Simulation-based analysis of 3D-printing industrial manufacturing processes

Department of Mechanics, Mathematics and Management
Mechanical Engineering and Management
Ph.D. Program
SSD: IIND-04/A – Manufacturing Technologies and Systems

Final Dissertation

Simulation-based Analysis of 3D-Printing Industrial Manufacturing Processes

by
Zahra Isania

Supervisors:

Prof. Giuseppe Casalino

Prof. Maria Pia Fanti

Coordinator of Ph.D. Program:
Prof. Giuseppe *Casalino*

Course XXXVII, 01/11/2022-30/04/2025

Department of Mechanics, Mathematics and Management
Mechanical Engineering and Management
Ph.D. Program
SSD: IIND-04/A – Manufacturing Technologies and Systems

Final Dissertation

Simulation-based Analysis of 3D-Printing Industrial Manufacturing Processes

by
Zahra Isania

Referees:

Prof. Raffaello Iavagnilio

Prof. Agostino Mangini

Supervisors:

Prof. Giuseppe Casalino

Prof. Maria Pia Fanti

Coordinator of Ph.D Program:
Prof. Giuseppe *Casalino*

Course XXXVII, 01/11/2022-30/04/2025

Every challenge is an opportunity for growth

Acknowledgments

I am deeply grateful to ***my family***, whose unconditional love, unwavering support, and constant encouragement have been the foundation of my journey. Their sacrifices, wisdom, and belief in me have guided me through every challenge and triumph. The values they have instilled in me—perseverance, integrity, and resilience—have been my compass, and I owe this achievement to their endless dedication and care.

I would also like to extend my heartfelt appreciation to ***Professor G. Casalino*** for his invaluable guidance, expertise, and support. His insights and advice have been instrumental in shaping this thesis, and I am truly fortunate to have had the opportunity to learn under his mentorship.

To ***Dr. Mohammad Zaeimi***, thank you for your boundless patience, understanding, and encouragement. Your presence in my life has been a constant source of inspiration and strength. I am especially grateful for the countless moments you stood by me with unwavering support during the most challenging times of this work.

To all who have contributed to this journey, directly or indirectly, I thank you from the bottom of my heart.

Abstract

In the evolving landscape of Additive Manufacturing (AM), achieving scalable, efficient, and cost-effective production remains a critical challenge. As industries advance toward the industrialization of 3D printing, they face complex operational demands, including machine utilization, part flow synchronization, and post-processing efficiency. This thesis tackles these challenges by developing a simulation-based framework utilizing Discrete Event Simulation (DES) to enhance AM workflow efficiency across multiple technologies.

Using FlexSim simulation software, the research models and analyzes production systems involving Selective Laser Sintering (SLS), Stereolithography (SLA), and Digital Light Processing (DLP). The DES approach enables detailed evaluation of workflow parameters, resource allocation, and job scheduling strategies. Through comprehensive case studies, the framework demonstrates its ability to identify system bottlenecks, minimize idle time, and improve throughput and labor efficiency.

This thesis contributes a domain-specific DES framework tailored to AM environments, validated through empirical modeling and performance evaluation. The findings underscore the value of simulation in both the design and operational optimization of AM production lines. Furthermore, the research demonstrates the role of simulation tools in supporting data-driven decision-making, reducing production costs, and improving reliability in large-scale additive manufacturing.

Ultimately, this thesis positions Discrete Event Simulation as a key enabler for the industrial adoption of AM technologies, offering a strategic path toward enhanced productivity, scalability, and operational resilience in modern manufacturing systems.

Keywords: Additive Manufacturing (AM), Discrete Event Simulation (DES), FlexSim, Industrialization of AM, AM Process Modeling

Contents

List of figures

List of tables

1 Introduction to the Industrialization of Additive Manufacturing

In today's increasingly competitive landscape of Additive Manufacturing (AM), organizations continuously seek to enhance the efficiency and reliability of their 3D printing workflows. Rising operational costs and intensifying market competition have brought renewed attention to critical production challenges, such as machine utilization, part flow optimization, and post-processing efficiency. These factors profoundly affect production costs, throughput, and the broader goal of industrializing AM.

To address these issues, manufacturers are adopting Discrete Event Simulation (DES) as a strategic tool to optimize 3D printing production systems. DES enables detailed modeling of workflows, facilitating the optimization of machine allocation, labor utilization, and post-processing activities. It empowers manufacturers to analyze production scenarios, assess system performance, and implement data-driven improvements that enhance throughput, minimize defects, and streamline operations [1].

With the advancement of 3D printing technologies, potential issues can be identified before a production line is fully operational by simulating printing and post-processing systems using specialized software. This enables manufacturers to refine printing parameters, assess the impact of machine downtimes, and identify critical bottlenecks in a data-driven manner [2]. Once the 3D printing workflow is in operation, DES models assist in monitoring real-time performance and optimizing resource allocation to ensure smoother operations. This simulation-based approach ensures improved reliability and better evaluation of AM system performance [3].

Compared to traditional manufacturing lines, AM systems present unique challenges such as build volume constraints, curing time, and complex material handling. DES provides a robust framework to simulate these specific characteristics, making it particularly valuable for optimizing print scheduling, buffer capacities, and post-processing workflows [4]. As a result, simulation-based approaches are gaining momentum as indispensable tools in scaling AM production.

A growing body of literature demonstrates the effective use of DES in enhancing AM processes. Researchers have applied simulation methodologies to refine build orientation, optimize support structures, and develop advanced scheduling algorithms. These studies have yielded tangible improvements in productivity, part quality, and cost reduction [5].

Recent investigations have extended the application of DES to simulate and optimize key AM processes, including Selective Laser Sintering (SLS), Stereolithography (SLA), and Digital Light Processing (DLP), enhancing job distribution and minimizing idle time [6]. By modeling job distribution strategies and machine interactions, these simulations have helped reduce idle time and increase resource efficiency, underscoring DES's potential to elevate AM into a mature, industrial-scale production method [7].

Furthermore, DES has facilitated progress in areas such as post-processing automation, defect rate mitigation, and material flow optimization. These advancements are vital for achieving higher levels of repeatability and scalability, core requirements for the industrialization of AM [8].

The literature review highlights the growing consensus around DES's value in refining 3D printing workflows. Key themes include improvements in print scheduling, material logistics, defect management, and post-processing. As demand for industrial-scale 3D printing continues to grow, DES emerges as an essential element in production planning, offering a pathway to greater operational efficiency, cost-effectiveness, and scalability in AM.

This thesis proposes a simulation-driven framework for optimizing additive manufacturing workflows by leveraging DES. Through detailed case studies involving SLS, SLA, and DLP, the research utilizes FlexSim software to model and analyze production line dynamics, assess resource efficiency, and propose improvements for large-scale industrial implementation.

1-1 Additive Manufacturing

Additive Manufacturing (AM), also known as 3D printing, is a transformative technology that fabricates physical objects by layering material based on designs created using Computer-Aided Design (CAD) software and exported in STL (stereolithography) file format [9]. Unlike traditional subtractive methods (e.g., cutting or drilling), AM enables the creation of intricate shapes and personalized designs that are often impractical or impossible with conventional techniques.

AM is a multi-phase process that includes pre-processing (design), processing (manufacturing), and post-processing (testing). During the design phase, detailed 3D models are created using CAD software, materials are selected, and the design is enhanced for maximum performance and efficiency. Analysis and simulation forecast material behavior and part performance. In the manufacturing phase, the part is constructed layer by layer using a sliced CAD model. Post-

processing steps, such as surface finishing or heat treatment, refine part quality. Testing involves dimensional inspection, mechanical property assessment, and non-destructive evaluation to ensure compliance with performance and regulatory standards.

AM simulation offers significant advantages, including increased print success rates, better design optimization, and failure prevention. It provides insights that enhance reproducibility and reduce shape distortion and costs. Simulation also helps eliminate waste and optimize material usage, ultimately improving overall production efficiency [10].

Factors affecting the choice of AM technology for specific applications include cost, material selection, post-processing requirements, surface finish and dimensional accuracy, sterilization possibilities, fabrication speed (layer thickness per unit time), and resolution (minimum feature area and minimum layer thickness) [11]. Specifications such as maximum build volume, fabrication speed, machine cost, and available materials are continuously evolving with advancements in AM technology. The International Standard [12] classifies AM technologies into seven categories, as illustrated in Figure 1:

1. Binder Jetting (BJ)
2. Directed Energy Deposition (DED)
3. Material Extrusion (ME)
4. Material Jetting (MJ)
5. Powder Bed Fusion (PBF)
6. Sheet Lamination (SL)
7. Vat Photopolymerization (VP)

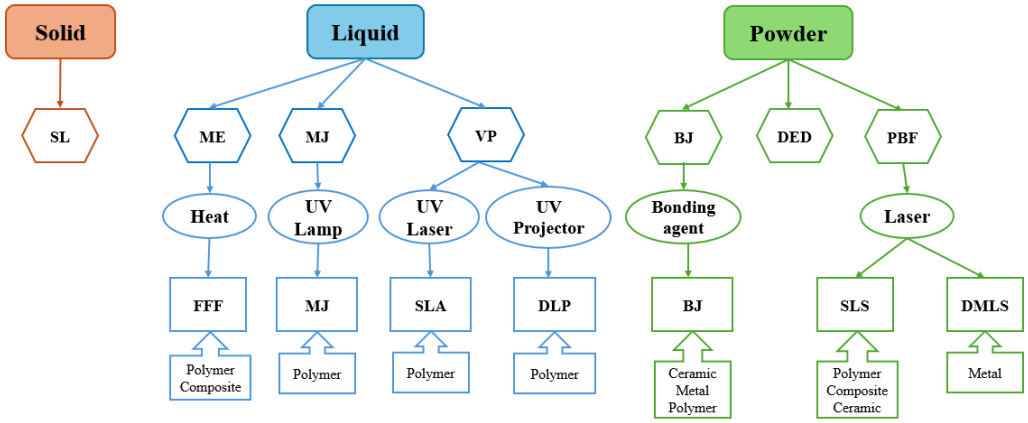

Figure 1 Classification of 3D Printing Technologies by Material State and Process Type

These processes can be liquid-, solid-, or powder-based [13]. The most common AM technology is Fused Filament Fabrication (FFF), followed by SLS, Material Jetting (MJ), SLA, Binder Jetting (BJ), and Direct Metal Laser Sintering (DMLS). The most commonly used AM machines include the EOS Formiga P100 (SLS), Stratasys Objet family (MJ), Stratasys Dimension family (FFF), and Stratasys Fortus (FFF) [14].

The expiration of key patents has significantly impacted the additive manufacturing landscape by making technologies like FFF, SLS, and SLA more accessible and affordable [15]. FFF is widely used for early-stage prototyping due to its low cost and seamless workflow from CAD models to physical parts [16]. SLS is valued for its robustness and material versatility, especially with Polyamide (PA), though it often produces a grainy surface finish that may be unsuitable for applications requiring smooth contact areas [17]. In contrast, SLA offers a superior surface finish and higher dimensional accuracy but typically involves additional steps, such as support structure removal, and is generally less cost-effective than SLS [16]. Technologies based on photopolymerization—such as SLA, Material Jetting (MJ), and DLP—are capable of producing highly detailed components. However, they are often limited by material brittleness and sensitivity to moisture and UV exposure [18]. Despite these limitations, such technologies are particularly well-suited for producing molds used in silicone-based product manufacturing.

Like any technology, AM comes with its own set of advantages and disadvantages. These are summarized below [19] and visually represented in Figure 2.

Advantages of Additive Manufacturing

- **Personalization without Tooling Costs:** One of the main benefits of AM is its capacity to

create customized products without requiring pricey tooling or special equipment for each item.

- **Reduced Material Waste:** By using only the required amount of material, AM significantly reduces waste and scrap production.
- **Design Flexibility:** AM allows the creation of complex geometries that would be difficult or impossible to manufacture with traditional techniques.
- **Cost-Effectiveness:** Since AM does not require pricey molds or tooling, it can be a cost-effective option for low-volume production runs.
- **Rapid Prototyping:** Quick iterations and modifications can be made to digital models, accelerating product development.
- **Localized and Distributed Manufacturing:** AM enables production closer to the end-user, reducing transportation costs and lead times.
- **Shorter Lead Times:** The ability to manufacture complex parts quickly speeds up time-to-market and development cycles.
- **Supports Sustainable Practices:** AM consumes less energy and material compared to traditional methods, promoting sustainability.
- **Encourages Innovation:** Designers have greater freedom to experiment and create products that would be difficult to achieve with conventional methods.

Disadvantages of Additive Manufacturing

- **Limited Material Selection:** AM currently supports fewer materials compared to traditional manufacturing, especially for applications that demand specific mechanical or thermal properties.
- **Post-processing Requirements:** AM parts often require additional finishing steps, such as polishing, painting, or heat treatment, to achieve the desired quality.
- **Size Limitations:** The size of printable objects is constrained by the printer's build volume.
- **High Equipment Costs:** The initial investment in AM machines can be prohibitively expensive for small businesses.

- **Sustainability Challenges:** The production of additives may generate harmful waste, which must be disposed of properly to avoid environmental and health issues.
- **Limited Scalability:** AM may not be cost-effective for high-volume production compared to traditional mass manufacturing methods.
- **Quality Control:** Achieving consistent quality and performance of parts produced through AM can be difficult, as it necessitates meticulous process control and testing.
- **Limited Production Speed:** While AM is efficient for small-scale production, it may not match the speed of traditional manufacturing for large-scale productions.
- **Accuracy Constraints:** Small and intricate parts produced using AM may have limited accuracy in comparison to traditionally manufactured parts.

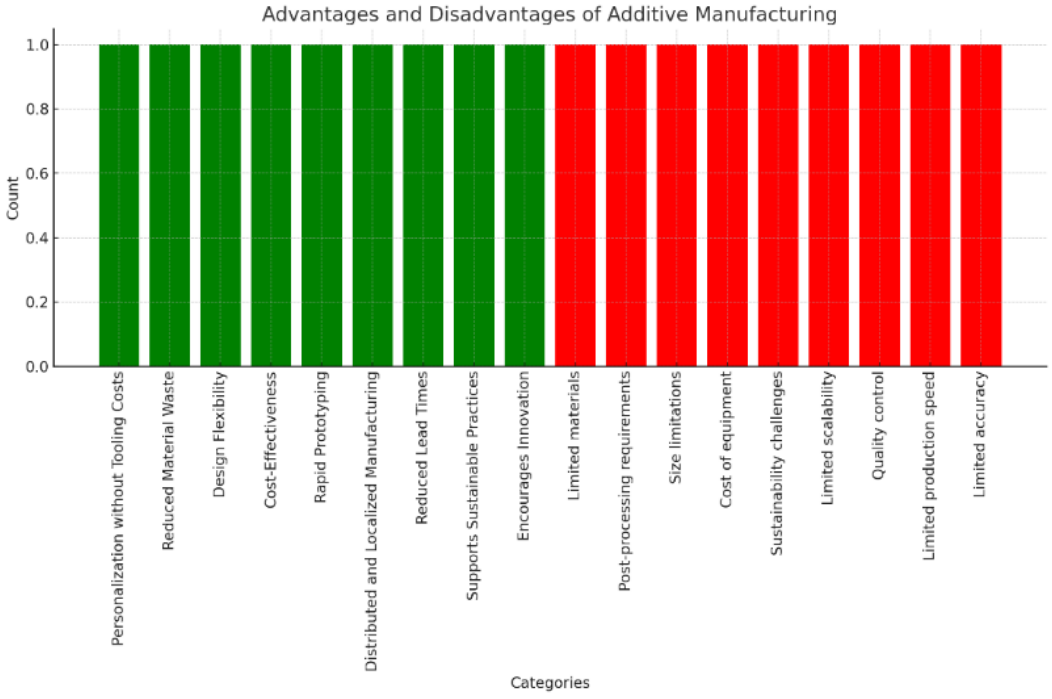

Figure 2 Overview of the Advantages and Disadvantages of Additive Manufacturing

Numerous studies have analyzed the advantages and limitations of different AM technologies and materials. For example, Petropolis et al.[20] found that PLA and FFF enable high-detail printing but may compromise user experience in certain applications due to hardness. SLS allows for rapid prototyping but requires post-processing to mitigate surface porosity and fluid absorption [21]. Furthermore, DMLS produces strong metal components but often requires intensive post-processing to ensure smooth finishes [22]. The shareability of AM-compatible digital 3D models further

enhances the reproducibility of scientific studies and enables easy adaptation to different user requirements [23].

With advancements in AM, affordability has improved due to expiring patents, increasing competition, open-source platforms, and cloud-based CAD software. These developments, along with user-friendly interfaces, enable non-experts to create products more easily [24]. Consequently, AM is expanding into custom, on-site production applications. Furthermore, the introduction of 4D printing has integrated smart materials capable of changing shape or physical properties in response to external stimuli, with applications in soft robotics, self-evolving structures, anti-counterfeiting systems, and active origami [25].

Advanced 3D printing systems are now integrated into Industry 4.0, combining automation, AI, and IoT for smart manufacturing. These systems are widely used in aerospace, automotive, healthcare, and consumer goods industries, offering cost-effective, customizable, and sustainable production solutions [26].

AM is particularly well-suited for advanced production needs due to its efficiency in creating detailed and lightweight components with minimal material usage. In aerospace, it is commonly used to manufacture parts that are both lighter and stronger than those made through traditional methods. In the healthcare sector, it supports the development of customized implants and prosthetic devices, precisely tailored to fit the unique physiological profiles of individual patients [27].

1-2 AM process at industrial scale

Since its inception in the late 1980s, Additive Manufacturing (AM) has experienced significant evolution. Initially, it was primarily used for rapid prototyping, enabling designers to produce physical versions of their designs quickly and cost-effectively. However, advancements in materials, technologies, and production methods have transformed AM into a robust manufacturing approach, now capable of producing functional, end-use components across various industries [28]. Today, AM enhances industrial productivity through digital systems and automation, extending its applications beyond prototyping to include direct production of components and manufacturing tools for industrial use.

A key enabler of AM's industrialization is the ability to accurately predict and control process outcomes. Given AM's capacity to produce parts with varying material properties within a single

component, the use of predictive simulation tools becomes essential. These tools support precise part design, particularly in mission-critical applications where reliability is crucial. By facilitating the analysis of manufacturing system behavior, simulation not only reduces the reliance on costly trial-and-error experimentation but also plays a vital role in optimizing AM processes. This, in turn, accelerates the adoption of AM in industrial environments and enhances overall production efficiency. As such, simulation serves as a cornerstone in the industrialization of AM, enabling cost-effective and high-quality production [29].

To successfully implement AM at an industrial scale, manufacturers must prioritize high levels of producibility, repeatability, and reproducibility. Achieving this requires adopting a structured approach to additive manufacturing that integrates advanced technologies, enforces rigorous process control, and adheres to standardized procedures.

1-2-1 Structured approach to additive manufacturing

The AM product realization process has been divided into eight distinct phases by researchers at the National Institute of Standards and Technology (NIST) [30], all interconnected through a digital spectrum. This spectrum refers to the creation, storage, and management of data required to guide the transition between each stage of the process, collectively known as the AM digital spectrum, which enables the formation of a cohesive digital thread. To enhance the practical application of this model, a simplified six-activity framework was derived from the original eight phases [31]. As illustrated in Figure 3, the six main steps include: (A1) generate AM design, (A2) plan process–machine independent, (A3) plan process–machine dependent, (A4) build part, (A5) post-process part, and (A6) qualify part [32]. These activities are elaborated as follows:

- **(A1) Generate AM design:** Using geometric dimensioning and tolerancing (GD&T) in mind, this exercise takes the conceptual design and creates a 3D tessellated model. This stage depicts the part's geometric shape and any feasible design justifications. In terms of topological optimization, internal lattice structure, assembly tolerance, and thickening/hollowing, a geometric model is altered. A watertight 3D model with tessellations is the result.

- **(A2) Plan process–machine independent:** This step involves defining aspects of the manufacturing process that are independent of the specific machine to be used. It focuses on planning parameters such as support structure requirements, optimal part orientation,

scheduling considerations, material selection, surface quality expectations, and estimated build times. The goal is to achieve a well-oriented 3D model with topologically optimized support structures that enhance manufacturability and minimize material usage and build duration.

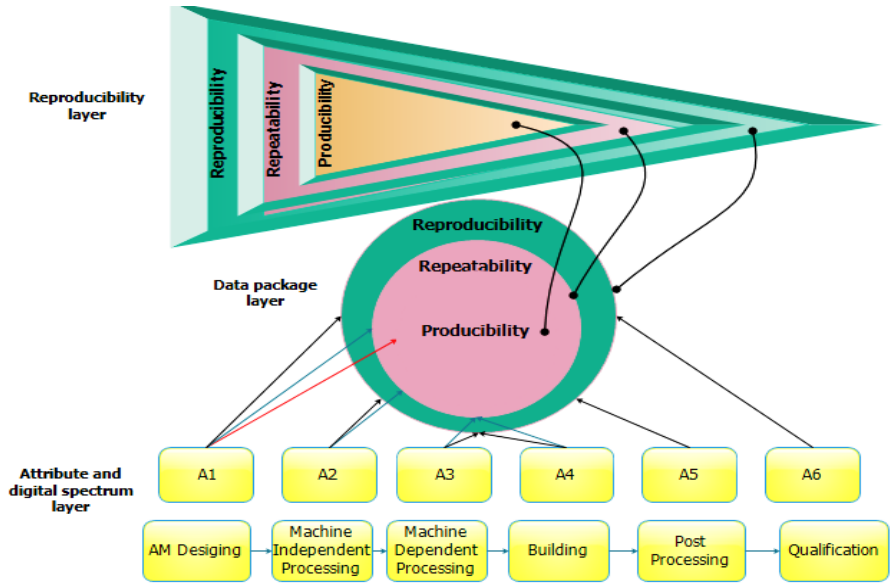

Figure 3 the AM product realization process into a six-activity model [33].

- **(A3) Plan process–machine dependent:** This step includes the definition of process-specific parameters such as slicing strategy, laser or light source power, scan speed, hatch distance, and scan-path planning. These parameters are tailored to the specific machine and material being used and directly influence the performance of the build. While optimization techniques can help determine suitable values, they typically yield near-optimal solutions due to the trade-offs between product quality (e.g., surface roughness, dimensional accuracy) and production efficiency (e.g., build time and operational cost). The output of this phase is the machine-specific build code, which guides the AM equipment during the fabrication process.

- **(A4) Build part:** Using the established process plans, a part is constructed during this activity. To selectively melt the powder layer, it is spread out to a layer thickness and scanned. Until the part is entirely constructed, the process is repeated. It is feasible to keep an eye on the melt-pool characteristics (such as size and form) throughout manufacturing to manage the microstructure and find flaws (like balls). The as-built portion is the output.

- **(A5) Post-process part:** This step is frequently required to complete a component to meet design specifications. It could involve the removal of a support structure, the improvement of

surface texture through shot peening and grinding, the increase of precision through machining, and the enhancement of properties through thermal procedures, including annealing and hot isostatic pressing (HIP). The post-processed portion is the output.

- **(A6) Qualify part:** This phase focuses on the final evaluation of the manufactured component. Any mechanical testing or non-destructive evaluation (NDE) of the manufactured part may be included. By adding test findings to part provenance data in this activity, a reference for any upcoming questions about part quality can be established.

Figure 3 illustrates the information map of AM, which comprises four levels: technical model, reproducibility layers, AM digital spectrum (conceptual model), and data packet (data model). Vertical integration reflects the refinement of information from abstract concepts to reproducible data, while horizontal flow highlights the transition from design (A1) to quality assurance (A6) [11]. This structure reinforces the foundation for establishing a digital origin and a reproducible digital discipline.

1-2-2 Producibility, Repeatability, and Reproducibility in AM

In the context of AM, producibility refers to the ability to reliably manufacture components that meet specified geometry, performance, and quality standards [34]. High producibility hinges on precise control of key process parameters such as temperature, scan speed, and material composition. This necessitates the adoption of rigorous design principles, standardized protocols, and advanced process control and monitoring systems.

Repeatability denotes the consistent production of identical parts within the same production setup, which is especially critical in high-precision sectors like aerospace and automotive manufacturing [35]. Reproducibility builds upon this, ensuring uniform outcomes across different production batches, times, and locations. Achieving reproducibility requires the standardization of materials, process parameters, and quality control protocols.

Producibility, repeatability, and reproducibility are closely aligned with the first four activities (A1–A4) of the NIST-AM digital spectrum (Figure 3)[11]. These activities are essential for structuring and validating an AM process. To support reproducibility, a comprehensive digital package is developed, encompassing all critical manufacturing, qualification, and validation data.

The digital spectrum layer establishes a data governance framework across AM systems. The feature

layer supplements this structure by enriching it with detailed part and process data that guide manufacturing decisions. At the process layer, geometry and machine parameters are aligned to standardize settings across platforms. Together, these layers create a robust, data-centric foundation that underpins the technical integrity of AM workflows.

These three metrics are not only technical indicators but also practical benchmarks for reliability in AM production. They are foundational to both process planning and quality assurance strategies and are heavily reliant on data traceability and integrity [11].

The first activity model (A1) plays a crucial role in supporting these objectives. It identifies key attributes required for achieving producibility, repeatability, and reproducibility. These attributes are organized into three subcategories: design, 3D tessellated model, and machine specification.

The design subcategory includes essential elements such as the 3D model and the selected material type (e.g., Ti6Al4V or IN625). To create the 3D tessellated model, two primary methods are commonly used: (1) boundary representation (B-rep) from CAD software, and (2) triangulation of point clouds collected via coordinate measuring machines (CMMs) or laser scanners using reverse-engineering technology [36, 37]. These design inputs serve as the foundation for reliable and standardized AM part fabrication.

Focusing on repeatability and reproducibility, the 3D tessellated model sub-category highlights critical attributes such as the method used for model generation, XYZ coordinate data, and their connectivity, surface resolution, and facet types (triangular or rectangular). Among these, surface resolution plays a pivotal role as it directly relates to chordal error—the deviation between the actual surface and the triangular mesh representation [38]. Minimizing such geometric errors is essential for preserving model fidelity, optimizing slicing accuracy, and ultimately enhancing both repeatability and reproducibility in the AM process.

The machine specification sub-category encompasses attributes such as build volume (in mm), dimensional accuracy, multi-material capability, and build speed. These parameters are all critical to achieving repeatability and reproducibility. In particular, consistent manufacturability of features, such as wall thickness, edge precision, and overhang geometry, plays a key role in ensuring reliable and high-quality part production [39, 40]. Machine capabilities directly affect whether parts can be manufactured within defined tolerances, thereby influencing process stability.

Once the first activity model (A1) has defined the foundational design and machine-based criteria to

ensure producibility, subsequent models shift focus toward repeatability and reproducibility to establish digital provenance. The second activity model (A2) introduces key attributes grouped under two sub-categories: part orientation and support structure. These two are closely interconnected, as part orientation inherently determines where support structures will be required during printing.

Part orientation is determined by considering multiple factors, including build time, surface quality, mechanical properties, and support needs. For example, poor orientation can exacerbate the "stair-stepping effect" on sloped surfaces. This effect can be mitigated by combining adaptive slicing techniques with optimal part orientation [41]. Additionally, orientation significantly affects mechanical performance due to the anisotropic nature of processes like Powder Bed Fusion (PBF). Attributes such as yield strength, ultimate tensile strength, stiffness, and fracture strain can vary depending on the part's alignment during printing.

Support structures are defined by several attributes [42], including their quantity, the number of contact points with the part and the build plate, the material used, the support type (e.g., block, point, or web), infill density, and the vertical offset between the part and the build platform. The ability to recognize complex geometric features, such as overhangs, undercuts, and assemblies with moving components, is essential for generating effective support structures that enhance both print stability and part quality.

In the third activity model (A3), key attributes related to repeatability and reproducibility are organized into three sub-categories: slicing, process setup plan, and process parameter determination.

Following the definition of part orientation and support structures, the 3D tessellated model (e.g., STL or AMF format) is discretized into 2D slice contours (e.g., CLI format) [43]. These contours define the reference geometry for subsequent process planning, including tool path generation and parameter assignment, and guide the machine's operation. Key slicing-related attributes include XY coordinate data for each layer and their piecewise linear connectivity. It is also crucial to identify instances where a layer contains multi-material regions or functionally graded materials, as these require differentiated treatment during processing.

The process setup plan involves attributes such as machine configuration, powder properties, and environmental controls. Machine-specific characteristics include heat source type, mode, and power, as well as air flow and temperature management. Powder characteristics [44] relevant to process consistency include thermal conductivity, absorptivity, specific heat capacity, thermal expansion coefficient, and bulk density. Additionally, the setup plan covers parameters like part placement on

the build plate, base elevation, cooling time after printing, and initial bed temperature—all of which influence build quality and repeatability.

Finally, process parameters play a critical role in determining final part properties. These include laser power, spot size, wavelength, laser mode, scan speed, hatch distance, layer thickness, scan pattern, and scan strategy [45]. Certain parameters—such as power, scan speed, hatch distance, and layer thickness—are often varied depending on the exposure type: pre-contour, core, skin, and post-contour. The skin category may be further refined into up-skin, down-skin, and side-skin to ensure surface quality and mechanical integrity.

In summary, Activity Model A3 addresses three interrelated components—slicing, process setup, and process parameter specification—that collectively underpin the repeatability and reproducibility of additive manufacturing workflows.

Activity A4, which focuses on the part build phase, is divided into two sub-categories: preparation for the build and the actual build process.

The preparation stage involves both machine setup and powder preparation. Key machine setup parameters that contribute to digital provenance include the initial bed temperature, inert gas/air ratio, laser focal point, build plate position and level, recoating blade wear, and build platform characteristics such as type, flatness, surface roughness, thickness, and its parallelism with the recoater. These attributes collectively establish a stable and repeatable build environment.

Equally important is the accurate characterization of the powder material, which is essential for predicting melt-pool behavior and thermal dynamics during the build. Critical powder attributes include particle size and distribution, morphology (including dimensional shape, sphericity, roundness, and perimeter), chemical composition, and multiple density metrics (apparent, tap, and skeletal). Thermal properties such as conductivity and diffusivity also play a central role. Additionally, the number of times the powder has been recycled can significantly impact material performance and must be carefully tracked.

The build process stage is concerned with maintaining process stability and is divided into two main areas: process consistency and motion/position accuracy. Key parameters for ensuring process consistency include laser beam power, wavelength, mode, inert gas/air flow rate and ratio, chamber pressure, ambient temperature, humidity control, and layer thickness.

Motion and positioning accuracy relate to the precise functioning of components such as the

recoating blade or arm, laser spot alignment, and Z-axis control. Deviations in any of these elements can compromise the geometric fidelity of the printed part. Maintaining stability across both consistency and positional accuracy domains is essential for producing high-quality, repeatable builds in additive manufacturing.

Activity A5 focuses entirely on reproducibility, as the part geometry has already been formed, and the emphasis transitions to finishing and post-processing. The key attributes associated with this phase can be categorized into four areas: support removal, property enhancement through thermal treatments, dimensional accuracy improvement, and surface texture refinement.

Consistency in the method and sequence of support removal is essential to prevent structural or dimensional variation. Often, parts undergo heat treatment with support structures still in place to alleviate residual stresses, after which cooling conditions and durations must be carefully managed to ensure proper heat dissipation. Common removal methods include wire electrical discharge machining (EDM) and bandsaw cutting, with critical parameters such as wire diameter, process settings, and fixture or positioning setups requiring strict control.

To enhance material properties, thermal post-processing techniques such as hot isostatic pressing (HIP) and annealing are frequently employed. These methods help reduce residual stress and internal porosity while improving microstructural uniformity and ductility. For example, Ti-6Al-4V components are typically treated using HIP at 926°C under 100 MPa, followed by annealing at 913°C for 2–4 hours and furnace cooling to below 427°C [46]. Important attributes in this context include the selected treatment method, peak temperature, applied pressure, processing duration, and cooling rate [45].

Due to the inherent geometric variability in additively manufactured metal parts, further post-processing is often required to achieve the desired dimensional accuracy. This is typically addressed through machining techniques such as adaptive raster milling, sharp edge contouring, and drilling. Relevant parameters include the machining strategy, tool path definition, process settings, and fixture or positioning arrangements. These operations play a critical role in minimizing dimensional deviations and aligning the final part with design specifications.

Poor surface roughness in additively manufactured parts may result from the stair-stepping effect or process instabilities such as irregular melt-pool formation. Surface texture improvement methods—such as shot peening, painting, and surface hardening—are essential for enhancing reproducibility, with implementation details serving as key attributes. For instance, in shot peening, parameters like

the size of the metallic spherical media and the applied air pressure are critical for achieving a uniform and consistent finish. In summary, Activity A5 ensures reproducibility through standardized support removal procedures, thermal property enhancement, dimensional accuracy improvements, and surface texture refinement.

Key attributes associated with Activity A6, which concerns the testing and qualification phase of a part, are crucial for assessing and validating reproducibility. These attributes are categorized into five areas: geometric dimensioning and tolerancing (GD&T), defect analysis, microstructure characterization, surface roughness, and part property evaluation.

Within GD&T, advanced inspection methods—such as industrial computed tomography (CT) scanning, 3D optical scanning, and coordinate measuring machines (CMMs)—are used to assess dimensional and geometric accuracy. Inspection plans often target parameters such as flatness, roundness, straightness, parallelism, perpendicularity, and concentricity, all of which are critical for ensuring measurement consistency and reproducibility [47].

Defect analysis focuses on critical AM issues such as cracks, porosity, and delamination [48, 49]. Non-destructive evaluation (NDE) methods, including CT scanning, dye penetrant inspection, and ultrasonic testing, play a vital role in identifying these flaws without damaging the part [50]. Detailed defect inspection plans—including controlled test conditions like temperature and the use of distilled water in density testing to reduce air bubble interference—are essential for establishing digital provenance and reliable quality assurance [51].

Microstructural analysis involves techniques such as optical microscopy and scanning electron microscopy (SEM) to evaluate grain size, morphology, and growth direction. Consistency in sample preparation—such as cutting orientation, coordinate selection, and polishing methods—ensures accurate and repeatable microstructural characterization.

Surface roughness is another important metric for assessing part quality and reproducibility. Measurement involves precise instrumentation, designated coordinate points, and metrics such as average roughness (Ra) and maximum roughness height (Rt). Reliable identification and consistent measurement protocols are fundamental for maintaining reproducibility standards.

Lastly, part of property testing encompasses mechanical, electrical, chemical, and thermal characteristics [52]. Mechanical testing techniques [53] assess both deformation characteristics, such as tensile strength, compressive behavior, and hardness, and failure-related properties, including

fatigue performance and fracture resistance. These assessments form a comprehensive basis for certifying the performance and repeatability of AM-produced parts.

2 The Role of DES for 3D-Printing Industrialization

The ability of AM to liberate designers from the constraints of traditional production is unmatched. This adaptability makes it possible to design components that are strong and perform well while using the least amount of material. Because AM can create designs that are lightweight and efficient, it has become widely used worldwide and has grown into a multibillion-dollar business with a wide range of materials and processes. However, there are obstacles to overcome in the industrialization of AM, including maintaining consistent quality, cutting costs, and maximizing production efficiency. DES emerges as a key enabler in overcoming these obstacles. In this study, DES is applied to simulate and optimize the industrialization of AM, improving process quality and encouraging wider adoption of 3D printing in manufacturing.

Mapping and simulating 3D-printing processes are essential for analyzing and improving production workflows. By employing DES, manufacturers can analyze system behavior, identify bottlenecks, and improve efficiency. In modern industrial settings, 3DP has evolved from an innovative concept into an essential part of production, governed by standards such as ISO/ASTM 52900:2015 [54]. It enables the design of complex geometries with reduced component counts, facilitating the transition from traditional molding techniques to layer-by-layer fabrication based on digital 3D models. As AM continues to industrialize, maximizing facility utilization and reducing costs remain critical. The integration of simulation-based approaches, including Digital Twins, further enhances the ability to streamline production, optimize resource use, and ensure high-quality outputs [55].

AM plays a pivotal role in the production of lightweight, integrated structures, especially in the aerospace, medical, and automotive industries. These technologies hold tremendous potential to revolutionize product design, supply networks, and manufacturing processes, enabling the production of more complex components at lower cost and with greater efficiency [56]. The need to maximize the utilization of AM facilities is expanding as AM materials and processes continue to advance, especially in terms of reducing the time and cost of 3D printing in industrial production [57].

Due to changing consumer needs and the requirement for quick modifications through flexible production layouts and processes, manufacturing organizations today face growing pressures in production planning and management. It may be particularly challenging to increase efficiency in complex production environments, especially when it comes to identifying and eliminating bottlenecks. The use of simulation tools is essential in meeting these challenges. These tools are

primarily used to speed up the manufacturing process from start to finish, including planning, implementation, and operational management [58].

In the context of 3D printing, the partnership between HP and Siemens at the DFactory in Barcelona is a significant step forward in 3D printing productivity and automation. The DFactory project aims to enhance productivity and automation in the HP Jet Fusion 3D printing production workflow by incorporating Siemens' advanced automation solutions, which allow for high-volume and continuous manufacturing with minimal human intervention. The objective is to accomplish “lights-out manufacturing,” where operations run autonomously without the need for human oversight, even during off-hours. In such a setup, all production-related tasks, including material handling, assembly, and quality assurance, are handled by machines, robots, and automated systems, enabling factories to run around the clock. In this way, labor costs are reduced, human error is minimized, and sustainable production is promoted [59].

The growing complexity and unpredictability of the present manufacturing and economic environment directly impact modern manufacturing system design. More automation, reduced lot sizes, shorter product life cycles, and greater product variability are among the key developments being facilitated by intelligent control systems. As a result, suppliers and manufacturers in the discrete manufacturing sector are placing increasing emphasis on automation, simulation, and digitization—all of which are critical at both the production line and equipment levels. These developments are forcing businesses to incorporate advanced technologies and redefine manufacturing methods [60].

Digital Twins (DTs) have become a key element of the changing landscape of digital technology. A virtual model that replicates its physical counterpart in real-time and is used for continuous monitoring, optimization, and decision-making is called a digital twin [61]. DTs are essential to modern industrial processes because they allow seamless communication between virtual and physical systems through real-time data exchange. The use of DTs has been further hastened by the emergence of Industry 4.0, which brings with it technologies such as IoT, Big Data, and predictive maintenance. These tools presently serve as the digital equivalents of Cyber-Physical Systems (CPS), establishing a constant data connection between the digital and real worlds [62].

Digital twins are particularly useful in AM. Industry 4.0 requires the ability to create complex, non-standard structures, which AM makes possible. While AM can speed up production and minimize material waste, improving mechanical characteristics is still difficult and frequently necessitates

expensive, time-consuming trial-and-error procedures. Manufacturers may significantly reduce the requirement for physical trials and increase the accuracy of parameter selection by simulating various manufacturing situations using DTs. This integration accelerates production, improves qualification speed, boosts quality, and optimizes the use of resources [63].

A crucial element of the Digital Twin structure is simulation. Production planning is enhanced, processes are streamlined, and production concepts are validated with the use of techniques like DES [64]. Near-optimal operational solutions can be obtained by combining simulation with optimization methods like genetic algorithms. Nonetheless, there are still issues with gathering high-quality input data and the time needed for comprehensive simulations. A connected data approach can assist in dealing with these difficulties by automatically extracting data and thus enhancing the connection between the physical and digital systems [65].

Creating a Digital Twin for Additive Manufacturing (AM) involves a structured, collaborative process that generally unfolds in three main stages: establishing the digital twin's scope, developing the digital master, and generating the digital shadow [66]. This includes defining the elements to be modeled, simulating production systems using DES, and gathering real-time data for traceability and continuous monitoring. From process and design to automation, every step needs teamwork to guarantee that the digital twin can precisely optimize output and decision-making. Even with continuous progress, more work remains in areas such as data fidelity, simulation accuracy, and strengthening the bond between digital and physical systems [67].

Among simulation methodologies, DES is one of the most used approaches for researching and improving manufacturing processes [68]. The modeling, simulation, optimization, and visualization of logistics, manufacturing systems, and other operational elements are made easier by DES technologies. Because of its adaptability, DES is especially powerful for conducting in-depth analyses of system features, identifying possible weak points or bottlenecks in process flows, and enhancing important performance metrics, including productivity, material handling costs, energy consumption, and resource usage [69].

For example, Omogbai and Salonitis [70] proposed using DES to simulate and assess lean manufacturing improvement initiatives before their use. Velumani and Tang [71]also demonstrated how to use DES to control production bottlenecks in batch processes and evaluate operational conditions. In addition, Prajapat et al. [72]created a DES model for a repair plant, giving decision-makers a tool to assess different facility layouts and configurations to maximize output.

2-1 BPMN Mapping Process

Business Process Modeling Notation (BPMN) is an internationally standardized visual language used to illustrate business processes and workflows in an organized and consistent manner. Developed by the Business Process Management Initiative (BPMI), it enables a smooth transition from process design to execution [73]. It provides a clear and structured representation of workflows, promoting effective communication and collaboration between business analysts and technical developers. Furthermore, BPMN supports the graphical representation of XML-based execution languages, such as BPEL4WS and BPML, ensuring consistency between process modeling and implementation.

BPMN diagrams consist of a range of elements, each representing different aspects of a process. These include flow objects, such as events (triggers or results), activities (tasks or subprocesses), and gateways (decision points that guide flow). Connecting objects—including sequence flows, message flows, and associations—define the relationships between elements. Additionally, BPMN incorporates swimlanes, which group activities by participants or roles, and artifacts, such as data objects and annotations, that provide supplemental information. These components allow for detailed yet intuitive process models that are both comprehensive and easy to interpret.

Within the broader field of Business Process Management (BPM), BPMN serves as a critical integration tool, linking various components of process automation, including modeling, simulation, workflow execution, Enterprise Application Integration (EAI), and Business-to-Business (B2B) collaboration [74]. Before BPMN, the absence of a unified modeling language created inconsistencies and challenges in managing business processes effectively [75]. Unlike traditional flowcharts or informal diagrams, BPMN was developed specifically to align with business execution languages and web services, incorporating advanced features for modeling message exchanges, events, and inter-organizational processes [76].

BPMN is widely adopted across industries to improve operational transparency and workflow efficiency. It enhances stakeholder communication through standardized visual representations, reducing ambiguity and ensuring alignment. BPMN also enables process optimization by helping organizations identify bottlenecks, analyze inefficiencies, and implement targeted improvements. Additionally, its compatibility with execution languages facilitates process automation and integration with Business Process Management Systems (BPMS). Applications range from workflow reengineering and compliance management to enterprise-wide digital transformation efforts [77].

With the growing emphasis on automation and digital transformation, BPMN continues to evolve. Future enhancements focus on improving its compatibility with other modeling standards, expanding automation features, and tailoring its use to specific industry needs. Innovations like artificial intelligence (AI) and machine learning present opportunities to expand BPMN's role into areas such as intelligent process automation and predictive analytics. As a globally acknowledged and standardized approach, BPMN remains vital for organizations aiming to optimize process efficiency, strengthen system integration, and drive innovation in process management [78].

While BPMN is specifically intended for modeling business processes, the Unified Modeling Language (UML) functions as a general-purpose modeling language, primarily used in software development. Though BPMN and UML Activity Diagrams both visualize workflows, BPMN offers distinct features for execution logic, event handling, and communication between process participants. UML, on the other hand, encompasses a wider range of applications, including modeling software architecture, system dynamics, and object relationships. Its ability to represent detailed system-level structures makes UML a key tool in software engineering, system design, and data modeling [79].

Despite their distinct purposes, BPMN and UML can be effectively combined in system development. BPMN is useful for outlining high-level business workflows, while UML diagrams can be used to specify internal system implementations and interactions supporting these workflows. This integrated approach helps align business process design with technical system implementation, ensuring a seamless transition between business and IT perspectives [80].

2-2 Discrete Event Simulations

Discrete Event Simulation (DES) has emerged as a powerful tool for modeling and optimizing complex manufacturing systems and assembly lines. It is particularly well suited for manufacturing environments due to its capability of explicitly modeling variations using probability distributions. This allows DES to answer key operational questions related to throughput, resource allocation, utilization, and supply and demand [81]. A key advantage is its capability to analyze procedures and information flows without interrupting real systems. Goldsman [82] developed a simulation model to observe a system in operation and predict its future performance. He emphasized that "a fully developed and validated model can answer a variety of questions about real systems." Simulation is therefore essential for evaluating new system designs, modifying existing operations, and testing

changes to control policies [83].

A DES begins in an initial state and transitions to a new state whenever an event occurs. This state-change mechanism continues over time, with the system maintaining certain states for defined durations before progressing [84]. As Goldsman [82] noted, "Of all the simulation techniques, DES models the operation of a system as a discrete sequence of events in time. Every event happens at a specific moment and signifies a change in the system's state." To fully understand DES, it is important to explore both its conceptual behavior and evolving applications.

DES is particularly effective in modeling systems where components transition between states at specific times, either due to internal behavior or interactions with other components. This method is especially useful when the system operates across discrete, non-overlapping time intervals, often under stochastic influences. In a DES model, the system is viewed as a collection of interacting, attribute-rich entities that carry out tasks and respond to events and actions.

Simulation contributes to manufacturing efficiency by identifying bottlenecks, reducing downtime, and addressing operational issues. DES has been widely applied in energy consumption analysis, bottleneck elimination, and line balancing [85]. Although DES has existed since the 1950s, recent technological advances have enabled its integration with virtual reality and automatic data acquisition for input generation [86]. For instance, Ingemansson et al. [87] demonstrated how DES can utilize IoT-generated data to support real-time decision-making and process improvements.

The first industrial revolution introduced machinery to replace manual labor, yet human operators remained essential for managing these systems. Today, advances in automation and robotics are increasingly substituting human labor, especially for repetitive and high-precision tasks like welding [88]. With human-like mobility, industrial robots can perform complex movements without fatigue. This robotization has delivered major benefits to companies, including a 50% reduction in production costs, a 30% increase in productivity, and utilization rates exceeding 85% [89]. While initial costs are high, robotization proves cost-effective in large-scale, repetitive production environments such as the automotive industry. Manufacturing systems now include various specialized machines along with human or robotic operators, often structured into production lines or cells. Due to this complexity, DES is essential for in-depth system analysis [90].

A major advancement in DES is its ability to update simulations dynamically using remotely stored, real-time data. In smart factories or Industry 4.0 environments, machines equipped with sensors generate data that represents the digital twin (DT) of the production system. DES serves as a core

component of a cyber-physical system (CPS) that synchronizes the virtual model with physical processes (Figure 4). Through internet-based communication, DES can retrieve updated parameters on a schedule, improving simulation accuracy and responsiveness.

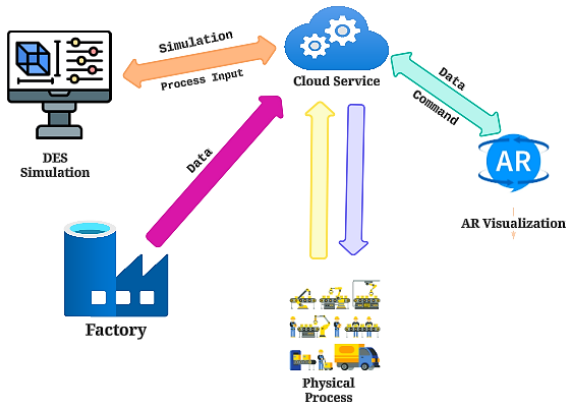

Figure 4 DES simulation concept from a smart factory.

A locally executed DES can process variables like standard deviation and averages, obtained via cloud-based services. The cloud functions as the user interface for a smart production center, where data collected from IoT systems is streamed into DES for real-time simulation and optimization. DES can then transmit its simulation outputs back to the cloud to assist in future planning. Augmented Reality (AR) further supports this by visualizing simulation outcomes in the physical workspace, enhancing operator understanding and system transparency.

The evolution of DES aligns with emerging trends in hybrid modeling practices and optimization algorithms, enabling simulation applications to transition from design-focused tools to real-time operational solutions [91]. Although DES does not directly interact with the physical system, it plays a critical role in evaluating operational changes based on input parameters like cycle time, resource usage, and labor assignment. With the integration of Industry 4.0 technologies—including AR, IoT, and digital twins—DES becomes more dynamic, interactive, and intelligent [92].

To further analyze DES methodologies, a comprehensive review of the literature on DES for optimizing assembly applications identified 52 relevant studies, classified based on domain, objective functions, model formulation, and optimization methods [81]. The results showed that the predominant trends in general production systems included time-based and throughput goals, commercial software applications, and what-if scenario analysis. Mansharamani [84] examined the field from a programming standpoint, identifying three key DES methodologies: event scheduling, activity scanning, and process interaction.

Goldsman [82] offers a comprehensive framework for constructing a DES model, which includes eight essential steps: problem formulation, setting objectives and planning, conceptual modeling, data collection, simulation model creation, experimental design, production runs and analysis, and documentation and reporting. Accurately modeling a system requires a thorough understanding of the real-world process being simulated. Several tools are available for characterizing operations, including those introduced by Ziarnetsky et al. [93], who developed modular components for modeling assembly lines. Their approach was validated through a case study, demonstrating its effectiveness in simulating inventory management. Likewise, Weigert and Henlich [94] investigated the role of graphing techniques in improving the comprehension of assembly systems, particularly in DES modeling.

Although DES offers several advantages, it also comes with certain limitations. One of its key benefits is the ability to analyze complex systems, test operational changes, and assess feasibility without affecting real-world production. However, developing simulation models requires specialized expertise, and the method involves inherent randomness [82]. According to Jamil and Razali [83], DES is particularly effective for large-scale applications since it prevents disruptions to ongoing operations. However, they also noted that DES does not fully capture inconsistencies in production variables or account for human errors and skills, as it primarily relies on quantitative data.

Detty and Yingling [95], explored the benefits of DES in lean manufacturing, emphasizing its ability to visualize overall system advantages. By simulating the transition to lean practices, businesses can more accurately predict the effects of process improvements. Jamil and Razali [83], echoed this perspective, arguing that simulation speeds up the line-balancing process and boosts efficiency by identifying and addressing inefficiencies.

Several case studies demonstrate the success of DES in diverse manufacturing settings. For instance, Kumar and Phrommathed [96] used Arena 7.0 to simulate key operations in a paper sheet-cutting process. Their four-step approach—process mapping, data gathering, resource utilization analysis, process redesign, and evaluation—showed that integrating simulation with data analysis reduces the likelihood of ineffective process changes. The study found that applying these techniques resulted in better machine utilization, shorter lead times, and more opportunities for quality control.

Ziarnetsky et al. [93] conducted a case study where they applied their simulation framework to an aircraft manufacturer to enhance inventory management. By simulating 210 days of production using AutoSched AP with a four-week warm-up period to exclude initialization effects, they concluded

that simulation effectively visualizes and tests various scenarios to identify optimal solutions. Similarly, Jamil and Razali [83] investigated the role of simulation in balancing mixed-model assembly lines. After mapping process flows and conducting time studies, they created a simulation model using ProModel software. By comparing the simulated system with the actual one, they identified inefficiencies caused by blockages and idle time. Through a what-if analysis, they redesigned the layout by adding buffers to eliminate blockages and increasing manpower to reduce idle time. Their findings showed that simulation-based improvements greatly enhanced the efficiency of the production line.

Dewa and Chidzuu [97] used DES to develop an optimal mixed-model production sequence. Their approach integrated queuing theory and simulation to resolve bottlenecks. Using the Showflow software, they constructed a model based on an actual assembly plant layout. A comparison between historical and simulated data showed only a 5% deviation, confirming the model's accuracy. The study demonstrated that DES-based bottleneck analysis could provide critical insights for optimizing production flow. Similarly, Detty and Yingling [95] used simulation to quantify the benefits of lean manufacturing. They developed models for both existing and lean systems, concluding that DES effectively estimates shop-floor savings. Their methodology offers a reliable framework for assessing the economic impact of lean principles.

In summary, DES is an essential tool for analyzing, optimizing, and reengineering manufacturing systems. Its ability to model complex interactions and simulate alternative scenarios supports informed decision-making. While DES depends on accurate data and expert model design, its value in operational planning is undeniable. Future research should examine how DES can be further enhanced through integration with artificial intelligence and real-time analytics. As DES evolves with digital technologies, it will continue to play a vital role in driving efficiency, agility, and competitiveness across modern manufacturing systems.

2-3 FlexSim software

FlexSim is a Windows-based software developed by the American company FlexSim, offering a comprehensive suite of tools for creating and executing simulation applications. The FlexSim environment includes three core components: the compiler, the developer, and the function items [98]. Fully integrated with the C++ compiler, FlexSim utilizes FlexScript (a pre-compiled C++ library) or C++ directly. FlexSim features a rich object model library, where object parameters can

represent almost any physical entity, enabling the simulation of numerous real-world systems [99].

Its graphical capabilities leverage OpenGL to render animations, supporting immersive virtual reality functionalities. The software offers multiple visualization modes, including tree view, 2D, 3D, and virtual reality. This flexibility allows users to display two different views simultaneously during model development or execution. These visualization strengths make FlexSim a preferred tool for simulations in manufacturing, logistics, and maintenance industries [99]. As a powerful platform for analyzing dynamic systems, FlexSim employs DES to capture the complexities and variabilities inherent in production environments. Enhancing a system requires a comprehensive understanding of the interactions among its components, and FlexSim excels in this area [100]. It is widely used for designing, evaluating, and optimizing production systems. The software includes an intuitive interface with drag-and-drop functionality, integration of stochastic elements, and monitoring tools for evaluating performance metrics.

With robust analytical capabilities, FlexSim enables comprehensive system simulations, displaying production line models within model windows. These windows visualize temporary entities, forklifts, operator activities, and product accumulation points [101]. The software is recognized for its cost-effectiveness, reliability, and rapid deployment in decision-making processes. Additionally, FlexSim seamlessly integrates with external software such as Microsoft Word and Excel, using spreadsheets for both data input and result analysis. Its simulation engine operates efficiently within a visual modeling environment, offering powerful tools for building complex systems. Object-oriented architecture supports rapid model construction and realistic 3D animations, enhancing both visual and analytical depth [102].

Traditionally, improving an error-check system in manufacturing could take months or even years; however, with FlexSim, this process can be accomplished in days or even hours. By increasing system efficiency and reducing production costs, FlexSim has been widely adopted across industries such as manufacturing, logistics, and warehouse management [103]. The software is especially effective for process reconstruction, plant layout planning, and production preparation. Its advanced 3D visualization capabilities and compatibility with other platforms make it one of the most powerful simulation tools available [104].

The basic steps in using FlexSim include defining the model layout and logistics, setting parameters, compiling and executing the model, generating output, and performing result analysis [103]. By leveraging operational data and research-based strategies, FlexSim supports the development of

practical solutions for optimizing production lines. Practitioners and researchers have consistently validated FlexSim's effectiveness, often integrating it with additional software and hardware tools to broaden its application scope.

This study explores the application of FlexSim DES in designing layout improvement strategies for factories to enhance productivity. By utilizing FlexSim, organizations can derive actionable insights into software utilization, problem-solving approaches, and performance optimization techniques. This research emphasizes the need for evaluating industrial system performance to increase productivity, achieve economic efficiency, and minimize total operational time. Consequently, businesses can streamline operations, identify bottlenecks, enhance workforce well-being, and reduce both costs and labor hours.

The process of creating a simulation model in FlexSim follows a structured methodology that ensures clarity and efficiency in optimizing production layouts. This approach is illustrated in Figure 5 and consists of the following key steps [105, 106]:

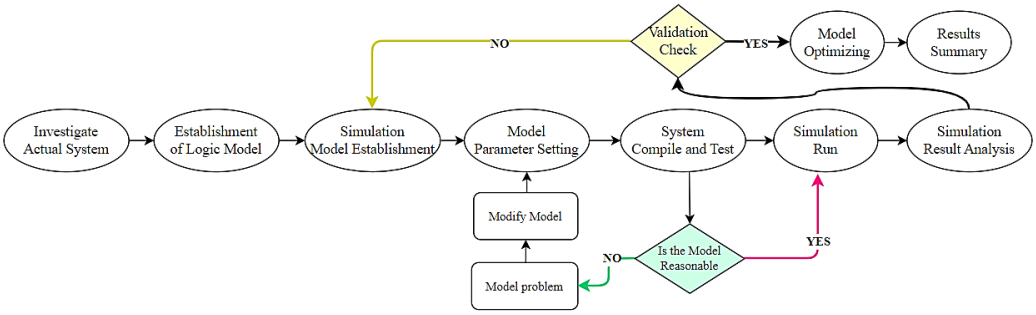

Figure 5 Steps for Simulation and Optimization of Production Line

Investigate the Actual System: This step involves examining the system's structure, developing a process flowchart, and conducting parameter analysis to define operational characteristics.

Establishment of a Logic Model: A layout diagram is created to represent logical relationships between system elements, ensuring accurate material flow and interaction modeling.

Simulation Model Establishment: The physical model is converted into a simulation model within FlexSim. This transformation supports computational analysis and system behavior replication.

Model Parameter Setting: Each simulation component is assigned specific parameters, such as processing time, resource availability, and machine reliability, to ensure a realistic system representation.

System Compilation and Testing: The model is compiled into an executable format. Errors are identified and corrected to guarantee accurate functionality.

Simulation Execution: The model is run using predefined iterations and termination conditions to evaluate system performance under various scenarios.

Simulation Result Analysis: Output data are statistically analyzed to assess key performance indicators such as throughput, resource utilization, and efficiency.

Model Optimization: Based on simulation outcomes, model parameters are refined. The optimized model is then compared with the original configuration to determine the most efficient layout.

The findings from the FlexSim simulation provide valuable insights into system performance, efficiency, and potential areas for improvement. When simulating a technological flow, two scenarios are typically encountered:

1. The technological flow already exists, and simulation is used to enhance it.

2. A new system is being designed, and simulation helps determine the optimal process flow before implementation.

In this study, the first scenario is focused on optimizing an existing technological flow to improve the production layout. The primary objective is to determine the number of parts that can be processed within a specified time frame while assessing equipment utilization levels. FlexSim is utilized as the primary tool for this analysis.

Figure 6, presents a flowchart illustrating a specific simulation scenario aimed at improving the production layout. The components of this scenario and their interactions are as follows:

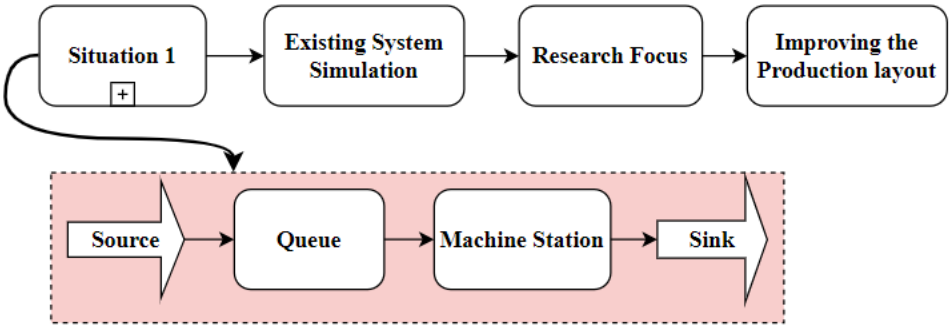

Figure 6 Diagram Showing the Technological Flow of Processes to Be Modeled

Situation 1: This stage represents the initial scenario where the current technological flow is

simulated to identify areas requiring improvement. The model includes essential elements such as sources, queues, machine stations, and sinks.

Existing System Simulation: The current system is simulated to gather performance data and identify bottlenecks or inefficiencies.

Research Focus: The simulation results are analyzed to pinpoint specific areas for improvement. This step provides a deeper understanding of the system's current state and evaluates the potential impact of modifications.

Improving the Production Layout: Based on research findings, modifications are applied to enhance efficiency and productivity. These changes are guided by insights gained from the simulation and statistical evaluations.

By systematically following the FlexSim simulation methodology, production layouts are successfully enhanced, and system efficiency is improved. The structured approach ensures that potential bottlenecks are identified early, allowing for targeted optimizations to be implemented. Ultimately, this results in reduced production times, lower costs, and better resource utilization, making FlexSim an invaluable tool for manufacturing system analysis and optimization.

3 Selective Laser Sintering (SLS) Mapping and Simulation

3-1 Process Description

SLS is an innovative AM process where a powerful laser selectively melts powdered materials like plastics, metals, or ceramics to form solid objects. It is widely used in both prototyping and large-scale production due to its ability to create detailed and accurate geometries without requiring additional support structures. The SLS process includes several crucial stages, such as powder preparation, laser sintering, recoating, cooling, and post-processing, each playing a key role in ensuring the final part meets the required quality [107].

The process begins with the even distribution of a fine powder layer across the build platform. The material—typically a thermoplastic, metal, or ceramic—is preheated to just below its melting point to improve sintering efficiency. Once the layer is prepared, a laser scans across the powder bed, fusing particles together at specific locations based on the digital part design. The laser energy causes the powder to partially melt and bond, forming the object layer by layer. After each layer is sintered, the build platform lowers slightly, and a new powder layer is deposited. This recoating and sintering cycle continues until the part is fully built.

Once printing is complete, the part is allowed to cool within the powder bed, which helps minimize warping and preserve dimensional accuracy. The cooling period may last several hours, depending on the material and part geometry. After cooling, the part is carefully removed, and any unused powder is collected for reuse.

Post-processing is a vital phase of the SLS workflow. Once removed from the powder bed, excess powder is cleaned off, and further treatments may be applied to improve mechanical properties or surface finish. These secondary operations can include annealing, polishing, or surface coating. Finally, the parts undergo quality checks to ensure compliance with specifications related to geometry, finish, and mechanical strength [108].

The quality and efficiency of the SLS process are affected by several factors, including the material properties, build time, and energy usage [109]. The type of powder selected significantly affects the mechanical strength, surface quality, and functional performance of the printed parts. Build times vary depending on the size and complexity of the design, while energy consumption remains a critical factor due to the sustained heating required for both sintering and cooling [110]. Effective

post-processing, such as powder removal and finishing, is equally important to ensure the production of high-quality parts.

SLS presents several advantages, such as enabling the production of complex geometries without the need for support structures, which increases design flexibility [111]. It also supports a broad array of materials, making it adaptable for industries like aerospace, automotive, and healthcare. Parts produced through SLS tend to have excellent mechanical properties and dimensional accuracy. However, challenges such as the cost of high-quality powders, part warping, and the degradation of unused powder over time can affect production costs and part quality.

To further advance the application of SLS in large-scale production (LSP), this research introduces a DES methodology designed to address the complex dynamics of SLS manufacturing in a large-scale environment. The complexity inherent in SLS LSP stems from the interplay of various factors, such as the manufacturing layout, material properties, and production schedules. These elements create a challenging environment that demands an advanced simulation framework to facilitate efficient analysis and optimization.

The proposed DES model utilizes a modular approach, simulating discrete events and activities that occur within the SLS LSP environment. The study focuses on modeling the setup and processing times in a Selective Laser Sintering case study, exploring how variability in machine and operator numbers affects cost reduction and production output. By incorporating hypothetical elements that emulate uncertainties typically found in large-scale manufacturing, the simulation remains robust and adaptable, offering valuable insights into potential production bottlenecks, resource utilization, and viable optimization strategies.

This research contributes to the advancement of SLS LSP by providing a scalable and practical simulation methodology for performance evaluation and operational improvement. One of the core goals is to propose strategies for improving production throughput through the optimization of layout design and process parameters. To achieve this, the study references the production system described in [112], with a focus on optimizing workstation configurations and integrating additive manufacturing technologies like SLS.

As part of this investigation, a prototype production layout is designed, leveraging selected 3D printing methods to improve the efficiency of SLS workflows within a hypothetical simulated manufacturing setting. The outcomes of this research aim to establish clear, actionable guidelines for developing efficient production environments. This contributes not only to the enhancement of SLS-

based systems but also to the broader objective of boosting the operational efficiency and industrial viability of additive manufacturing technologies.

3-2 Case Study

To begin the optimization process, it is essential to simulate the reference model using FlexSim. This baseline simulation is based on the production plan described in [167], which aims to produce 20,000 parts annually. The reference model incorporates several key assumptions that define the constraints and operational parameters of the system:

- Each SLS machine is capable of printing eight parts simultaneously.
- The production system operates for 250 working days per year.
- The production schedule consists of two shifts per day.
- The work breaks are assumed to occur daily from 12:00 to 12:30 PM.

The recommended number of machines, their setup, and processing time are displayed in Table 1, along with the number of machines required, calculated using a specific formula. The optimization process involves determining the most efficient machine utilization while maintaining the required output of 20,000 parts annually. Table 1 visually illustrates the factory layout, emphasizing key areas for processing, material storage, and workflow efficiency.

Table 1 Recommended Machinery from ref [112]

Machine Names	Quantity	Setup Time (min)	Process Time (min)
Powder Mixing	2	10	15
Sifter	1	10	5
SLS Device	4	30	320
Cabin Sandblaster	1	10	5
Grinder	2	15	8
Varnishing	1	10	5
Packing Station	2	10	7

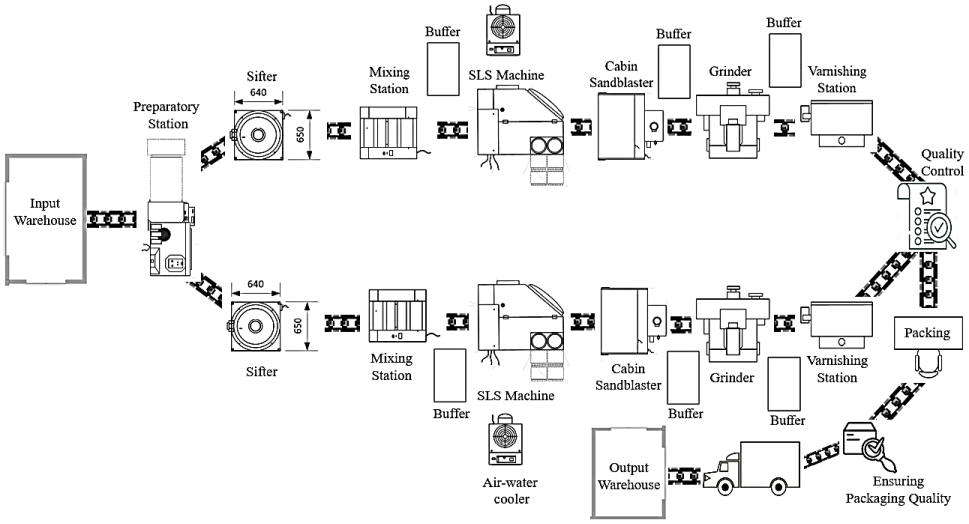

Figure 7 Exemplary Layout Plan for 3D Printing Machines and Devices, modified from [112].

The layout plan has been meticulously designed to optimize workstation efficiency by ensuring a streamlined and logical sequence of manufacturing operations. The design ensures product receipt on one side of the production hall and material supply on the opposite side. By structuring the layout in this manner, the facility promotes continuous material flow, reduces unnecessary movement, and increases overall operational efficiency. The aim is to establish a highly productive and well-organized work environment, ultimately improving the performance and productivity of the manufacturing plant.

3-3 BPMN Mapping

A Business Process Model and Notation (BPMN) diagram is used to visually represent the business processes. BPMN's visual approach helps identify and address issues such as infinite loops, ensuring correctness and coherence in process descriptions [113]. The SLS production process is depicted in Figure 8, providing a clear and comprehensible visual representation of the layout and workflow. This facilitates better understanding and clarity in the process description.

The production simulation task consists of three basic phases, as follows (Figure 8).

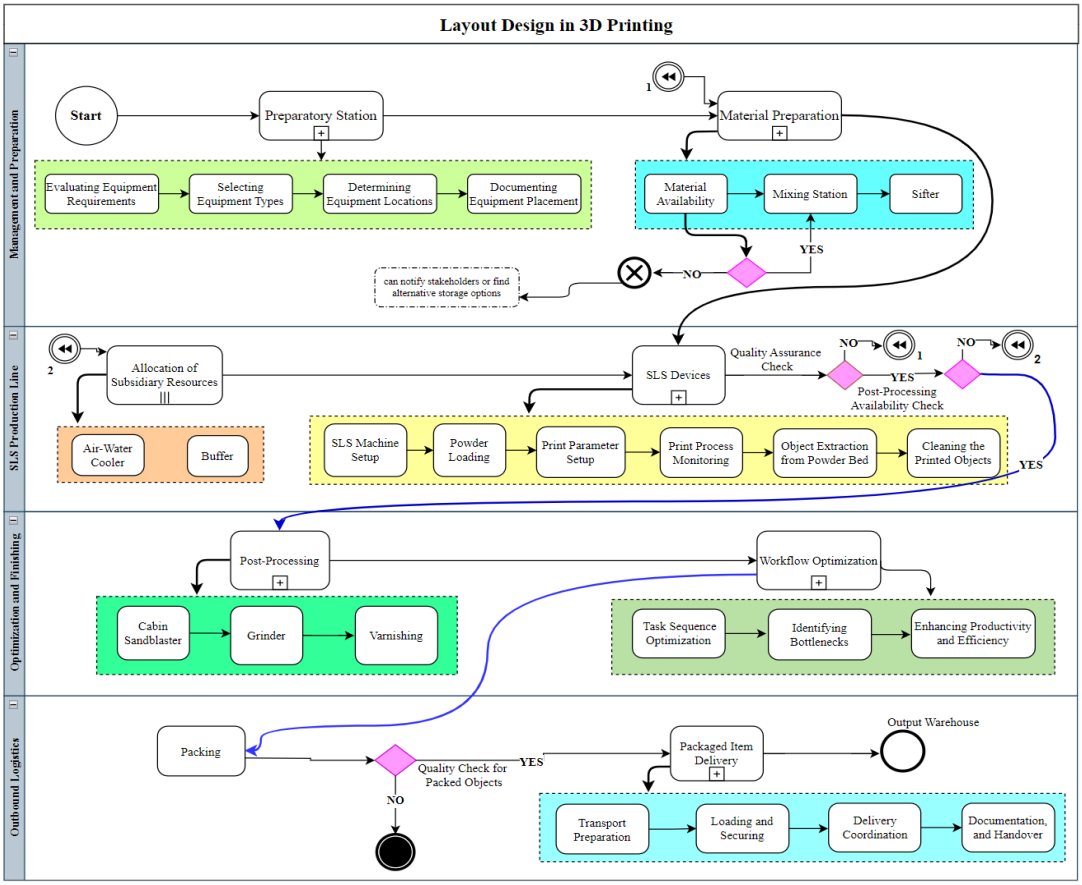

Figure 8 BPMN Diagram of the SLS Workflow

Preprocessing: First, the process begins in the first swim lane where activities progress sequentially. The first stage involves the preparatory station, encompassing tasks such as equipment evaluation, selection, positioning, and documentation. After completing these steps, the process proceeds to the material preparation station. Here, activities include checking material availability, preparing materials at the mixing station, and using the sifter.

A gateway follows the material availability check. If materials are available, the process continues; if not, the workflow ends, as indicated by a thick-lined circle symbol with a cross inside, representing the end event cancel symbol. A text box notes that stakeholders can be notified, or alternative storage options can be found. All tasks are represented with rectangles with rounded corners, indicating activities performed as part of the process. Sub-processes are shown with rectangles with a plus sign (+) at the bottom, signifying complex activities that can be detailed further.

Processing: This section focuses on the SLS procedure. The SLS Device is considered a key component of the manufacturing process. It is designed to work seamlessly with Industry 4.0 environments, making it a forward-looking production platform. The SLS technique, developed by

Desktop Manufacturing Corporation [114], uses a laser beam to solidify powdered materials layer by layer. A 3D CAD model is loaded, converted to STL format, and then sliced into layers [114]. Before laser sintering, plastic powder is placed and heated, causing the powder to fuse selectively by the cross-section of the model. After printing, the product is cleaned and may go through finishing procedures like varnishing and sandblasting [115]. The use of 3D printing equipment, such as the EOS GmbH FORMIGA P 110 and related support equipment, at a recently built facility is the basis of this process. The SLS technique is used by these devices [116].

After the material preparation station is completed, the process moves to the SLS machine station. This station consists of several subprocesses that must all be completed: SLS Machine Setup, Powder Loading, Print Parameter Setup, Print Process Monitoring, Object Extraction from the Powder Bed, and Cleaning the Printed Objects. Following these subprocesses, a gateway ensures quality assurance. If the quality check is successful, it proceeds to another gateway for the post-processing availability check. If this is also successful, the process moves to the next pool, the post-processing station. If the quality check gateway result is "no," the process returns to the material preparation station. However, if the post-processing gateway result is "no," the process returns to the buffer in the subsidiary resources station. In this scenario, a double-lined circle with two arrows inside the symbol indicates waiting for the necessary conditions before continuing. Before the SLS station, subsidiary resources are allocated. This task is represented by a rectangle with three vertical lines at the bottom, indicating that it is performed multiple times in parallel. This includes subprocesses such as the air-water cooler and buffer, which are operated in parallel with certain stations, including the SLS station.

Post-processing: After being moved to the post-processing station, subprocesses such as the cabin sandblaster, grinder, and varnishing must be completed. Once these are finished, the process transitions to workflow optimization, which involves subprocesses like task sequence optimization, bottleneck identification, and productivity and efficiency enhancement.

Upon completing workflow optimization, the process proceeds to the final pool, the packing station. A gateway is placed after packing to check the quality of packed objects. If the quality check is successful, the process moves to the packaged item delivery station, which includes subprocesses like transport preparation, loading and securing delivery coordination, and documentation and handover. After completing these steps, the process ends at the output warehouse, indicated by a thick-lined circle symbol representing the end event. However, if the quality check in the packing station fails, the process terminates, represented by a circle with a thick black outline and a solid

black interior, indicating a termination event.

3-4 FlexSim Model

In FlexSim, modeling and simulating a technological flow (a system) involves several basic steps:

- Create a layout using library objects.
- Make port connections.
- Edit the look and behavior of objects.
- Run the simulation.
- View the results.

The main topic of this study is the layout plan of a reference production line, designed to meet the processing requirements of FlexSim software. The model requires 21 processors, 4 temporary storage spaces, 1 pallet temporary storage zone, and 1 input and output warehouse.

In the model, a source is used to generate workpieces. Before any operation, the workpieces wait in a queue to be processed. Therefore, a queue is placed before each operation. Materials are routed from the input warehouse to the powder selection buffer, and the powder is then fed into the powder mixing machines for blending once the setup is complete. After the processing time, the mixture is transferred to a sifter machine, which separates larger grains from smaller ones.

Figure 9 presents the layout created in FlexSim, reflecting the technological flow of the processes being modelled.

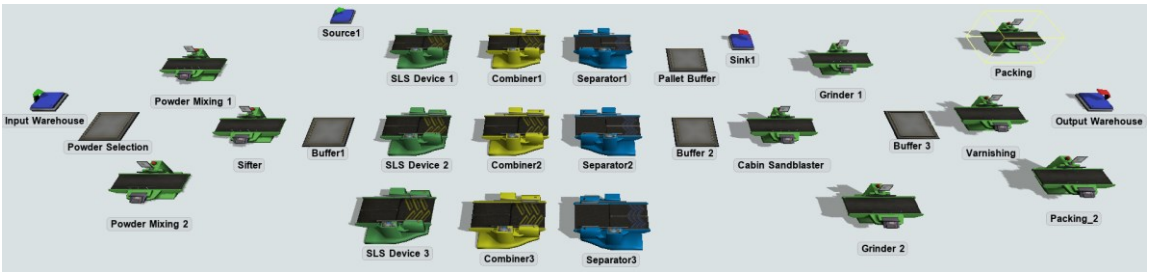

Figure 9 Layout create in FlexSim.

To ensure that workpieces (flow items) move according to the technological flow, connections between the ports must be established. Figure 10 illustrates the connections between resources in the

FlexSim simulation model, which is based on the reference layout [112]. Building the model and accurately adjusting its parameters are crucial for the success of the simulation.

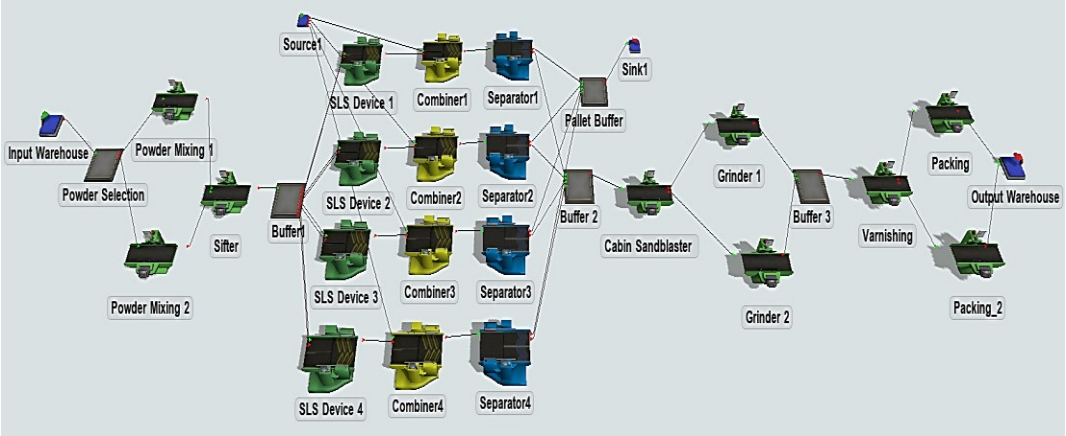

Figure 10 FlexSim Simulation Model of the Ref [112] Production Line

Following this, the layout was designed with the optimal number of machines, as shown in Figure 11. The parameters, which are explained in detail subsequently, were thoroughly checked to ensure optimal performance.

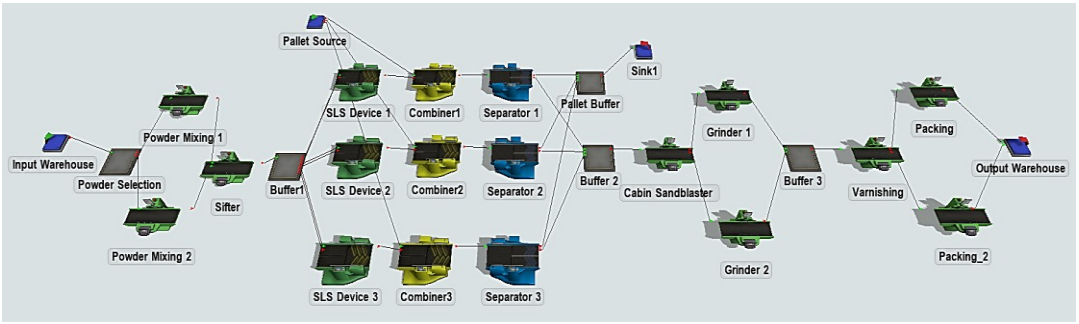

Figure 11 Optimized Production Line Layout with Optimal Number of Machines

To establish a connection between objects, follow these steps:

1. Use the Toolbar: The toolbar provides several options, including the frequently used 'Connect Object' option, as shown in Figure 12 This option is essential during modeling to define the types of connections.

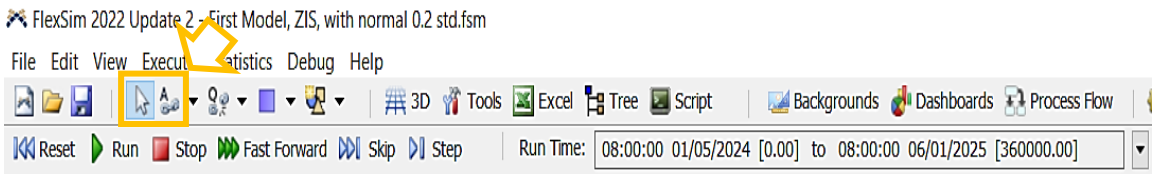

Figure 12 Connections Between Resources

Simply placing the desired objects in the FlexSim simulation space is not sufficient to make the model functional. Necessary connections between these objects must be created. Use the Connection Section in the Toolbar:

- **Connect Objects:** This mode is used to connect fixed resource objects.
- **Connect Center Ports:** This mode is used to connect task executors to fixed resources. For example, if you define an operator or a dispatcher for a processor object and want to assign them to your processes, you must use this type of connection (as shown in Figure 13(a)).
- **Disconnecting Connections:** If you need to disconnect these connections, use the 'Q Disconnection' option, following the same method explained for connecting objects (as shown in Figure 13(b)).

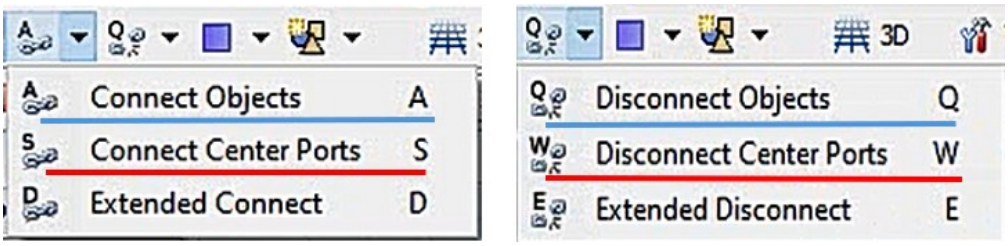

Figure 13 (a, b): Creating Functional Connections in FlexSim

Note: In the model simulated using FlexSim software, only the 'Connect Objects' connection was employed, as no task executors are included.

In a model, the first step involves adding a source, which is essential for the model's creation. This source is used as the initial storage for raw materials. In Figure 14, the process of editing this object is illustrated.

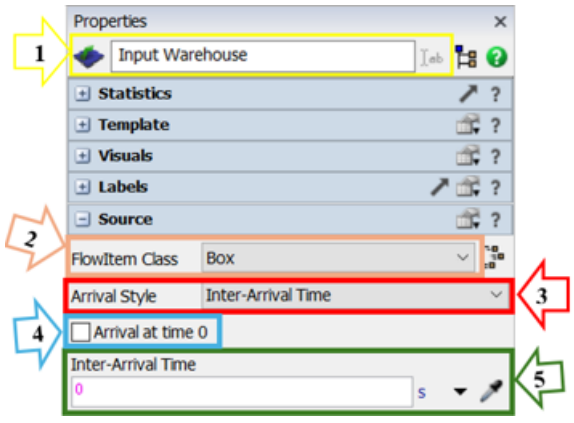

Figure 14 Setup the properties for the source

1. Object Name: Assign a name to the object. For example, in this model, the source is named “Input Warehouse”.

The following properties are unique to the source and do not exist in other objects:

2. Flow Item Class: Specifies the type of material used, such as a box, pallet, or tote.

3. Arrival Style: Defines how parts enter the system. In this model, Inter-Arrival Time is selected, meaning arrivals are based on time intervals. Other options include “Arrival Schedule” (based on a predefined timetable) and “Arrival Sequence” (based on a specified order).

4. Arrival at Time 0: If selected, the first flow item enters the simulation at time zero. This option is enabled in the model.

5. Inter-Arrival Time: Specifies the arrival time for parts in the model. Clicking the triangle next to the box allows selection from various options, such as predefined distributions or a fixed value.

Next, two processor machines labeled Powder Mixing are added. As shown in Figure 15, double-clicking on a machine opens a new window displaying its object properties. In the statistics section, various aspects of the machine’s operation can be observed:

1. Machine State: Indicates whether the machine is idle, processing, etc.

2. Throughput: Displays input and output quantities.

3. Contents: Shows the current quantity of items in the machine.

4. Stay Time: Provides maximum, minimum, and average waiting times.

These properties apply to all processor objects used in the FlexSim model.

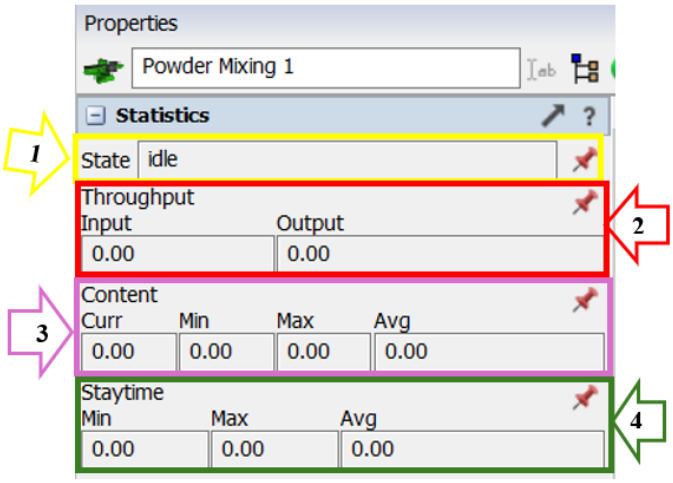

Figure 15 Processor Machines Properties in FlexSim

Next, the Visuals section in the machine's Properties Panel is explored, as shown in Figure 16.

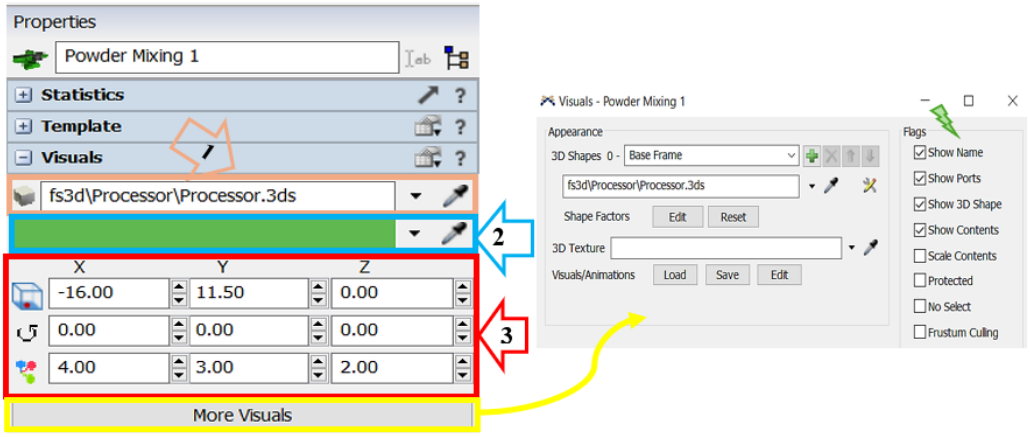

Figure 16 Visuals Customization in the Properties Panel

1. Appearance: Modify the machine's appearance by clicking the small triangle next to the “Card” to select from pre-made figures provided by the software or click Browse to upload a custom figure.

2. Colour: Adjust the machine's color.

3. Size: Modify the machine's position along the X, Y, and Z axes, rotate it, and resize it as needed. Additionally, clicking "More Visuals" opens a new window for further adjustments, such as unchecking the "Show Name" box to hide machine names.

Figure 17 illustrates the setup of properties for the machining process. For example, in the powder mixing process, the setup time is fixed at 10 minutes, while the process time follows a normal distribution with a mean of 15.0 minutes and a standard deviation of 3.0 minutes.

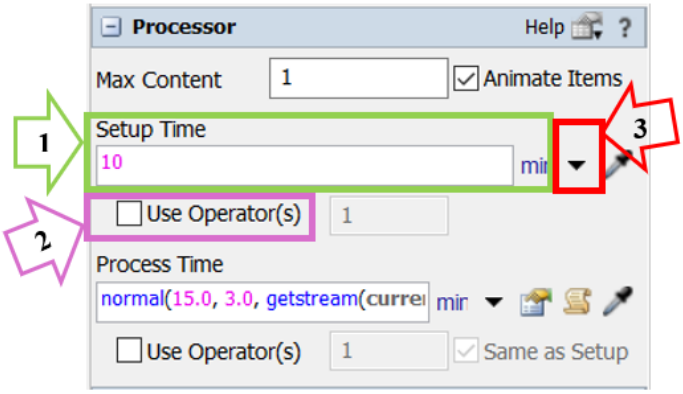

Figure 17 Configure Machine Processing Properties

1. Processing Time: In the Settings section, the processing time for the machine is configured. Next to this section is the Time Units area, where the desired time units can be specified.

2. Use Operator: Selecting the "Use Operator" checkbox indicates that an assigned operator is required to perform the task.

3. Time Units Options: Clicking the triangle next to Time Units opens a window with multiple options (arrow 3), including the "Statistical Distribution" option, which allows selecting a suitable distribution model.

Note: In this model, machine processing time is evaluated in two ways: first, using a fixed value, and second, by setting the standard deviation to 20% of the mean value.

This section is labeled "Output" and provides three primary options, as illustrated in Figure 18:

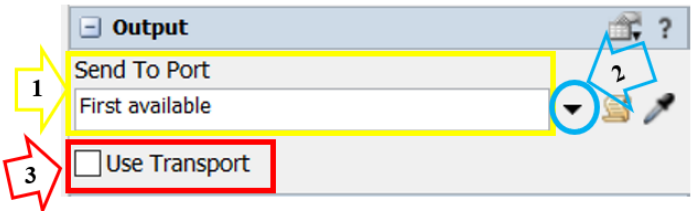

Figure 18 Configuration Options for Output Distribution

1. Send to Port: Determines how content is distributed. For example, selecting "First Available" directs content to the first idle machine. Other distribution methods are also available. In this model, a buffer is placed before the SLS machine, utilizing FlexSim's "Round Robin if Available" setting at the buffer's output. This ensures that content is sent sequentially to available machines, balancing the workload and optimizing resource utilization.

2. By Percentage: Clicking the triangle icon reveals an option to specify percentages for defective and healthy parts. This option is not used in this model.

3. Transporter Requirement: Selecting this option indicates that a transporter is required to move the content.

Note: The described machine settings apply to all equipment, including Powder Mixing machines, sifter machines, cabin sandblasters, grinders, varnishing machines, and packing systems.

Before any operation or process, items must wait in a queue to be processed. In this model, multiple queues are designated to prevent bottlenecks in the production line. While most settings for this object are similar to others, there are specific distinctions, as illustrated in Figure 19:

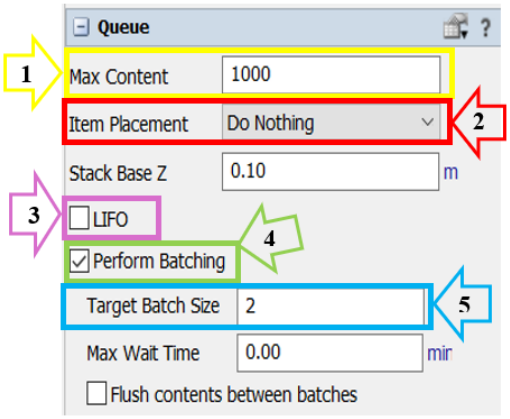

Figure 19 Queue Configuration Settings

1. Maximum Content: Specifies the maximum number of parts the queue can hold at any given time. In this model, the maximum is set to 1,000 parts, aligning with the software's default recommendation, which effectively meets the requirements.

2. Item Placement: Determines how items are arranged within the buffer. Selecting "Do Nothing" minimizes the visual representation of items in the buffer, simplifying the display without affecting functionality.

3. LIFO (Last In, First Out): Enabling this option ensures that the most recently added item is the first to be processed and exit the queue. By default, this model uses FIFO (First In, First Out), where the first item to enter the queue is processed first.

4. Perform Batching: Activating this feature allows items to be sent in batches according to specified settings.

5. Batch Size: Defines the number of items in each batch sent to the next machine. For instance, setting the batch size to 5 means that items will be sent in groups of five.

In this model, all buffers use the default maximum content settings provided by the software, except for the buffer preceding the SLS machine. This buffer is set to a maximum content of 50,000 to accommodate the SLS machine's processing time and prevent bottlenecks.

It is important to note that all machines in this model are of the Processor type, except for the SLS machine, which is a Combiner type. Processor machines handle parts individually, whereas the SLS machine processes eight parts simultaneously, necessitating the use of a combiner, as shown in Figure 20.

To facilitate this process, a single source is established to supply pallets for the machines. The combiner receives the required parts from the buffer before the machines and, once the batch is ready, sends it to the next machine in groups of eight. The combiner is configured to operate in Batch Mode.

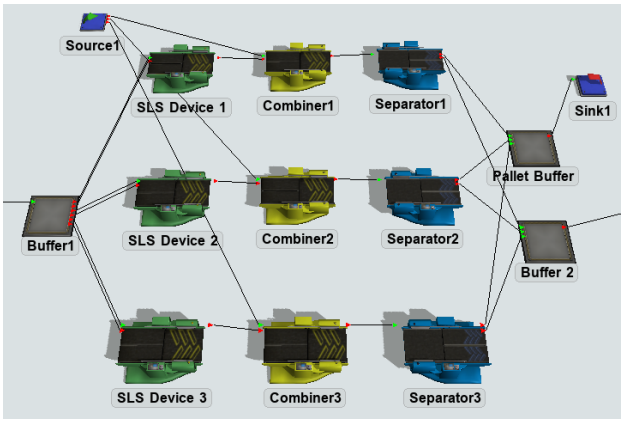

Figure 20 Configuration of the SLS Machine

The machine following the combiner is the Separator, which is set to Unpack Mode. Since this setup is not directly supported by the software, an additional combiner is placed between the combiner and the Separator. The second combiner's role is to receive the parts from the SLS machine in batch form, pack them, and then send them to the Separator machine for unpacking.

In the Separator machine, the products are separated, and two buffers are placed afterward: one to receive the processed parts and another to collect the pallets. These pallets are removed from the workspace and sent for reuse in the next production line.

This explanation outlines the configuration of the model. The setup of the combiner machine, as

implemented in the model, is illustrated in Figure 21.

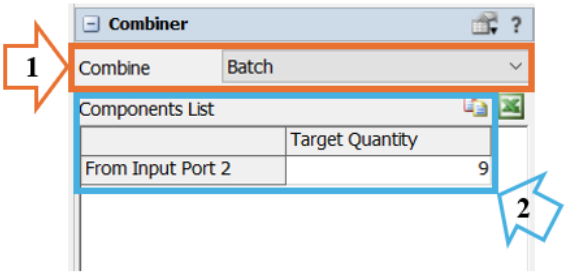

Figure 21 Combiner layout

To operate the combiner machine, at least two inputs are required, which is a fundamental rule for using the combiner. The settings for the combiner machine are similar to those of other machines, except for the Combine Mode.

1. Combine Mode: There are three formats for the combine mode: batch, pack, and join.

- Pack: In this mode, a specified number of parts enter the machine together, but they exit the machine one by one.
- Batch: In this mode, the same number of parts that enter the machine exit together as a batch.
- Join: This mode merges parts into a single item. Unlike the batch and pack modes, which allow for the items to be unpacked later, the join mode permanently combines the parts into a single unit that cannot be unpacked.

2. Component List: Specifies the number of parts and components (such as pallets) that will exit the combiner machine. For example, if '9 parts' and '1 pallet' are entered, it means that 9 parts will exit along with one pallet that entered the machine.

Next, the parts move to the cabin sandblaster, where they undergo a procedure using highly accelerated abrasive compounds. This process enhances the overall finish of the parts by smoothing uneven surfaces and removing surface defects. Afterward, the parts are moved to the grinder station. Here, the surface polish is improved, any remaining support structures or build platform attachments are removed, and any dimensional errors from the printing process are corrected. This meticulous procedure ensures that the parts meet the necessary quality standards before moving to the next stage.

Following this, the parts are queued to prevent bottlenecks and then proceed to the varnishing

station, where they receive a layer of decorative or protective varnish. The parts are cleaned and, if needed, prepped before coating to ensure an even application. After drying or curing, thorough quality inspections are performed before the parts are packaged for storage or further processing.

Finally, the parts move to the packing station. Here, they are packaged according to standardized procedures and then delivered to the output warehouse for distribution.

Once the model is configured according to the reference situation, the simulation can be run. To initiate the simulation, the simulation period must be established, which in this case is set to 250 days.

As previously stated, the main objective is to find the optimal number of machines by exploring different scenarios to enhance production. These scenarios are designed to determine the required number of SLS, sifter, cabin, varnishing, and packing machines to reach output levels that match or surpass the reference [112].

Before running these scenarios, it is essential to assess the feasibility of adjusting the number of SLS machines. To do this, the reference layout design serves as the foundation for evaluating the performance of the SLS machines. A low machine utilization rate indicates the potential to reduce the total number of SLS machines. The optimal number of SLS machines determined through this evaluation is then used to define the scenarios.

Handling bottlenecks and equipment configurations are crucial aspects of manufacturing processes that significantly impact production efficiency. To improve production line productivity, eliminate bottlenecks, and maximize equipment utilization, it is vital to examine variables such as processing time, blocking time, and idle time [117]. The final system model aims to enhance equipment usage while minimizing idle times. A key step in assessing the production line's operational state involves evaluating the number of SLS machines in operation.

In the study, the initial test's machine count was set according to the guidelines in the article. The output was calculated using four SLS machines over 250 days. In the second test, the number of SLS machines was reduced to three, while all other machine quantities were kept consistent with the article's specifications. The objective was to determine the output within the same 250-day period. Similarly, in the third iteration, the number of SLS machines was further reduced to two, while the other machine quantities were maintained as specified in the article.

Four key parameters—the sifter, cabin sandblaster, varnishing, and packing machines—were used to

determine the number of additional machines in the FlexSim model. For each of these parameters, both lower and upper limits were set to explore various scenarios within FlexSim's flexible framework. Specifically, cabin sandblaster machines range from 1 to 3, sifter machines from 1 to 2, varnishing machines from 1 to 3, and packing machines from 1 to 2. By analyzing the output from the best-performing SLS configuration, as examined in the next section, the optimal number of these machines was identified.

Table 2 Scenarios for Machines

Scenarios #	**1**	**2**	**3**	**4**	**5**	**6**	**7**	**8**	**9**	**10**	**11**	**12**	**13**	**14**	**15**	**16**	**17**	**18**
Cabin Sandblaster	1	1	1	1	1	1	1	1	1	1	1	1	2	2	2	2	2	2
Sifter Machine	1	1	1	1	1	1	2	2	2	2	2	2	1	1	1	1	1	1
Varnishing Machine	1	1	2	2	3	3	1	1	2	2	3	3	1	1	2	2	3	3
Packing Station	1	2	1	2	1	2	1	2	1	2	1	2	1	2	1	2	1	2
Scenarios #	**19**	**20**	**21**	**22**	**23**	**24**	**25**	**26**	**27**	**28**	**29**	**30**	**31**	**32**	**33**	**34**	**35**	**36**
Cabin Sandblaster	2	2	2	2	2	2	3	3	3	3	3	3	3	3	3	3	3	3
Sifter Machine	2	2	2	2	2	2	1	1	1	1	1	1	2	2	2	2	2	2
Varnishing Machine	1	1	2	2	3	3	1	1	2	2	3	3	1	1	2	2	3	3
Packing Station	1	2	1	2	1	2	1	2	1	2	1	2	1	2	1	2	1	2

Furthermore, an analysis was performed to evaluate the impact of applying a distribution function to the deterministic processing time values shown in Table 2. It was assumed that the distribution followed a normal distribution, with the mean values aligned with those in the reference, and the standard deviation set to 20% of the mean (std = mean * 0.2).

3-5 Model's Results and Discussion

The production rate obtained from constructing the model using data from the reference model precisely matched that of the reference model. Consequently, the validation process was successfully completed.

Table 3 presents the results of the simulation experiments, which were conducted in two formats: one using a fixed processing time and the other incorporating a distribution for processing time (std = mean * 0.2). As shown in the table, the differences between the results of these two approaches were minimal.

Table 3 SLS layout Output Comparison

Experiment Number	Number of SLS Machines	Parts Produced in 250 Day	
		Without distribution	With distribution
1	4	23,438	23,309
2	3	23,446	23,315
3	2	18,094	18,003

After 250 days, utilizing four SLS machines resulted in a total production of 23,438 parts. According to FlexSim, the equipment utilization rates for SLS machines 1, 2, 3, and 4 are displayed in Figure 22(a), with processing times of 58%, 57.97%, 57.96%, and 57.96%, respectively. Furthermore, the collection percentages for these machines are recorded as 33.86%, 32.68%, 33.90%, and 32.68%.

A probability distribution analysis of the four SLS machines indicates a total output of 23,309 parts. The collection percentages for SLS machines 1, 2, 3, and 4 are 33.15%, 33.44%, 33.87%, and 33.09%, while their processing times are 58.04%, 57.79%, 57.37%, and 58.14%, as illustrated in Figure 22(b).

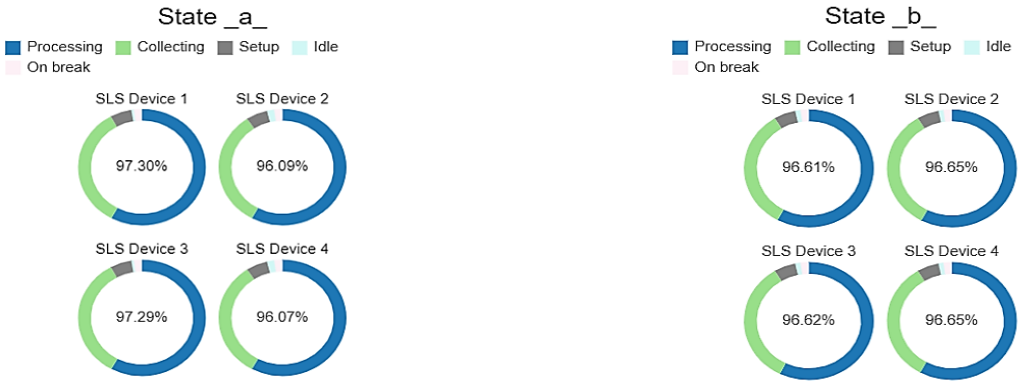

Figure 22 Production Analysis for 4 SLS Machines in 250 Days: (a) Fixed Processing Time, (b) Distribution-Based Processing Time

In a subsequent test utilizing three SLS machines with distribution-based processing, a total of 23,315 parts were produced. The equipment utilization rates for this scenario are depicted in Figure 23(b), with machine processing times recorded at 76.76%, 76.78%, and 76.77%, and corresponding collection percentages of 13.72%, 13.71%, and 13.71%.

In contrast, when fixed processing times were applied, as shown in Figure 23(a), the equipment utilization rates resulted in collection percentages of 13.32%, 13.34%, and 13.37%, with machine processing times of 77.33%, 77.31%, and 77.27%.

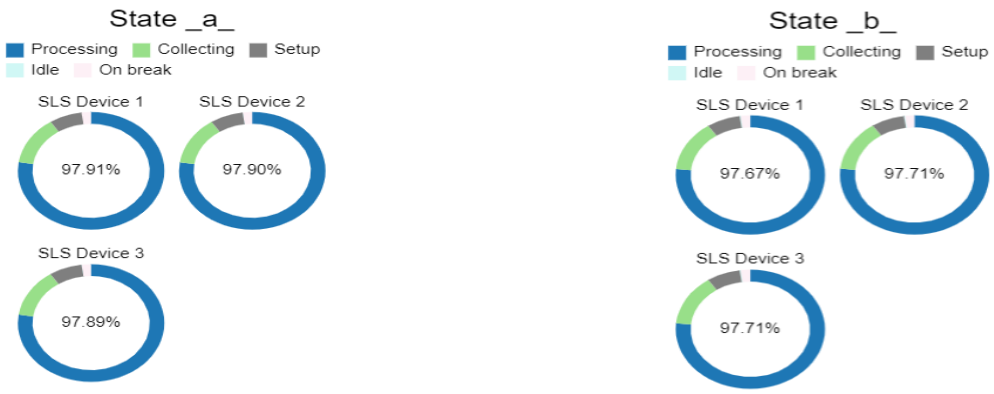

Figure 23 Production Analysis for 3 SLS Machines in 250 Days: (a) Fixed Processing Time, (b) Distribution-Based Processing Time

When the study was extended to a scenario with only two SLS machines, a total of 18,094 parts were produced over 250 days. A similar experiment, incorporating a normal distribution for processing times with the same parameters, yielded 18,003 parts. This outcome is not ideal, as it falls significantly short of the production target.

A thorough analysis confirms that three SLS machines provide the most effective configuration. The results, whether based on fixed or distribution-based processing times, exhibit minimal variation, reinforcing the conclusion that three machines offer the optimal balance. This setup ensures adequate production over the 250-day period while enhancing daily operational efficiency. Moreover, operating three machines is more cost-effective than using four, as it maximizes output without requiring additional equipment, making this configuration the most economical option.

The State Gantt chart in Figure 24 visualizes the operational states of the three SLS machines over a 48-hour period. Each state is represented by different colors: processing time (orange) indicates active production while collecting (pink) represents material handling after processing. Setup (purple) covers preparatory tasks like calibration, and idle time (light blue) shows periods of inactivity. Blocked time (light red) highlights operational interruptions, whereas on break (cream) denotes scheduled downtime for maintenance or operator breaks.

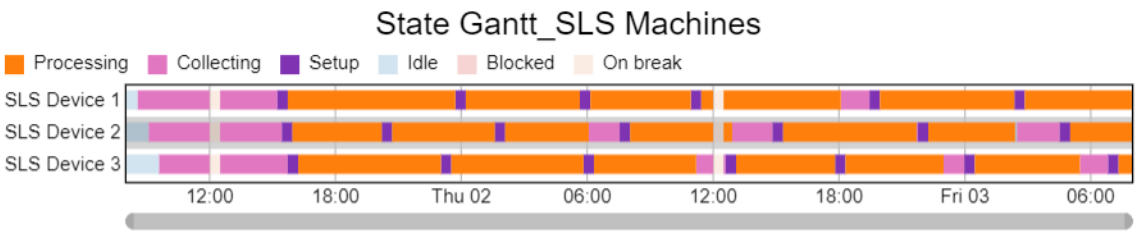

Figure 24 Operational State Gantt Chart of SLS Machines

The chart monitors the three devices over a two-day period, illustrating their operational cycles and downtimes. SLS Device 1 demonstrates consistent processing activity with minimal idle or blocked states. In contrast, SLS Device 2 experiences slightly higher idle and collecting times, possibly due to variations in processing complexity. SLS Device 3 exhibits longer setup and idle periods, indicating more frequent or extended setup requirements. This Gantt chart offers a comprehensive overview of machine efficiency and downtime patterns, aiding in the identification of bottlenecks and opportunities for optimization. By addressing blocking issues, extended setup durations, and idle periods, the overall performance of the SLS machines can be enhanced.

The objective is to track the flow of items entering the sink (output warehouse). Figure 25 presents three tables displaying the throughput of the Output Warehouse over consecutive time intervals: one day, two days, and three days. These tables illustrate the cumulative output over time, providing a clear insight into the warehouse's productivity.

Output First Day

Object	Throughput
Output Warehouse	44

Output for Two Days

Object	Throughput
Output Warehouse	136

Output for Three Days

Object	Throughput
Output Warehouse	228

Figure 25 Throughput Analysis of the Output Warehouse Over Three Days

On the first day, the warehouse processes 44 parts, establishing a reference point for daily performance. By the second day, throughput rises to 136 parts, reflecting an increase of 92 parts, which suggests consistent productivity or enhanced efficiency. By the end of the third day, the total throughput reached 228 parts, with an additional 92 parts processed. The steady increase in throughput (92 parts per day after the first) indicates stable and predictable operations over the three days.

The warehouse maintains a steady and predictable output rate, showcasing efficient operations without significant delays. This information offers valuable insights into system performance and productivity patterns, aiding in the identification of opportunities to enhance resource allocation or scheduling for improved throughput.

Figure 26 presents an analysis of Staytime data for various parts throughout a 250-day operational cycle. The tables summarize key metrics, including average, minimum, and maximum Staytime, offering a detailed overview of different stages within the system.

Staytime_ A

Object	Avg Staytime	Min Staytime	Max Staytime
Buffer1	37.32	0	276.83
Buffer 2	198.10	0	487.85

Staytime_ B

Object	Avg Staytime	Min Staytime	Max Staytime
Powder Selection	308.05	0	345.41
Buffer 3	19.82	0	116.59

Figure 26 Staytime Performance: Buffer Analysis in Manufacturing Process

In the 'Staytime_A' table, Buffer 1 has an average Staytime of 37.32 parts, with values ranging from 0 to 276.83 parts. This variation indicates that while some tasks pass through quickly, others experience considerable delays. In contrast, Buffer 2 has a significantly higher average Staytime of 198.10 parts, with a maximum of 487.85 parts, suggesting a broader range of task durations and a higher likelihood of bottlenecks.

The 'Staytime_B' table provides insights into the Powder Selection process and Buffer 3. The Powder Selection stage records an average Staytime of 308.05 parts, with a maximum of 345.41 parts, highlighting it as a critical stage with extended processing times. Meanwhile, Buffer 3 exhibits the shortest average Staytime at 19.82 parts, with a maximum of 116.59 parts, indicating a more efficient flow compared to other areas of the system.

Overall, the staytime analysis reveals notable differences in processing durations across various manufacturing stages. Extended staytimes in Buffer 2 and the Powder Selection process suggest potential bottlenecks that could impact overall efficiency. Conversely, Buffer 3 demonstrates higher efficiency with its shorter staytimes. These findings offer valuable insights into areas where adjustments in buffer management and resource allocation could enhance operational performance.

The variation in Work-In-Progress (WIP) over time is monitored using a line chart to visualize this dynamic. The number of items in Buffer 2 is depicted as a continuous line, revealing a fluctuating pattern due to the probabilistic nature of machine timings. Figure 27, titled 'Content vs Time,' illustrates these changes over three days. The horizontal axis represents time, while the vertical axis indicates the WIP level in Buffer 2, ranging from 0 to 30 parts.

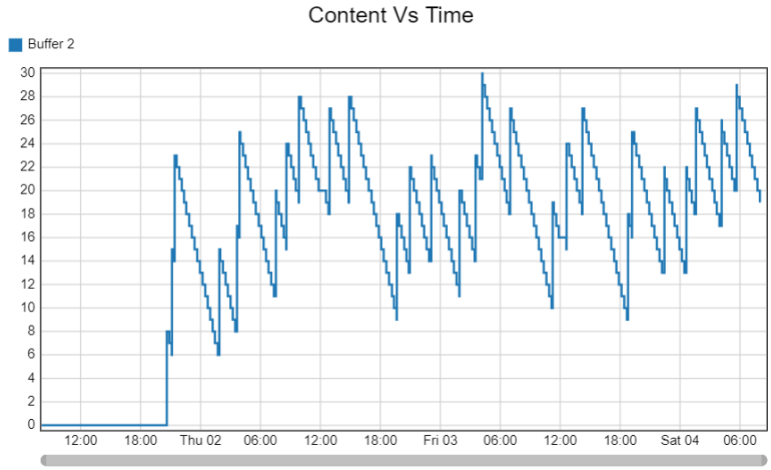

Figure 27 Temporal Analysis of Work-In-Progress (WIP) Levels in Buffer 2

At the beginning of the period, up until around 18:00 on the first day, the buffer content remains at zero, indicating no accumulation or processing activity. This is followed by a sharp increase to approximately six parts, suggesting a sudden influx of material or data into the buffer. Subsequently, the content level exhibits a sawtooth pattern, characterized by alternating rises and drops, reflecting a repetitive cycle of accumulation and depletion. The fluctuations occur consistently, with the buffer content peaking at approximately 26 parts before declining again.

This sawtooth behavior indicates a system in which material or data is introduced in discrete amounts and subsequently consumed or processed at regular intervals. Such a pattern is typical in batch processing or buffer management systems, where content is periodically replenished and utilized in a controlled manner.

Overall, the graph demonstrates the dynamic regulation of buffer capacity over time, highlighting periodic accumulation and reduction. This behavior is particularly relevant in real-time data processing and manufacturing operations, where maintaining steady input-output cycles is crucial for system efficiency. The consistent rise and fall of buffer content suggest a well-balanced process in which a stable inflow is counteracted by regular consumption or processing.

Table 4 provides a comprehensive comparison of production outcomes across multiple scenarios. A detailed examination of the data reveals three distinct production rate tiers. The first tier aligns with the target production of 20,000 parts over the designated 250-day period. Scenarios 1, 3, 7, and 13 successfully achieve this goal, with Scenario 1 standing out as the most efficient, as it meets the production target with the fewest machines required.

Table 4 Production Rate Comparison

Scenario #	Production		Scenario #	Production	
	*	(Mean, std) **		*	(Mean, std) **
1	20688	(20562.93, 9.96)	19	20691	(20567.03, 9.98)
2	**23446**	(**23312.16, 9.96**)	20	23450	(23452.21, 9.10)
3	20688	(20686.57, 10.27)	21	20691	(20682.39, 10.19)
4	23446	(23313.64, 9.90)	22	27135	(27126.44, 99.00)
5	20688	(20688.14, 10.36)	23	20691	(20684.56, 10.31)
6	23446	(23313.70, 9.98)	24	27135	(27126.34, 99.06)
7	20691	(20566.93, 9.99)	25	20688	(20563.07, 10.00)
8	23450	(23440.57, 8.80)	26	23446	(23313.53, 10.27)
9	20691	(20691.17, 10.30)	27	20688	(20664.27, 10.05)
10	23450	(23451.51, 10.50)	28	23463	(23321.06, 10.96)
11	20691	(20692.76, 10.37)	29	20688	(20667.24, 10.31)
12	23450	(23451.47, 10.50)	30	23463	(23320.96, 10.96)
13	20688	(20563.03, 10.02)	31	20691	(20567.03, 9.98)
14	23446	(23313.46, 10.32)	32	23450	(23452.26, 9.07)
15	20688	(20664.77, 10.48)	33	20691	(20682.36, 10.18)
16	23463	(23320.99, 10.89)	34	27135	(27126.29, 98.96)
17	20688	(20667.29, 10.03)	35	20691	(20684.67, 10.16)
18	23463	(23320.97, 10.93)	36	27135	(27126.37, 98.91)

* Using deterministic processing time

** Applying a normal distribution for processing time

The second tier reflects a higher production capacity, reaching 23,000 parts, with Scenario 2 emerging as the optimal choice due to its effective balance between output and resource allocation. However, the third tier, which is aimed at a production rate of 28,000 parts, is found to considerably exceed the target. Achieving this level would require a significant increase in the number of machines, contradicting the goal of maintaining efficiency and minimizing resource use.

Additionally, the dataset was reanalyzed under conditions where processing times followed a normal distribution. As shown in Table 4, the results indicate that production rates in both scenarios are almost identical.

The final evaluation of both approaches highlights the following optimal scenarios: Scenario 1, with three SLS machines and four auxiliary machines, successfully achieves the target production rate of 20,000 parts as outlined in the study. Scenario 2, with three SLS machines and five auxiliary machines, reaches a production rate of 23,000 parts, offering a higher output.

Ultimately, two key factors guide the decision-making process. If the goal is to meet the 20,000-part target with minimal cost, Scenario 1 is the preferred choice. However, if resource uniformity and increased production are prioritized, Scenario 2 stands out as the better option, as it delivers the highest production rate with five machines. Therefore, the final decision hinges on which parameters—cost efficiency or maximized output—are deemed most critical.

4 Stereolithography (SLA) Mapping and Simulation

4-1 Process Description

AM, widely recognized as 3D printing, encompasses various processes that build intricate 3D structures layer by layer using diverse materials. These technologies enable the creation of advanced components with complex geometries, functions, and material compositions [118]. AM is applied across various fields, including electronics, actuators, biomedical engineering, and sensors. The three primary methods in AM are extrusion-based 3D printing, SLS or selective laser melting (SLM), and SLA [119].

SLA, the earliest form of additive manufacturing, creates 3D objects by selectively solidifying liquid resin through photopolymerization. Its ability to deliver high precision and material versatility has led to its significant popularity [120]. Introduced in 1986 by 3D Systems [112], SLA was the first rapid prototyping method to be commercialized, marking a pivotal moment in the development of AM. However, the origins of modern stereolithography trace back to the 1970s [121]. Swainson [122] patented a system using intersecting radiation beams to build 3D objects by cross-linking or degrading polymers, while Herbert [123] developed a method to construct solid objects layer-by-layer using photosensitive polymers. Despite these early advancements, the contemporary form of stereolithography is primarily attributed to the work of C.W. Hull [124]. Hull's method, as illustrated in Figure 28 involves creating 3D objects layer by layer using photosensitive materials that are cured by ultraviolet (UV) radiation.

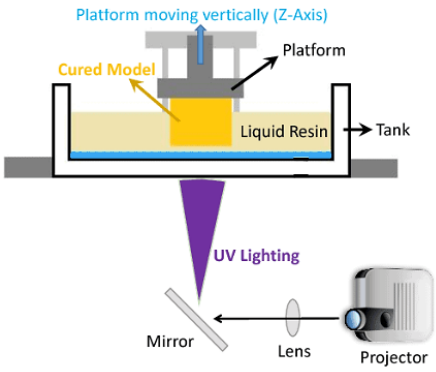

Figure 28 Hull's stereolithography system. [125]

An SLA printer is composed of four key components:

- A tank containing liquid resin, typically a transparent liquid plastic;
- A perforated platform that is submerged in the resin tank and can be adjusted vertically on the Z-axis to accommodate the printing process;
- A high-powered ultraviolet (UV) laser;
- A computer control unit that coordinates the movements of both the platform and the UV laser.

Over time, stereolithography has evolved across multiple generations, each introducing significant improvements in efficiency and capability. The first generation, exemplified by Hull's work, involved scanning a laser beam over liquid materials to create 3D products, though this method was limited by low efficiency. The second generation, known as projection stereolithography, overcame this limitation by curing entire layers simultaneously using photomask technology. In 2015, Tumbleston et al.[126] introduced the third generation with their continuous liquid interface production (CLIP) process, dramatically increasing print speed and enabling parts to be produced in minutes rather than hours. Most recently, volumetric stereolithography, considered the fourth generation, emerged, enabling the production of 3D objects with complex aperiodic volumes in just seconds [127-129].

The SLA process is based on the layered polymerization of epoxy or acrylic resin using a laser beam. Support structures, usually thin rods, are required during the printing process and are typically removed mechanically after printing [130]. The SLA printing workflow follows a structured sequence of tasks that directly align with the BPMN model, starting with print preparation, moving through the printing process, and concluding with post-processing. The process begins with designing a model in a 3D CAD system, which is converted to the STL format. The liquid resin is placed in the machine's vat, and a scraper smooths the resin layers and removes air bubbles before each layer is hardened. The laser scans the areas representing the current cross-section of the model, causing polymerization. The build plate is then lowered by the thickness of one layer, and this process repeats until the final geometry is achieved. Post-printing, the finished object is cleaned of any unbound resin, usually by rinsing in isopropanol or acetone, and the support structures are removed. The final step involves additional UV irradiation to complete polymerization throughout the model [131]. The object may undergo finishing processes such as grinding, smoothing, or varnishing. These post-processing steps ensure that parts produced via SLA not only meet functional requirements but also fulfill the aesthetic and performance demands of their intended applications.

SLA 3D printing was originally developed as a "bottom-up" method, where the light source illuminates the resin from beneath the vat. The first layer is formed at the bottom of the tank, with the build plate moving upward as each layer solidifies. This causes objects to emerge from the vat in an upside-down orientation. While most resin 3D printers utilize this bottom-up approach, some "top-down" systems exist, where the light source is positioned above the resin tank, curing the surface rather than the bottom. The build plate moves downward to accommodate new layers on top of the previous ones, resulting in the object being completed in an upright position.

Various types of resins are used in SLA, each suited to different applications. Standard resin is typically used for concept models and prototypes [132, 133], while ABS-like resin is selected for parts requiring high strength and elongation. Elastic resin is used for products that need to be elastically compliant. Other specialized resins include high-temperature, foundry, and medical-grade materials [134]. Common SLA materials range from rigid plastics to silicone rubbers. For instance, polycarbonate-like materials offer high-temperature resistance but require post-curing, while ceramic-like materials are used in automotive and electrical applications for their strength and heat tolerance. ABS-like resins and biocompatible silicones are also frequently employed.

By integrating this process description with the BPMN model, the connection between real-world SLA manufacturing and its digital simulation using DES becomes clearer. This structured approach allows for an accurate representation of machine operation, material flow, and post-processing in the simulation, making the analysis more applicable to real-world scenarios.

4-2 Case Study

This study aims to demonstrate the benefits of integrating FlexSim with DES to improve operational efficiency, minimize bottlenecks, and enhance production output in a hypothetical additive manufacturing production line. While the modeled scenario is conceptual, the configuration and logic are transferable to real-world production environments, thus justifying the use of specific values and assumptions detailed below.

The FlexSim-based simulation model is designed to produce 341 parts within a 20-day production window. Since the simulation focuses on system performance rather than product characteristics, the geometries and properties of the parts are not explicitly defined. However, the physical dimensions of the machines were incorporated into the model to ensure clear visualization and realistic spatial layout within the software.

The simulation operates under the following assumptions:

- The total operational time spans 480 hours across 20 days, assuming uninterrupted 24-hour production.
- Four SLA (Stereolithography) machines function in parallel to ensure higher throughput, increased system flexibility, reduced bottlenecks, and built-in redundancy.
- The washing and post-curing machines can process 10 parts simultaneously.
- Four transfer carts, one per SLA machine, are used to transport printed parts from the SLA machines to the washing station.
- All equipment is arranged in a U-shaped configuration. This layout, commonly adopted in lean manufacturing systems, enhances space efficiency, promotes flexible operator movement, reduces idle times, and facilitates smoother workflow. Additionally, it improves communication, supports multitasking, and allows early detection of issues, thereby contributing to continuous improvement and overall system performance [135].
- Four operators work simultaneously across the entire production system.
- The probability of producing a compliant part is 98%, while the probability of producing a defective part is 2%.

Table 5 summarizes the proposed machine setup and its respective processing times. The selection of process time distributions reflects realistic variability within additive manufacturing operations. For the SLA machines, a triangular distribution was applied, suitable for scenarios where minimum, most likely, and maximum values can be estimated despite limited empirical data. In contrast, uniform distributions were used for the washing and post-curing stages, reflecting equal likelihood across a defined range of durations, thereby avoiding any processing time bias. These assumptions provide a practical approximation of real-world process variability for simulation purposes.

Table 5 Machine Numbers and Times

Machine Names	Quantity	Process Time
SLA Machine	4	Triangolare (4.5, 5.5, 5) Hour
Washing Machine	1	Uniforme (0.5, 1) Hour
Post Cure Machine	2	Uniforme (1, 1.5) Hour

4-3 BPMN Mapping

Business Process Model and Notation (BPMN) is a universally recognized visual modeling standard used to depict and document intricate workflows. It offers a systematic and user-friendly approach to process representation, making it comprehensible for both technical professionals and general

stakeholders. In this research, BPMN is utilized to map the SLA 3D printing process, providing a structured and holistic view of the key operational phases required to produce high-quality parts.

As shown in Figure 29, the BPMN diagram outlines the SLA production workflow through three primary stages: Print Preparation, Printing, and Post-Processing. These phases are organized into separate swimlanes within a single process pool, enabling a clear and detailed depiction of task flows, process interrelations, decision points, and dependencies. This visualization technique enhances the overall understanding of the production workflow and contributes to efforts aimed at optimizing process efficiency and maintaining quality standards.

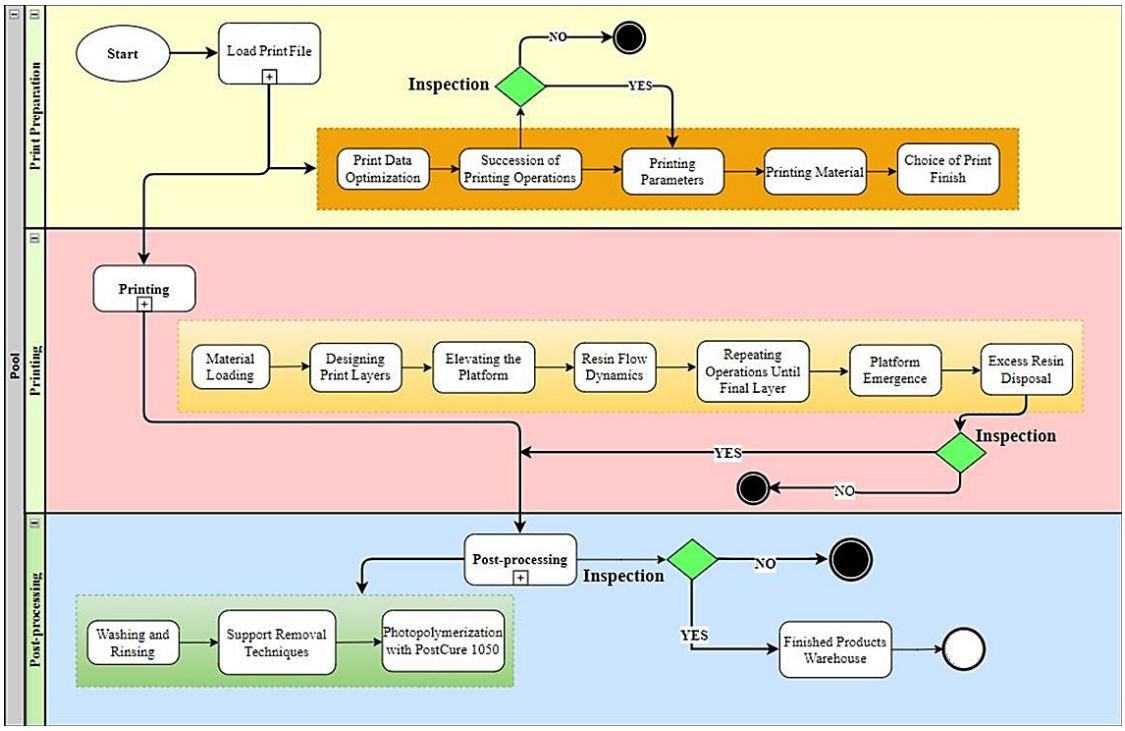

Figure 29 Stereolithography BPMN Diagram

While the BPMN model includes pre-processing steps for completeness, it is important to note that these stages are not explicitly simulated in the FlexSim environment. The simulation focuses primarily on the printing and post-processing phases to assess workflow efficiency and resource allocation.

- **Print Preparation:** Before the printing process can begin, several preparatory actions must be completed. This stage initiates with the start event in the first swimlane and proceeds with the loading of the print file, represented by a subprocess task. Following this, a sequence of operations is carried out, starting with the optimization of print data and continuing with the setup for printing. These tasks involve refining the digital model to ensure efficient and high-

quality printing. At this point, an inspection gateway is introduced—if the outcome is satisfactory, the process advances; if not, it is terminated.

Upon passing the inspection, critical preparatory tasks are performed in parallel, including configuring the printer settings, selecting a suitable printing material, and defining the desired print finish. Printer configuration involves setting key parameters such as exposure time, layer thickness, and print speed to achieve high accuracy and efficiency. Material selection ensures that the chosen resin meets the required mechanical and chemical specifications of the final part. Meanwhile, defining the print finish determines surface texture, the necessity of support structures, and any additional post-processing steps. These preparatory measures ensure that the system is fully optimized before initiating the printing phase, minimizing potential errors and maximizing the quality of the printed object.

- **Printing:** After the print preparation phase is completed, the workflow advances to the printing station, represented as a subprocess task. This stage involves a series of sequential operations, including loading the printing material, designing print layers, elevating the build platform, controlling resin flow, depositing layers iteratively, raising the platform upon completion, and removing any excess resin. Once these steps are finalized, an inspection gateway is introduced—if the product fails the inspection, the process is halted; if it passes, the workflow proceeds to the post-processing stage in the final swimlane.

  SLA printers commonly employ 3D SPRINT software for managing files, editing, and preparing prints. Key operations in this phase include preparing the printer with resin material, directing the UV laser for layer-by-layer fabrication, and executing precise lifting and sliding movements to achieve the desired geometry. As the process progresses, the printed component gradually takes form, with surplus resin eliminated in the concluding step of this stage.

- **Post-processing:** The final phase of the SLA workflow is post-processing, which plays a critical role in enhancing both the mechanical performance and visual quality of the printed parts. After completing the preceding stages, the process transitions into this subprocess, where a series of steps are executed to ensure the part meets the desired standards of functionality and appearance. The phase begins with washing and rinsing the printed object to eliminate any remaining resin. If the design includes support structures, these may be removed to improve surface finish and usability.

Following cleaning, the part is placed into a post-curing machine, where it undergoes photopolymerization under UV light. This curing process strengthens the material by increasing its hardness, durability, and resistance to chemicals. After curing, the product undergoes a final inspection to ensure compliance with quality standards. If approved, the product is moved to the finished goods warehouse, signaling the successful completion of the production cycle. If it fails the inspection, the process is halted to prevent defective parts from continuing downstream. This post-processing stage is essential in SLA manufacturing, as it significantly affects the final properties and ensures the printed parts meet performance and quality expectations.

4-4 FlexSim Model

In the simulation conducted for this study, the SLA printer is represented as a single unified processing entity, without modeling its internal components separately. This level of abstraction enables a simplified yet effective analysis of production workflows, equipment utilization, and overall operational performance. The FlexSim model takes a comprehensive approach to assessing the SLA production process, with an emphasis on enhancing resource allocation, minimizing bottlenecks, and boosting throughput.

The simulation incorporates essential parameters such as print cycle duration, machine availability, and post-processing requirements. While individual SLA printer components contribute to the physical printing process, their internal mechanics do not significantly impact the overall production system at a macro level. As such, the printer is modeled as a single functional unit within the simulation to enhance computational efficiency and maintain a clear analytical focus.

To maintain clarity between the technical aspects of SLA printing and the goals of the simulation-optimization approach, the discussion on SLA technology is presented separately from the simulation methodology.

The primary focus of this study is the development of a reference manufacturing line layout designed to meet processing demands within the FlexSim simulation environment. The complete simulation model, including system connections, configurations, and layout arrangements, is depicted in Figure 30 A legend to interpret the symbols in the figure is as follows:

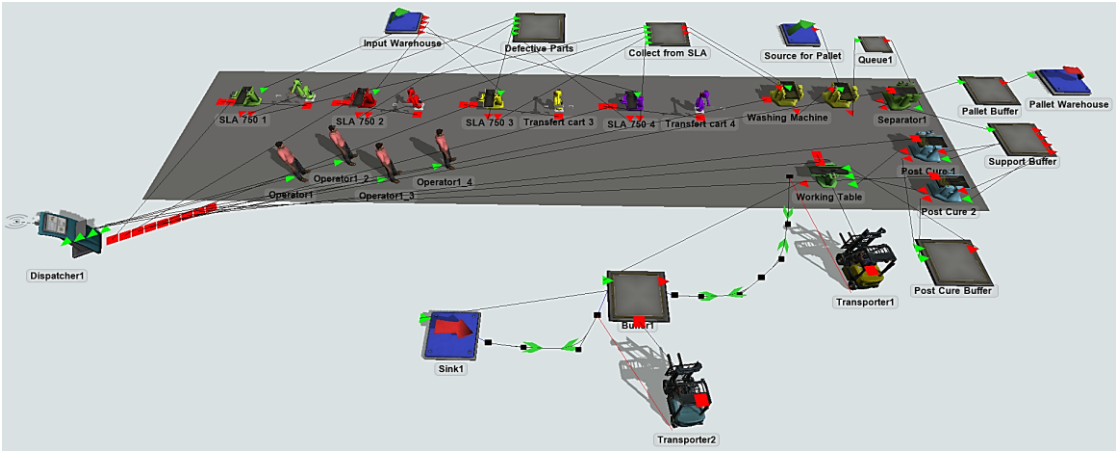

Figure 30 Simulation Model of SLA Production Line in FlexSim

The red square (■) symbolizes the central or "connection center" port, which facilitates the linkage between operators (or task executors) and fixed resources, ensuring efficient communication and coordination. The triangular icon (▲) represents the connection between fixed resources and is referred to as the "connect object." When this symbol appears green at the input of an object, it indicates that the port is open and ready to receive a new flow item. Conversely, if the symbol is red at the output, it signals that the port is closed. When the red indicator is present at both the input and output of an object, it means the device is currently engaged in processing and cannot accept additional flow items until the ongoing task is completed.

The simulation model comprises two principal sections: processing and post-processing. Several model adjustments were implemented to support efficient task distribution, optimize resource usage, and improve workflow within the simulated environment.

FlexSim was selected for this project due to its advanced capabilities in discrete event simulation, particularly within manufacturing and logistics contexts. Its intuitive 3D modeling interface, comprehensive statistical tools, and ease of use make it well-suited for analyzing SLA production lines [136]. Compared to other simulation tools, such as AnyLogic, Simul8, and Arena, FlexSim offers a user-friendly interface with drag-and-drop modeling, allowing for efficient setup and analysis of complex manufacturing systems [137]. While AnyLogic focuses on hybrid modeling (DES + agent-based), FlexSim excels in simulating manufacturing processes, providing a better fit for analyzing machine utilization, bottlenecks, and process optimization. Its scripting flexibility and real-time decision modeling features also give it an edge over Simul8 in managing complex workflows. These advantages position FlexSim as the most suitable tool for this research, enabling precise production optimization and effective resource management tailored to SLA-based additive

manufacturing.

Furthermore, FlexSim has a proven track record in industrial process optimization, having been extensively used to model resource allocation, machine utilization, and workflow efficiency. Previous research has validated its usefulness in manufacturing system design, lean process enhancements, and production scheduling—all of which align closely with the goals of this study. Although alternative simulation tools are available, FlexSim was selected not only for its accessibility but also because its specialized capabilities aligned best with the study's requirements, facilitating in-depth analysis of SLA printer performance, pinpointing bottlenecks, and refining production parameters to improve overall efficiency [138].

The model's processing area includes four concurrently operating SLA machines, each supported by a dedicated robotic unit. A shared input warehouse serves as the material supply point, with pre-processing tasks assumed to be completed externally. This assumption streamlines the simulation, focusing solely on processing and post-processing activities. A structured scheduling mechanism ensures that each SLA machine adheres to predefined cycle times to meet production targets.

To maintain operational efficiency and support effective simulation analysis, the model includes four operators. Their activities are managed through a dispatcher, which functions as a central control unit that collects information from fixed resources. The dispatcher interacts with the machines, retrieves necessary data, and distributes tasks accordingly. Operator assignments follow a predefined connection structure, which also governs task prioritization and execution order.

The dispatcher enables various task allocation strategies, with this study employing the round-robin approach. This method ensures that operators engage with all machines as needed, promoting an equitable distribution of tasks. As a result, each operator handles a fair share of the workload, supporting balanced involvement and enhancing overall resource utilization.

Accurate machine setup and calibration are crucial for ensuring consistent operations. In the simulation model, specific configuration parameters are included to guarantee that each SLA machine is properly initialized by the assigned operators. Furthermore, the model features two distinct buffer systems: one designated for defective parts and another for all successfully manufactured parts. Since each SLA machine yields approximately 98% conforming parts and 2% defective ones, the defective parts buffer is strategically placed to collect and segregate non-compliant items. Machine connections are designed to prioritize the transfer of functional parts first, with defective parts handled subsequently.

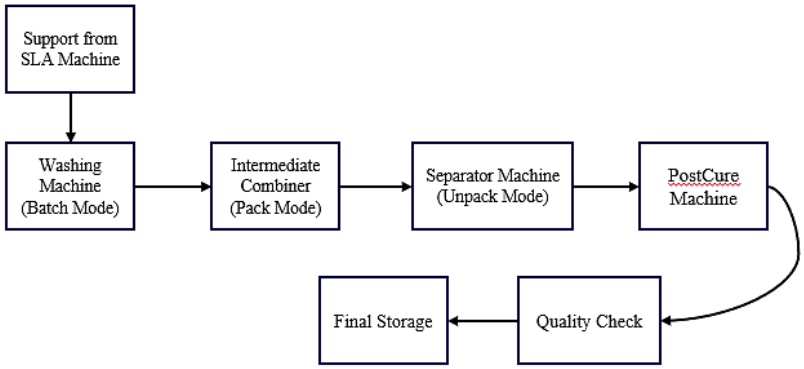

Figure 31 Post-Processing Workflow in SLA Production

As shown in Figure 31, the workflow features a designated washing machine, followed by a structured sequence of combining and separating operations to prepare parts for the post-curing stage. All pallets used in this process originate from a single source, promoting uniformity and simplifying setup procedures. A combiner machine is employed to enable the simultaneous washing of 10 parts within a defined cycle time. This setup requires the integration of both a combiner and a separator, with batch selection playing a vital role in configuring SLA machine parameters.

However, since the separator is set up for unpacking tasks, it cannot directly receive items from the combiner operating in batch mode. To overcome this challenge, an intermediate combiner machine, configured in pack mode, has been added between the two. In this arrangement, parts are washed in the first combiner (batch mode), transferred to the second combiner (pack mode), and then moved to the separator for further processing. These adjustments are tailored to the FlexSim simulation environment and were made to ensure precise modeling and effective process optimization.

To address workflow disruptions caused by machine congestion, a buffer has been strategically placed between the separator and the combiner. This buffer helps reduce queuing by temporarily holding parts that are waiting to complete the washing phase. Furthermore, this segment of the process requires operators to be involved in machine setup and configuration.

Two additional buffers are located downstream of the separator—one for pallet collection and another for temporarily storing parts before they are moved to the post-curing equipment. To enable the curing and transfer of 10 parts simultaneously to the next processing stage, two post-cure machines configured as combiners are utilized. These machines also require operator setup and supervision. After completing the curing cycle, parts are sent to a quality check station for final inspection before being transferred to the finished goods warehouse. A buffer is included at this stage to support a steady workflow and to avoid delays or machine idling due to the accumulation of parts.

The model does not explicitly address the batching strategy or scheduling for transferring parts to the output warehouse, as these elements fall outside the primary scope of the simulation. The equipment is arranged in a U-shaped layout. While a direct path from the quality check to the final warehouse would be technically possible, real-world manufacturing settings often involve spatial or logistical limitations that restrict such direct transport. To reflect these practical constraints, the model visually represents an alternative transport route, simulating the realistic movement of components within the facility.

4-5 Model's Results and Discussion

Bottleneck mitigation and equipment configuration are pivotal elements in enhancing the efficiency of manufacturing processes. Achieving optimal production line performance requires a systematic analysis of critical variables such as equipment processing time, blocking time, and idle time—factors that significantly influence overall productivity [117]. In this study, the simulation model was refined with a specific focus on minimizing idle time and maximizing equipment utilization.

The principal aim of the analysis is to determine the optimal number of machines required to meet the defined production targets. To this end, multiple operational scenarios were developed and assessed to identify the most effective allocation of SLA machines, post-curing units, quality inspection stations, and operator resources. These configurations were designed to align with the study's production constraints while maximizing system throughput and resource efficiency.

Before defining the simulation scenarios, evaluating the feasibility and implications of adjusting the number of SLA machines is essential. This preliminary step facilitated the identification of the most suitable machine configuration, serving as a foundation for subsequent scenario development. Although the base simulation model was initially configured with four SLA machines, additional experiments were carried out to evaluate the impact of altering machine quantities on production output and resource utilization.

As summarized in Table 6, operating with three SLA machines (Experiment 1) resulted in the production of 253 parts over a 20-day period, which fell considerably short of the required output. In contrast, increasing the number to four SLA machines (Experiment 2) yielded 341 parts, effectively meeting the production goal and validating this setup as the baseline scenario for the study.

Table 6 SLA Machine Quantity and Output Comparison

Experiment Number	Number of SLA Machines	Parts Produced in 20 Day
1	3	253
2	4	341
3	5	451
4	6	550

Experiment 3, which introduced a fifth SLA machine into the system, led to a notable increase in production output, reaching 451 parts over the 20-day simulation period. This improvement underscores the potential efficiency gains achievable through moderate investment in additional equipment. Provided that financial resources are not a limiting factor, the configuration employing five SLA machines may be considered a more scalable and productive alternative, offering a favorable balance between throughput and system flexibility.

In contrast, Experiment 4, which incorporated six SLA machines, produced an output of 550 parts. While this reflects continued improvement in production capacity, the incremental gain does not justify the associated increase in equipment and operational costs. The resulting output also significantly exceeds the production target, indicating potential overcapacity and leading to concerns about underutilization and reduced cost-efficiency. Therefore, although increasing the number of machines improves output, it is not economically viable beyond five machines within the current production objectives.

To further evaluate system performance, Figure 32 illustrates a comparative analysis of SLA machine utilization across two key configurations: four SLA machines (State_a) and five SLA machines (State_b). This visualization complements the production output data presented in Table 6 by offering insight into the operational efficiency of each setup.

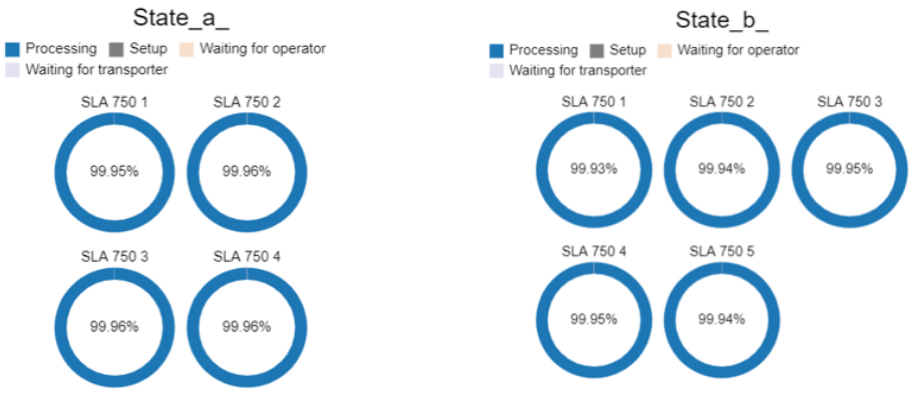

Figure 32 Production Analysis for SLA Machines in 20 Days: (a) 4 machines, (b) 5 machines

In both configurations, SLA machines demonstrate exceptionally high utilization rates, consistently exceeding 99.9%. Specifically, in State_a, utilization ranges from 99.95% to 99.96%, while in State_b, it spans from 99.93% to 99.95%. These results indicate that the system achieves near-maximum equipment utilization in both scenarios, reflecting minimal idle time and effective coordination between processing tasks, operator interventions, and material handling.

Moreover, the marginal increase in output observed in the five-machine setup does not correspond to a significant change in individual machine utilization. This finding reinforces the conclusion that while the five-machine configuration provides a modest improvement in total output, it does not proportionally enhance system efficiency. Depending on budgetary considerations, such a setup may not be economically justifiable.

Therefore, the analysis presented in Figure 32 supports the selection of the four-machine configuration as a highly efficient and well-balanced system. It successfully meets production targets while ensuring optimal utilization of available resources and avoiding unnecessary capital expenditure.

Figure 33 presents the Support Buffer WIP Analysis, illustrating fluctuations in WIP levels over a seven-day simulation period. The y-axis denotes the number of WIP items (i.e., parts) in the buffer, while the x-axis represents time. The analysis focuses on the Support Buffer using a “Content vs. Time” chart, revealing that buffer levels generally remained low, typically fluctuating between 0 and 1. However, three notable peaks were observed. The most significant occurred on Friday the 15th, when the buffer content spiked to 7 parts, indicating a temporary downstream delay, likely due to limited capacity at the quality check station or transport constraints. Additional moderate increases were observed on Sunday and Monday, reaching 4 and approximately 2–3 parts, respectively. These intermittent surges may reflect batch releases from upstream processes or temporary inefficiencies in resource allocation, such as transporter or operator availability. Overall, the Support Buffer maintained a stable performance with only occasional pressure during peak periods, suggesting the system functions efficiently under normal conditions but remains vulnerable to short-term bottlenecks.

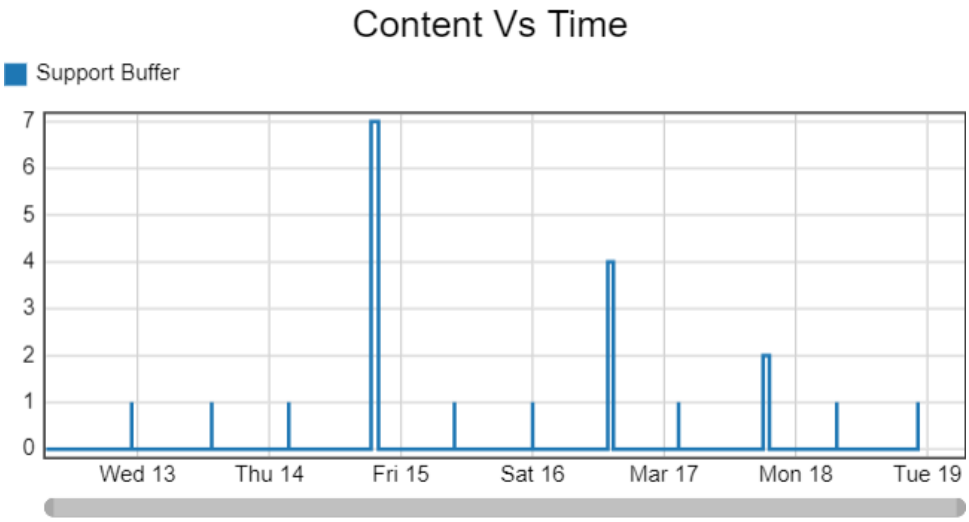

Figure 33 Temporal Analysis of Work-In-Progress (WIP) Variation in the Support Buffer

Figure 34. (a) State Gantt chart of Post Cure 1 and Post Cure 1_2 over one week, showing prolonged collecting phases and intermittent processing activity. (b) Output by Hour chart of the Washing Machine over a 20-day simulation period, revealing a largely flat throughput with a single pronounced spike around March 24. Together, these charts highlight the irregular flow of parts within the system, providing a clear justification for the extended collecting states observed in the post-curing process.

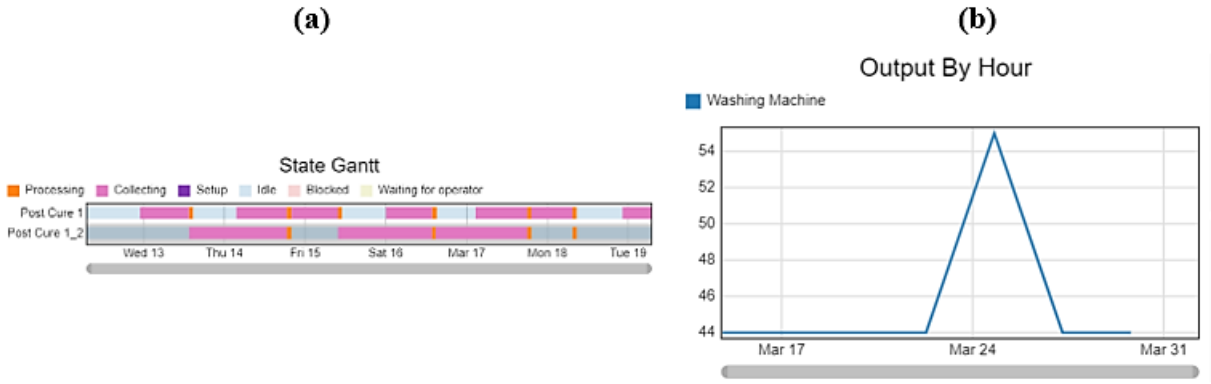

Figure 34 Machine State Behavior and Throughput Analysis in the Post-Processing Phase

To assess the synchronization and continuity of post-processing stages within the simulated SLA 3D printing workflow, both machine state and throughput data were analyzed. The State Gantt chart indicates that the post-curing units frequently remained in a collecting state due to insufficient part arrivals, thereby limiting the frequency of batch-based curing operations. This underutilization is further explained by the Output by Hour chart, which shows that the Washing Machine produced parts at a steady but low rate, with a single surge in output. This pattern suggests that upstream

processes (SLA printers and transporters) delivered parts in irregular intervals, disrupting the flow of materials into downstream stations. The combined analysis of these visualizations underscores a critical flow imbalance in the production line and emphasizes the importance of upstream-downstream coordination and batch timing optimization to enhance system-wide performance.

Building on the utilization analysis illustrated in Figure 32, which demonstrates consistently high utilization rates of the SLA machines under two primary configurations (State_a and State_b), a subsequent phase of the study focused on optimizing the allocation of downstream resources. Specifically, this stage investigated the roles of supporting elements such as operators, post-curing units, and quality control stations. For each factor, upper and lower limits were established to define a range of potential scenarios within FlexSim's flexible framework—for instance, operators (3 to 5), Post_cure machines (1 to 3), and quality check (1 to 2). The optimal configuration for these parameters is determined based on the most effective SLA setup, as presented in Table 7.

Table 7 Scenarios for Machines

Scenarios #	Operator	post-cure	Quality Check
1	3	1	1
2	3	1	2
3	3	2	1
4	3	2	2
5	3	3	1
6	3	3	2
7	4	1	1
8	4	1	2
9	4	2	1
10	4	2	2
11	4	3	1
12	4	3	2
13	5	1	1
14	5	1	2
15	5	2	1
16	5	2	2
17	5	3	1
18	5	3	2

To ensure a thorough and systematic evaluation, both lower and upper bounds were established for each resource type, allowing for an extensive exploration of system performance across a range of operational conditions. The outcomes of the corresponding simulation scenarios are presented in Table 8, which details the average production output and associated standard deviation for each configuration over a 20-day simulation period.

Table 8 Production Rate Comparison

Scenario #	Production (Mean, std)	Scenario #	Production (Mean, std)
1	(356.71, 1.32)	10	(350.43, 2.56)
2	(356.71, 1.32)	11	(350.24, 2.61)
3	(350.16, 2.57)	12	(350.24, 2.61)
4	(350.17, 2.57)	13	(356.71, 1.32)
5	(350.11, 2.62)	14	(356.71, 1.32)
6	(350.11, 2.62)	15	(350.24, 2.57)
7	(356.71, 1.32)	16	(350.27, 2.57)
8	(356.71, 1.32)	17	(350.09, 2.61)
9	(350.43, 2.56)	18	(350.09, 2.61)

Among the 18 scenarios evaluated, Scenarios 1, 2, 7, 8, 13, and 14 consistently achieved the highest production output, averaging 356.71 parts with minimal variation (standard deviation of 1.32). Notably, Scenario 1 emerged as the most resource-efficient configuration, achieving this maximum throughput with only three operators, one post-curing machine, and one quality check station. This lean setup demonstrates a high level of coordination and effective scheduling, as evidenced by the near-complete utilization of the SLA machines illustrated in Figure 32.

In contrast, Scenario 9, representing the baseline model aligned with the initially recommended layout, employed four operators, two post-curing machines, and one quality check station. While this configuration ensured stable system performance and minimized the risk of bottlenecks, it yielded a lower output of 350.43 parts. The additional resources in Scenario 9 did not translate into increased throughput, suggesting potential underutilization and inefficiency relative to Scenario 1.

A more detailed comparison between these scenarios highlights several key insights. In terms of workforce allocation, scenarios employing three operators, such as Scenario 1, demonstrated that a reduced labor force can sustain high performance when task coordination is optimized. Conversely, configurations with four or five operators (e.g., Scenarios 9–12) offered marginal improvements in operational resilience but did not significantly increase productivity, indicating diminishing returns beyond a certain staffing threshold.

Regarding post-processing, a single post-curing unit, as used in Scenario 1, did not pose a constraint on production, underscoring the effectiveness of upstream scheduling. In Scenario 9, the addition of a second post-curing machine improved flexibility but had a limited impact on actual output. This emphasizes the importance of synchronizing post-processing tasks with both printing and material

handling operations. Furthermore, the presence of only one quality check station across all scenarios was sufficient to meet inspection demands, indicating that quality control did not present a production bottleneck. Thus, increasing the number of inspection resources would yield minimal benefits relative to the added cost.

Scenarios categorized within the second performance tier—including Scenarios 3–6, 9–12, and 15–18—achieved slightly lower average outputs, ranging from 350.09 to 350.43 parts. Within this group, only a few scenarios, such as 3, 4, and 9, attained respectable performance with moderate resource consumption. Others, while delivering similar outputs, required significantly more equipment, resulting in less favorable cost-performance ratios.

In summary, the comparative results presented in Table 7 and Table 8 identify Scenario 1 as the most efficient and cost-effective solution among all evaluated configurations. It maximizes output while minimizing resource use, reflecting a lean and well-coordinated system design. While Scenario 9 meets production objectives and provides enhanced operational flexibility, it does so at the expense of resource efficiency, highlighting the trade-off between system resilience and optimization.

The application of a simulation-optimization framework to SLA production lines demonstrates measurable benefits in terms of productivity, cost-efficiency, and workflow integration. Through strategic adjustments in machine configurations and labor assignments, the optimized model achieves a sustained production output of 341 parts over a 20-day period using four SLA machines. This configuration delivers a high machine utilization rate of 99.9%, ensuring maximum throughput while avoiding unnecessary capital expenditure.

Additionally, the integration of a U-shaped production layout and a dispatcher-driven operator assignment system reduces idle time and effectively mitigates bottlenecks, enhancing overall responsiveness. Cost-efficiency is further reinforced by maintaining a low defect rate of 2%, contributing to reduced material waste. Optimized scheduling of post-processing stages, such as washing and curing, shortens lead times and supports continuous part flow with minimal buffering delays.

These findings underscore the potential of DES, as implemented in FlexSim, to support data-driven decision-making in the industrialization of SLA-based additive manufacturing. The results confirm that large-scale production can be achieved in a manner that is both economically viable and operationally efficient.

5 Digital Light Processing (DLP) Mapping and Simulation

5-1 Process Description

Additive manufacturing, also known as 3D printing, creates parts layer by layer through different techniques. Among these, DLP stands out for its efficiency and precision. Much like SLA, DLP is a photopolymer-based 3D printing technique, but the main distinction is its light source. DLP uses a standard light source, like an arc lamp paired with a liquid crystal display (LCD) panel, to illuminate the entire surface of the photopolymer resin vat in a single pass, which generally makes it faster than SLA. The process uses a UV-sensitive resin that solidifies when exposed to UV light, allowing for the production of detailed, high-resolution components. Like SLA, DLP requires support structures and post-curing steps. A notable advantage of DLP, however, is its use of a shallow resin vat, which helps reduce material waste and operational costs.

DLP technology operates by projecting UV light at a specific wavelength onto a liquid resin that is sensitive to UV exposure, as shown in Figure 35. The fundamental material, called resin, is liquid and contains monomers that, when exposed to UV light, form polymers and harden. This process occurs in layers, building the object from the bottom up.

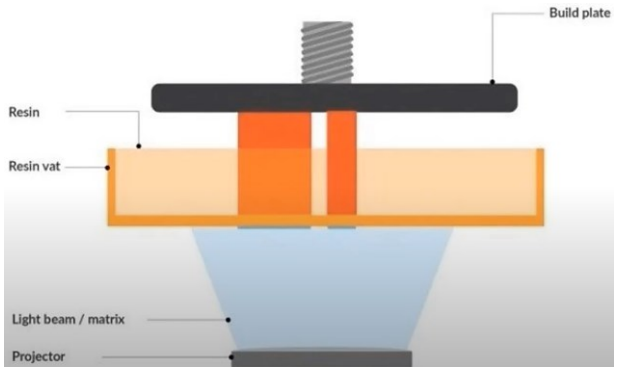

Figure 35 Basic Components of a DLP 3D Printer

The resin is poured into a transparent container that allows the UV light to pass through. At the bottom of this container is a flexible, transparent slide, which is essential for ensuring the layer-by-layer formation of the part. A UV display located underneath the transparent slide projects the image of the layer to be printed. This image is typically exposed for less than a second. As soon as the resin is exposed to UV light, it hardens, forming one layer of the part. After the first layer hardens, the build platform (which holds the forming part) rises slightly, and the next layer is projected and

hardened in the same manner. This cyclical process repeats until the entire part is printed.

The entire build process is highly sensitive to UV light, and the resin must be carefully handled since it is both liquid and chemically reactive. Wearing protective gear like gloves is essential to prevent direct skin contact with the resin, which may lead to irritation or chemical burns.

After the printing process is complete, the part undergoes several essential post-processing steps to achieve its final mechanical and aesthetic properties. The first step is resin drainage and cleaning, where excess uncured resin is drained from the part, and automated ultrasonic cleaners can be used to ensure thorough cleaning. Once cleaned, the part is rinsed with water and then dried with paper towels. If the part was printed with support structures, these are carefully removed using pliers or cutting tools. The next critical step is post-curing, where the part is exposed to controlled UV light in a UV curing chamber for a specific period to enhance its mechanical strength, thermal resistance, and chemical stability. Finally, for parts requiring high surface quality, sanding and finishing may be necessary. This involves light sanding to smooth visible layer lines or imperfections, with additional painting, coating, or polishing applied depending on the final requirements of the part.

These post-processing steps are critical in both the BPMN diagram and DES modeling, as they contribute to the overall production time and resource allocation. Including them ensures a more accurate representation of the real-world DLP workflow.

In DLP systems, the projection of UV light is often achieved using a Digital Micromirror Device (DMD), which rapidly reflects light patterns to selectively cure specific regions of the photopolymer resin. Depending on the system configuration, DLP printers can follow either a bottom-up or top-down printing approach. The bottom-up configuration is more common and economical, as it minimizes resin usage and reduces material costs by employing a shallow resin vat. However, it requires careful adhesion control to prevent parts from detaching during printing. In contrast, the top-down configuration simplifies part detachment and is better suited for high-viscosity resins, though it typically demands a larger volume of material. As DLP printing systems scale toward higher volumes and greater complexity, workflow optimization becomes increasingly critical. This includes managing differences in processing times, machine utilization, and operator tasks, especially in environments with diverse part geometries. To address these challenges, this study applies DES in later sections to analyze and optimize the DLP production process, supporting strategic decisions in resource allocation and system design.

5-2 Case Study

The initial step in the workflow is the selection of the appropriate material. For this purpose, the 'TYPE D TOUGH' high-precision UV resin from DruckWege has been chosen, as shown in Figure 36 This resin is specially designed for 3D printing technologies like DLP and SLA, providing outstanding durability and accuracy for functional applications. DruckWege's TYPE D TOUGH is a robust, stiff material with high toughness, tailored for the demands of DLP/LCD 3D printing systems. Its high reactivity allows for fast curing speeds, enhancing production efficiency—ideal for both industrial and rapid prototyping environments. Additionally, it provides excellent contour sharpness and has an extremely low odor profile, making it suitable for various settings [139].

Figure 36 Resin for DLP 3D Printing

With a high modulus of elasticity and enhanced tensile strength, this acrylic-based resin is classified as a functional resin. It is characterized by elongation at a break of approximately 6%, making it highly rigid and impact-resistant once polymerized, ensuring that accuracy and strength are maintained under moderate physical stresses. Specifically designed for optimal performance with DLP 3D printers, the quick-curing properties of TYPE D TOUGH resin are well-suited for applications that demand high-detail and durable parts. The resin's photopolymer components undergo a reaction to UV light, enabling precise layer-by-layer solidification, which is essential for achieving high-quality, detail-oriented results.

In this setup, specific equipment is employed, as illustrated in Figure 37 Equipment Setup for Processing and Post-Processing in the Additive Manufacturing Workflow: (a) Elegoo Saturn 3 Ultra Desktop MSLA 3D printer, (b) Elegoo Mercury XS Bundle Wash & Cure(a). For the printing stage, the Elegoo Saturn 3 Ultra Desktop MSLA 3D printer, featuring an impressive 12K resolution, is utilized. This printer offers a spacious working volume of 218.88 x 122.88 x 260 mm, with a variable printing speed

ranging from 30–70 mm/h and a maximum speed of up to 150 mm/h. The cost of this model is approximately €369.99.

(a) (b)

Figure 37 Equipment Setup for Processing and Post-Processing in the Additive Manufacturing Workflow: (a) Elegoo Saturn 3 Ultra Desktop MSLA 3D printer, (b) Elegoo Mercury XS Bundle Wash & Cure

For the post-processing phase, as shown in Figure 37 Equipment Setup for Processing and Post-Processing in the Additive Manufacturing Workflow: (a) Elegoo Saturn 3 Ultra Desktop MSLA 3D printer, (b) Elegoo Mercury XS Bundle Wash & Cure(b), the Elegoo Mercury XS Bundle Wash & Cure Set, which includes a handheld UV lamp, is used. This equipment is specifically designed for handling larger prints and features a rotary knob with a display for the service interface, along with a time setting range from 0 to 30 minutes. The washing machine accommodates objects up to 180 x 121 x 153 mm with the platform, or 201 x 124 x 255 mm without it. For curing, it supports objects with a maximum size of Ø 200 x 260 mm. The wash machine dimensions are 255 x 155 x 385.5 mm (2.27 kg), and the curing device measures 246 x 230 x 353.5 mm (2.4 kg). Priced at €169.99, this bundle provides a cost-effective and versatile solution for post-processing.

Two different designs were explored to produce distinct parts, as shown in Figure 38 DLP 3D Printing: (a) geometry I and (b) geometry II. In DLP 3D printing, support structures are typically required for overhangs or large, unsupported spans. However, due to the simplicity of the part's geometry, no additional supports are needed in the CHITUBOX software. The printing process is simplified as each layer is cured simultaneously by DLP technology, reducing the risk of sagging in small unsupported areas. As a result, greater efficiency is achieved for straightforward geometries compared to other 3D printing methods.

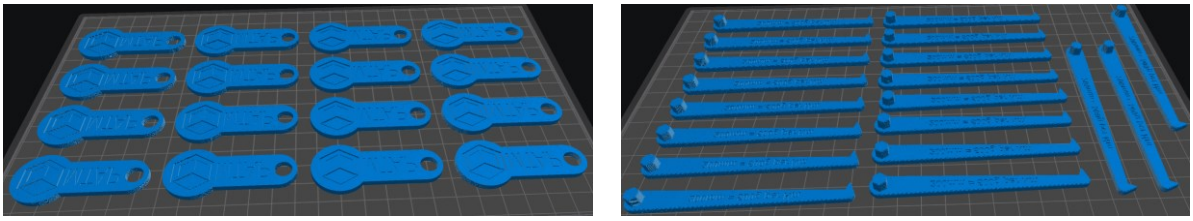

Figure 38 DLP 3D Printing: (a) geometry I and (b) geometry II

For this process, CHITUBOX software will be used to prepare the design for printing. Essential settings for the sample are configured in CHITUBOX before exporting it as an STL file, which is ready for the DLP machine. Figure 39 shows the configuration settings for the ELEGOO Saturn 3 Ultra DLP 3D printer within CHITUBOX, which are used for setup and calibration.

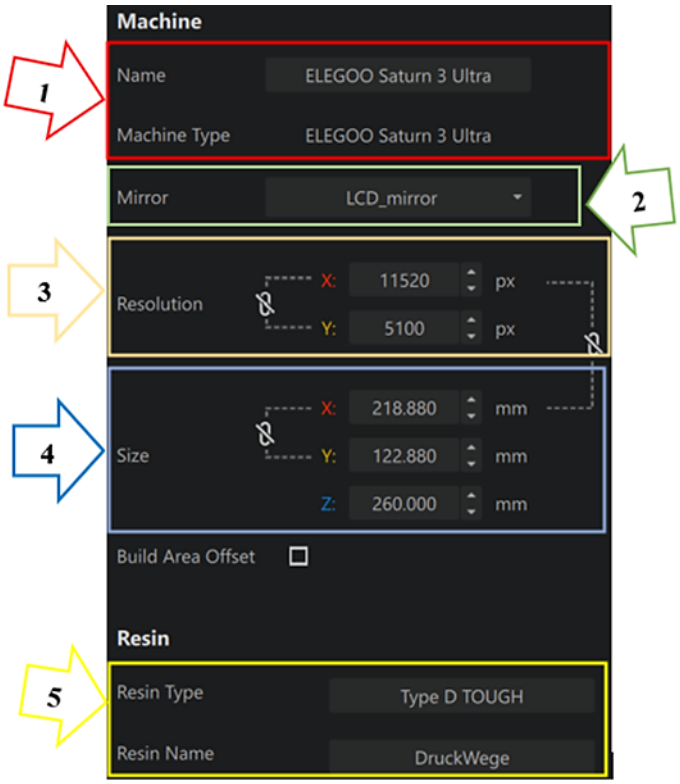

Figure 39 Configuration Settings for DLP 3D Printer

1. The ELEGOO Saturn 3 Ultra printer is designated as the primary equipment for high-precision printing tasks utilizing DLP technology.

2. In the settings, the mirror is configured as LCD_mirror, specifying the mirror mode for the LCD or projection screen employed in DLP printing. This setting directly impacts the orientation and reflective properties of the projected image, ensuring precise layer alignment during printing.

3. Furthermore, the resolution settings, encompassing the X, Y, and Z dimensions, define the

machine's printable area or build volume. The dimensions of the LCD screen are specified in millimeters, with an X resolution of 11520 pixels and a Y resolution of 5100 pixels. Higher resolutions enhance the printer's ability to achieve finer details in each layer, directly affecting the overall quality and smoothness of the printed parts.

4. The build size settings define the machine's printable area, or build volume, across the X, Y, and Z dimensions. Specifically, X is 218.880 mm, Y is 122.880 mm, and Z is 260.000 mm. The X and Y dimensions represent the width and depth of the machine's LCD, while the Z dimension indicates the maximum printable height. These specifications are essential for determining the maximum object size that this printer can produce.

5. Lastly, the resin type used is selected based on compatibility with the printer and project requirements, highlighting the importance of choosing the appropriate material for successful prints.

This section provides an in-depth analysis of the printing parameters configured for the DLP 3D printer, as illustrated in Figure 40. Each setting plays a critical role in determining the quality, accuracy, and speed of the printing process.

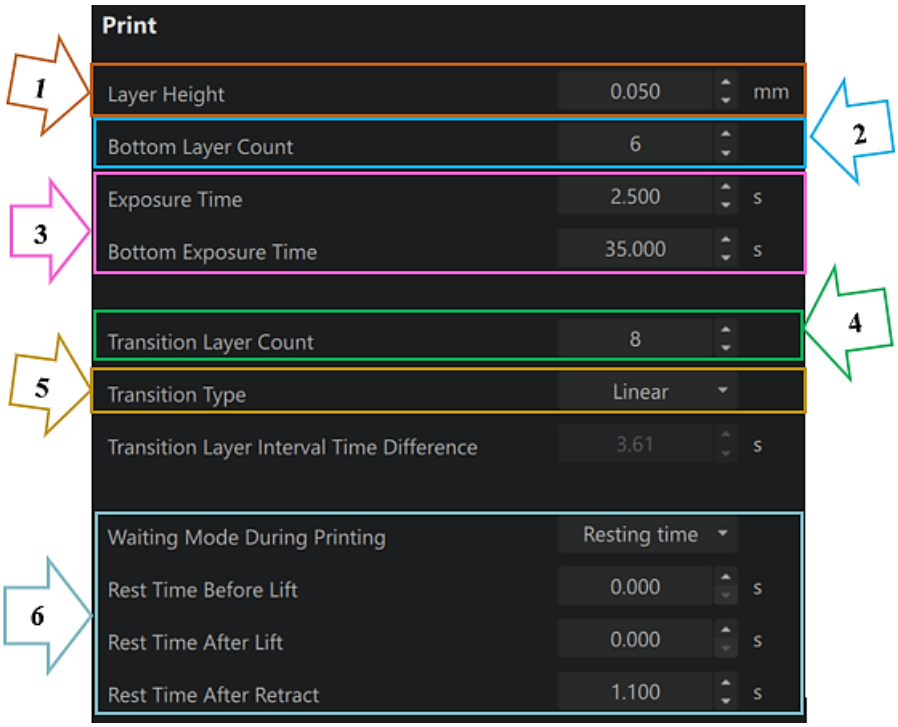

Figure 40 Configuration of Print Settings for DLP 3D Printing Process

1. The layer height determines the thickness of each layer applied in the printing process. In this setup, each layer is 0.05 mm thick. Reducing the layer height can enhance print resolution by

producing finer details; however, it also increases the printing time as more layers are needed to build the part. In this specific case, lowering the layer height below 0.03 mm is not feasible, as the resin cannot effectively support such thin layers. Additionally, this layer height setting influences other parameters, such as exposure time, to ensure optimal curing and part quality.

2. In resin-based printing, a specific number of initial layers, known as bottom layers, is defined to ensure secure adhesion of the part to the build platform, which is critical for successful printing. The number of bottom layers can be adjusted based on the requirements of the print. In this setup, 6 bottom layers have been specified, each with a layer height of 0.05 mm. These initial 6 layers are set with specific conditions to maximize adhesion, while the remaining layers are printed under different settings tailored to optimize speed and material use.

3. Exposure time refers to the duration that each layer is exposed to UV light, which is crucial for curing photopolymer resins that harden under light exposure. This parameter significantly impacts print quality, as inadequate exposure can result in incomplete curing, while excessive exposure may lead to over-curing, affecting dimensional accuracy and detail.

For standard layers above the initial bottom layers, an exposure time of 2.5 seconds was selected. Initial tests with exposure times of 4 and 3 seconds resulted in slight protrusions on the first few layers, which affected the surface quality and required post-processing, such as sanding, to smooth out. Based on these observations, the exposure time was refined to 2.5 seconds to achieve a balanced cure with improved accuracy.

For the initial bottom layers, a significant Bottom exposure time of 35 seconds is applied, which is approximately 10 to 20 times the exposure time. This extended duration ensures that the first layers adhere firmly to the build platform, which is vital for handling the high tension these layers experience during the initial stages of printing. This robust adhesion prevents detachment and ensures stability throughout the print process.

4. Transition Layer Count serves as an intermediary between the bottom and normal layers, gradually adjusting the exposure settings to minimize stress on the print. This means that instead of an abrupt shift from the initial layers to the standard layers, the transition occurs gradually, creating a smoother change in exposure. In this setup, 8 transition layers are used to ensure a gradual adjustment between the higher exposure time of the bottom layers and the standard exposure time, reducing the likelihood of layer separation or warping.

5. A linear transition type is selected to gradually decrease the exposure time in evenly distributed steps across the transition layers, reducing the chances of layer separation or warping.

6. During the printing process, the printer enters a "resting" mode at specific points to allow the resin to settle, which helps minimize defects and enhance layer quality. The Rest Time Before Lift setting specifies the pause before lifting the build plate after each layer is cured. Here, it is set to zero, meaning the lift happens immediately after curing to maximize printing speed. Similarly, the Rest Time After Lift is also set to zero, allowing the build plate to transition to the next layer without delay. After the lifting and retraction process, a Rest Time After Retract of 1.1 seconds is applied. This brief pause allows the resin to settle back into place before starting the next layer, which can help reduce resin artifacts and improve surface smoothness.

Figure 41 pertains to the movement settings, detailing how far the build platform will lift, the speed at which it ascends, and the speed at which it retracts. These settings control the platform's motion during the printing process, influencing both the initial lift distances for the bottom layers and the standard layer lift distances, along with their respective speeds for lifting and retracting.

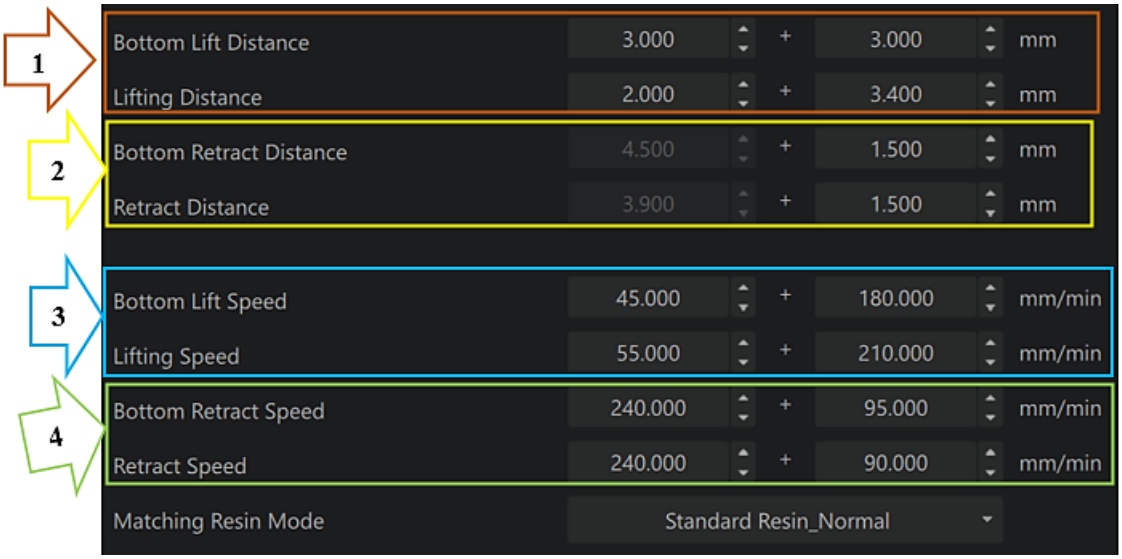

Figure 41 Platform Movement and Speed Settings for 3D Printing Process

1. The movement is divided into two stages. In the first stage, the platform is kept closer to the LCD screen for an initial lift of 3 mm, and then raised an additional 3 mm in the second stage, increasing its distance from the screen. This two-stage lifting method is used to optimize print speed and reduce overall printing time by adjusting the platform’s movement based on its proximity to the LCD.

In the Bottom Lift Distance, the platform is raised after each of the initial 8 layers, set at 3.000 mm,

with an adjustable range that extends to 6.000 mm (3.000 + 3.000). Similarly, in the Lifting Distance, which defines the distance the build platform moves up after each layer is printed, a setting of 2.000 mm is used, with a maximum adjustable range of 5.400 mm (2.000 + 3.400).

2. The Retract Distance refers to the height at which the build plate returns to the resin tank after lifting, typically lowering by the same distance it was raised. Additionally, the Bottom Lift Speed determines the rate at which the plate moves back into the resin tank for all layers following the initial 8 layers, ensuring a consistent return speed throughout the remaining layers.

3. The Bottom Lift Speed represents the speed at which the build plate rises from the resin tank during the first 8 layers. This initial lifting speed is generally reduced to allow the plate to emerge more slowly from the resin for each layer. This slower speed is crucial to ensure that the print adheres firmly to the build plate. In contrast, the Lifting Speed specifies the platform's lifting speed after each subsequent layer, excluding the initial 8 bottom layers. This speed is adjusted for efficiency once the initial layers have secured the print to the plate.

4. These two speeds regulate the plate's descent back into the resin tank. In the model, for instance, the plate is first lowered by 4.5 millimeters at a speed of 240 mm/min, then slowed to 90 mm/min for the final 1.5 millimeters as it nears the LCD. This gradual reduction in speed as it approaches the LCD helps minimize the risk of resin spillage.

After configuring the necessary print settings, the slicing process was executed, providing estimates for print duration, material volume, and part weight. Figure 42 presents the sliced layouts of two different geometries prepared using CHITUBOX software. In Figure 42(a), a batch arrangement of 16 parts for Geometry I is shown, while Figure 42(b) illustrates the layout of 19 parts for Geometry II. These visualizations highlight the efficient use of the build plate in batch printing, demonstrating how multiple components can be optimally positioned for simultaneous fabrication.

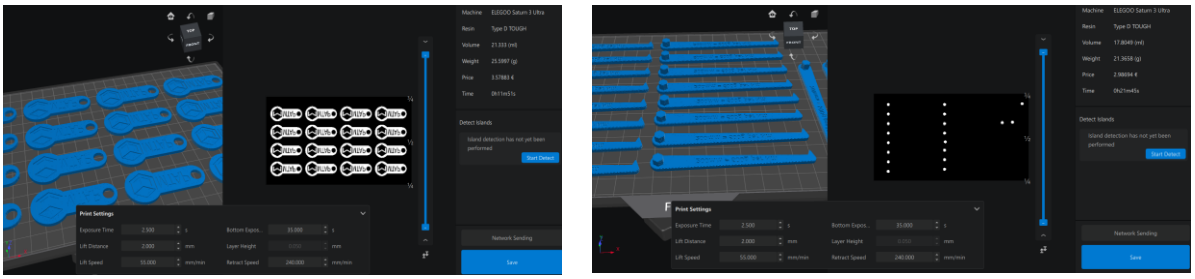

(a) (b)

Figure 42 Slicing and Part Layout for the Geometry (a) I and (b) II, in CHITUBOX

This study also involved the development of a prototype layout, guided by empirical data obtained from a real-world 3D printing environment. The data were collected from a small laboratory located in Berlin. During the experimental phase, two parts with distinct geometrical features were fabricated separately. Each part was initially modeled in FlexSim software to reflect individual production workflows. Subsequently, both models were integrated into a unified simulation environment within FlexSim, enabling the analysis of production line efficiency and layout optimization.

5-3 BPMN Mapping

Figure 43 presents the BPMN (Business Process Model and Notation) diagram that outlines the complete workflow of the 3D printing process using DLP technology, followed by essential post-processing operations to ensure part quality and functionality.

The process initiates with a Start event, indicated by an empty circle, and progresses to the "Printing with DLP" subprocess. This stage, denoted by a rectangular shape with a plus symbol, encapsulates the core printing operations. It includes three preparatory tasks: File Preparation, Machine Setup, and Setting Process Time, represented by individual task elements. These tasks collectively prepare the system for initiating the DLP printing cycle based on predefined settings and geometrical requirements.

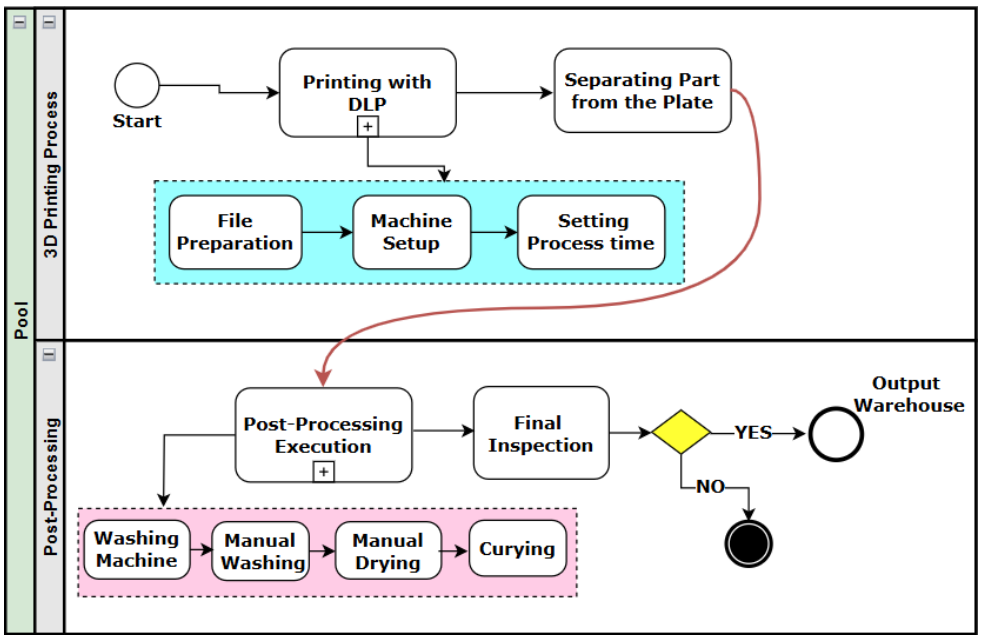

Figure 43 BPMN Diagram of the DLP 3D Printing

Upon completion of the printing operation, the part is separated from the build plate, a standalone task represented in the diagram. This marks the transition from the 3D printing phase to the post-processing phase.

The Post-Processing Execution is represented as a separate subprocess, comprising essential steps designed to improve both the mechanical strength and surface quality of the printed component. Initially, the part is cleaned in an ultrasonic washing machine to remove any uncured resin. This is followed by a manual rinse with water to clear away any residual material, and then manually dried to eliminate moisture in preparation for the curing stage.

The curing process is subsequently conducted in a UV chamber. This step is designed to polymerize any residual resin and to strengthen the part. The curing occurs in two stages: initially, the part is exposed to UV light for five minutes while rotating inside the machine. After manual repositioning to ensure even surface exposure, the part undergoes a second round of UV exposure for an additional five minutes.

After curing, the part advances to the Final Inspection stage, where a decision gateway assesses whether it meets predefined quality standards. If the part satisfies the inspection criteria, it is sent to the Output Warehouse. In the event of a quality failure, the part is discarded, as denoted by the end event symbol (a filled black circle).

This BPMN workflow ensures that each part produced via the DLP process is systematically prepared, printed, post-processed, and inspected to meet stringent quality standards, thereby supporting consistent and reliable production outcomes.

5-4 Production scenarios

To enhance production efficiency, the system model was optimized by reducing idle times and improving the use of available resources. The main goal was to identify the ideal number of machines needed to increase throughput while maintaining efficient resource allocation. To this end, various configurations were explored under different production scenarios, focusing on determining the suitable number of DLP machines, manual washing machines, and Operator 1 required to achieve the production goals. The simulation model, built using FlexSim, was systematically improved to minimize downtime and boost equipment usage, ultimately improving overall system performance. Several configurations were analyzed to understand their effect on output, with an emphasis on

maximizing resource efficiency and system productivity. The FlexSim model specifically examined three key variables: the quantity of DLP machines, manual washing machines, and Operator 1. For each of these, the number of units was varied between one and three. A comprehensive list of the tested configurations is provided in Table 9.

Table 9 Configurations for Machines

Configuration #	DLP Machine	Manual Washing Machines	Operator 1
1	1	1	1
2	1	1	2
3	1	1	3
4	1	2	1
5	1	2	2
6	1	2	3
7	1	3	1
8	1	3	2
9	1	3	3
10	2	1	1
11	2	1	2
12	2	1	3
13	2	2	1
14	2	2	2
15	2	2	3
16	2	3	1
17	2	3	2
18	2	3	3
19	3	1	1
20	3	1	2
21	3	1	3
22	3	2	1
23	3	2	2
24	3	2	3
25	3	3	1
26	3	3	2
27	3	3	3

Table 10 presents the setup and processing times associated with each machine involved in the production workflow. For clarity, time values are expressed in seconds, and processing times are distinguished between Geometry I and Geometry II.

Table 10 Setup and Processing Times

Machine Names	Setup Time (second) for Geometry I & II	Process Time (second) for Geometry I	Process Time (second) for Geometry II
DLP Machine	30	831	1425
Washing Machine	30	600	600

Curing Machine	60	600	600

5-5 Production scenario for geometry I

For Geometry I, illustrated in Figure 42(a), several key assumptions were defined and implemented within the FlexSim simulation model:

- The DLP machine is capable of printing 16 parts simultaneously.
- The simulation runs for 30 days.
- The production schedule consists of two shifts per day.
- A lunch break for the operator is assumed to take place from 12:00 PM to 12:30 PM.
- Saturdays and Sundays are designated as non-working days.
- Working hours are assumed to span from 8:00 AM to 4:00 PM.
- A defect rate of 10% to 15% is anticipated for the produced parts.

The defect rate was derived from preliminary testing, in which three out of 16 parts were defective in the first trial and one part was defective in the second trial, resulting in an average defect rate of 12.5%. To incorporate variability in production quality, a defect range of 10% to 15% was adopted in the simulation.

Table 10 provides details regarding machine setup and processing times, while Table 9 outlines the number of machines used in each production configuration. These assumptions collectively enable a thorough assessment of production performance and layout efficiency across various DLP-based manufacturing configurations.

5-6 Production scenario for geometry II

For Geometry II, depicted in Figure 42(b), a separate simulation was developed in FlexSim, building upon the foundational assumptions established for Geometry I. The core simulation structure remains consistent, with the following key distinctions:

- The DLP machine is assumed to be capable of printing 19 parts simultaneously.

- A defect rate of 15% to 25% is anticipated for the produced parts.

This defect rate range was determined based on initial testing, where 3 out of 19 parts were defective in the first trial and 5 parts were defective in the second, resulting in an average defect rate of 21%. To reflect potential fluctuations in production quality and enhance the robustness of the model, a conservative defect rate range of 15% to 25% was adopted for the simulation.

As with the previous scenario, machine setup and processing times are detailed in Table 10, and the number of machines assigned to each configuration is presented in Table 9.

5-7 Mix production line for geometry I and II

Following the individual simulations of Geometry I and Geometry II, a final integrated simulation was conducted to model a unified production line encompassing both geometries. To maintain consistency and clarity, all general assumptions from the Geometry I simulation were retained, with the following additional parameters specific to the integrated model:

- The DLP machine can print 16 parts simultaneously for the first geometry Figure 42(a).
- The DLP machine can print 19 parts simultaneously for the second geometry Figure 42(b).
- A 10% to 15% defect rate is anticipated for parts corresponding to Geometry I.
- A defect rate of 15% to 25% is anticipated for Geometry II.
- It is assumed that each geometry contributes equally—50%—to the total production output.

The number of machines, along with their respective setup and processing times, are specified in the Global Table within the FlexSim environment, in accordance with the values presented in Table 10. The Global Table in FlexSim serves as a flexible data repository, enabling the storage, management, and centralized access of custom data throughout the simulation model. This functionality facilitates parameter definition, variable tracking, and inter-component communication, ensuring a cohesive and adaptable simulation framework.

6 Modelling in FlexSim

The study aims to design an optimized production line layout to meet processing requirements using FlexSim. The simulation model, illustrated in Figure 44, visually represents the production system, showing connections, configurations, and the overall layout. The model emphasizes two key areas: processing and post-processing, providing a detailed depiction of the system's workflow and structure.

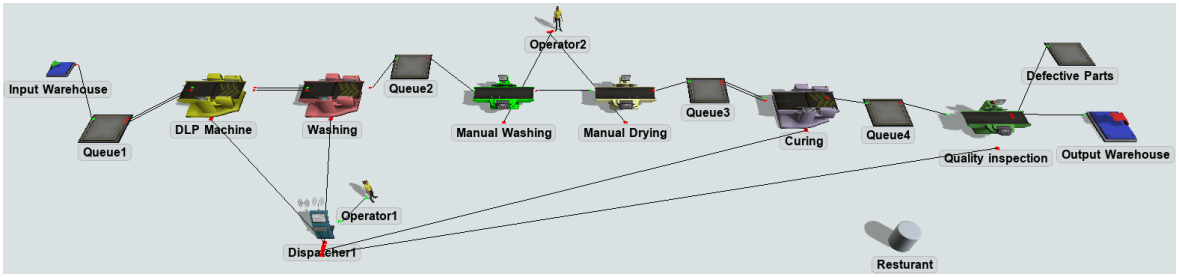

Figure 44 Simulation Model of DLP Production Line in FlexSim

Figure 44 presents a comprehensive simulation model of a production line, which was developed using FlexSim software to facilitate the analysis and optimization of the manufacturing process. The layout is systematically arranged in a linear sequence, commencing with the "Input Warehouse," where raw materials or resin required for the production line enter the workflow. Subsequently, the resin bottles are stored in "Queue 1" to ensure sufficient resin is available prior to initiating production.

Subsequently, the DLP station carries out the printing of the parts. Prior to initiating the print process, the resin is manually stirred using a spatula, and the machine is configured for operation. The layout of the simulation model remains consistent for both geometries, as illustrated in Figure 42(a) and (b). Upon completion of the printing cycle, the machine is paused, and the build plate is carefully removed. The printed parts are then detached from the build plate using a spatula—a task performed by the operator, who is also responsible for both machine setup and part separation.

After printing, the parts proceed to the washing station, where they undergo a thorough cleaning process to remove any residual resin. The washing machine setup is handled by the operator. Following the initial wash, the parts are rinsed with water to eliminate remaining resin traces, and then manually dried using paper towels. These tasks are overseen by a designated operator responsible for the manual operations in this phase.

To pre-emptively manage potential delays in the post-processing phase, Queue 3 was incorporated before the Manual Washing station in the FlexSim simulation model. This station was expected to experience delays due to Operator 2's workload, potentially causing upstream idle times. Likewise, Queue 4 was introduced after the curing step to temporarily hold parts before they entered Quality Inspection, helping to smooth the flow and reduce disruptions. These design choices were embedded in the simulation to evaluate their impact on reducing process congestion and balancing operator tasks.

Once washed and dried, the parts are transferred to the curing machine, which is also prepared by the operator. Upon completion of the curing cycle, each part undergoes a quality inspection. Depending on the inspection outcome, conforming parts are routed to the "Output Warehouse", while defective parts are redirected to a designated Defect Queue. The introduction of Queues 3 and 4 significantly improves production flow continuity, reduces operator strain, and minimizes system-wide delays during periods of peak activity.

A dispatcher coordinates all tasks assigned to Operator 1, ensuring balanced workload distribution and timely execution of tasks across the various stations. To realistically represent work schedules, a restaurant area was integrated into the simulation model, allowing operators to take breaks during predefined intervals.

To maintain equal production output between the two geometries, an empirical distribution was employed. This mechanism assigns an equal probability (50%) to the production of Geometry I and Geometry II. The part type is determined at the Input Warehouse using trigger-based logic, which labels each part according to the defined distribution parameters. To ensure an equal 50% distribution of production between all parts, an empirical distribution is applied, as illustrated in Figure 45.

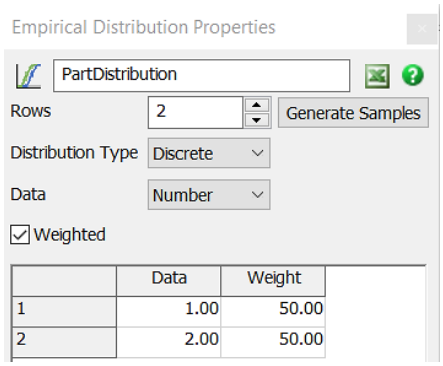

Figure 45 Empirical Distribution for Part Production

In FlexSim, the empirical distribution is configured with two data points, each representing a part

type (1 and 2), with both assigned a weight of 50%. This setup ensures that the simulation randomly selects parts in a balanced manner, reflecting an equal production share for each geometry. The model is designed to follow this distribution strictly, ensuring that 50% of each part type is produced as defined.

To implement this in the Input Warehouse, a trigger is set up in the On Exit section, as shown in Figure 46. In this configuration:

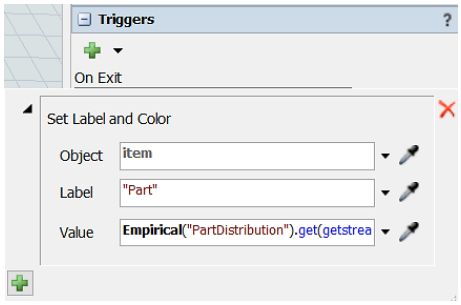

Figure 46 FlexSim Trigger Setup for Part Distribution

- Object: Set to item, indicating that the trigger applies to each part exiting the warehouse.
- Label: Defined as "Part", which categorizes the parts based on the type.
- Value: The function **Empirical**("PartDistribution").get(getstream(current)) is used to assign part types according to the empirical distribution.

By defining the label and assigning values through the empirical distribution, the model ensures that exactly 50% of each geometry type is produced. This setup allows the simulation to adhere to the predefined distribution, maintaining balanced production between the two part types.

To allocate process times defined in the Processing Time table, the setup is configured in the DLP machine's processing time section, as shown in Figure 47. After this allocation, the processing times are retrieved from the global table previously defined.

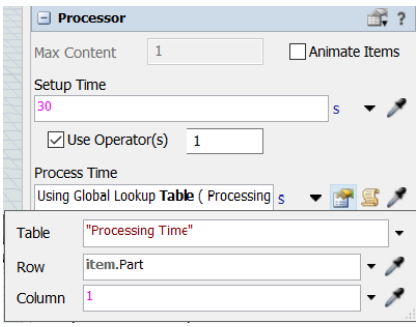

Figure 47 Processor Setup for Processing Time

In this setup:

- Table: The table name is "Processing Time", which matches exactly with the name assigned to the global table. This ensures that the processor pulls the correct data.
- Row: The entry “item.Part” is used here because the Part label was defined earlier in the model. This tells the software to reference the specific row based on the part type. For example, if Part 1 is processed, the first row of the table is used; if Part 2 is processed, the second row is referenced.
- Column: Set to 1, as there is only one column in the global table containing the processing times.

By defining these parameters, the model dynamically assigns the correct processing times for each geometry, ensuring accurate simulation of the production process.

The defective percentage for each geometry in the model is defined in the parameter section of FlexSim. Two separate failure rates are specified: FailureRate1 for Geometry I and FailureRate2 for Geometry II. Figure 48 illustrates the configuration for Geometry I, where a continuous distribution is used to define the defect rate. The lower bound is set at 10%, and the upper bound at 15%, representing the expected defect rate range. The final value displayed in the table is the average of these bounds, which is used in the simulation.

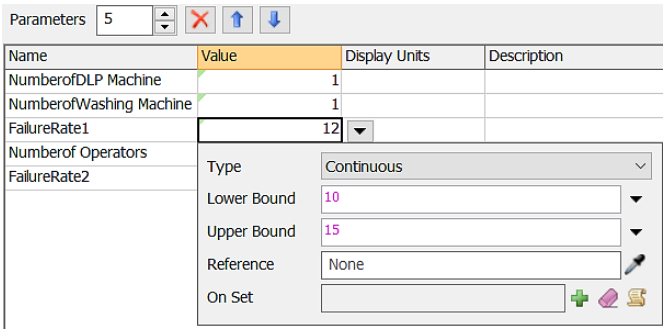

Figure 48 Failure Rate Definition in FlexSim

Defective percentages are defined within the Quality Inspection Machine in the model, where parts are inspected before being sent to the Output Warehouse. To implement this, the Send to Port section of the machine’s output settings is configured. As shown in Figure 49, Port by Case is selected, and two additional cases are added using the plus (+) button. This results in the creation of Case 1 and Case 2, directing parts based on their geometry.

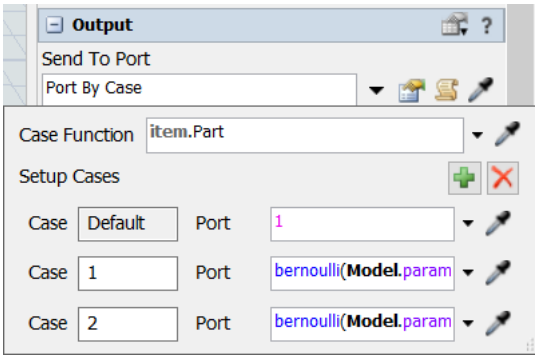

Figure 49 Defective Part Routing Setup

To define the routing logic, a Bernoulli distribution is used, as it models a binary outcome—either the part is defective or not. By clicking the small black triangle next to the port field, the Statistical Distributions menu is accessed, and Bernoulli is selected. The Bernoulli function in FlexSim is structured as: bernoulli(50,5,10, getstream(current)).

- 50 represents the defect percentage, which is replaced with Model.parameters.FailureRate1 for Geometry I.
- 5 and 10 are parameters replaced with 2 and 1, where 2 represents defective parts and 1 represents healthy parts.

For Geometry II, the same logic is applied, but FailureRate1 is replaced with FailureRate2 to reflect its specific defect rate. Additionally, in the Case Function field, "item.Part" is specified, referring to a label named Part that was previously defined in the Input Warehouse. This ensures that parts are accurately categorized before being processed by the Quality Inspection Machine. Once these parameters and assumptions are set in the FlexSim model, the simulation is executed.

7 Simulation results and discussion

This section presents the simulation outcomes for the three production scenarios, with a focus on evaluating system performance through key indicators such as throughput, queue times, machine utilization, and bottlenecks. Among these, throughput is emphasized as the primary measure of productivity, representing the total number of defect-free parts completed and transferred to the output warehouse during the simulation period. In the context of additive manufacturing, where processing times and resource coordination significantly impact overall efficiency, analyzing throughput provides a clear benchmark for comparing the effectiveness of different production configurations.

7-1 Production line for geometry I

To analyze production flow patterns, Figure 50 illustrates the Work-In-Progress (WIP) levels in Queue 2 over time for Geometry I. The cyclic nature of the flow is evident, demonstrating a repetitive pattern of sharp peaks and troughs due to the deterministic timing of the system. The x-axis represents simulation time, while the y-axis indicates the number of parts in the queue, with content levels peaking at approximately 350 units.

These periodic fluctuations reflect a well-regulated production flow, where the timing and coordination of automated or scheduled operations contribute to overall system stability. Additionally, the scrollbar beneath the figure highlights that the visible time frame is a segment of a longer simulation period, underscoring the consistency and robustness of the production process over time.

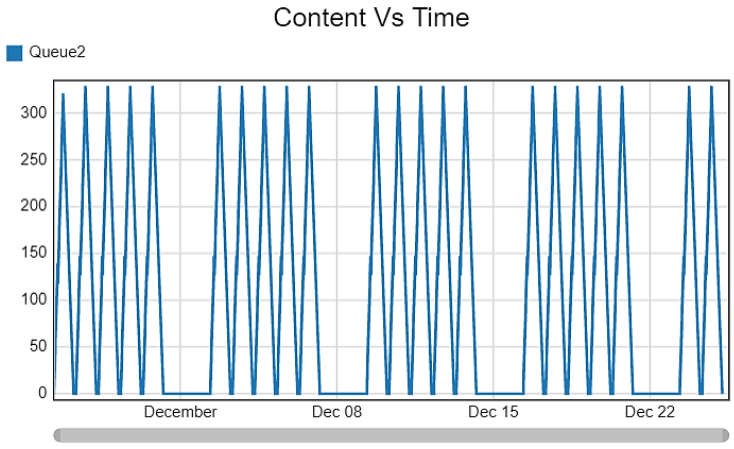

Figure 50 Cyclic analysis of WIP levels in Queue2 over time for Geometry I.

The total monthly output was evaluated using a tabular representation for clarity. Table 11 presents the throughput of the Output Warehouse over one month, confirming a total output of 11,193 parts. This concise numerical format ensures precise reference and facilitates clear evaluation of production performance.

Table 11 Output Analysis – Geometry I

Object	Throughput
Output Warehouse	11,193

To identify the most efficient production configuration, Table 12 summarizes the simulation results across multiple scenarios, each representing a distinct machine setup. This comparative evaluation enables a clear assessment of production performance under varying operational conditions. For each configuration, the simulation was repeated 50 times independently to ensure statistical reliability. The reported values represent the mean and standard deviation of the resulting production outputs.

Table 12 Production Rate Comparison- geometry I

Scenario #	Production (Mean, std)	Scenario #	Production (Mean, std)
1	**(11683.90, 38.12)**	15	(10649.44, 608.71)
2	(11719.06, 37.50)	16	(6850.20, 652.40)
3	(11719.06, 37.50)	17	(10362.66, 1273.98)
4	(11568.34, 313.20)	18	(10221.76, 1212.12)
5	(11592.82, 312.61)	19	(7376.32, 684.35)
6	(11600.68, 316.67)	20	(6784.04, 999.27)
7	(11774.26, 52.83)	21	(7058.02, 1141.00)
8	(11817.84, 57.04)	22	(6135.68, 1299.62)
9	(11760.90, 37.83)	23	(4991.20, 1023.79)
10	(10439.34, 1110.95)	24	(3974.76, 1011.57)
11	(10616.62, 1255.74)	25	(6090.96, 749.69)
12	(10751.08, 782.50)	26	(7284.10, 1348.36)
13	(6758.02, 30.88)	27	(5903.22, 664.24)
14	(10802.44, 642.51)		

The results indicate that Scenarios 1–9 yield the highest production rates, averaging between approximately 11,600 and 11,800 parts per month. Notably, Scenario 1 emerges as the most optimal configuration, achieving the highest output of 11,683.90 parts with a low standard deviation of 38.12, highlighting both high performance and strong consistency. This indicates that the simplest configuration was not only the most productive but also the most stable for the production of

Geometry I parts. Scenario 2, while achieving a comparable production rate of 11,719.06 parts, shows a slightly higher variability (standard deviation of 37.50) compared to Scenario 1 (38.12). Although both scenarios exhibit excellent stability and high outputs, Scenario 1 still maintains a slight advantage in terms of overall efficiency and consistency, positioning it as the preferred choice for maximizing performance while minimizing resource usage.

A noticeable decline in production performance was observed in Scenarios 10 to 14, where two DLP machines were employed. These scenarios achieved moderate production rates between 10,439 and 10,802 units but showed an increase in variability compared to the best-performing group. This suggests that adding an additional DLP machine without adequately adjusting the number of supporting resources, such as washing machines and operators, did not lead to an improvement and, in some cases, even reduced overall system efficiency.

The poorest performance was recorded in Scenarios 15 through 27, where the mean production rates dropped significantly to values between 6,850 and 3,974 units. These scenarios, often involving three DLP machines, exhibited large standard deviations, frequently exceeding 600 units and in some cases surpassing 1,000 units. This high variability indicates that the system became unstable and inefficient when additional DLP machines were introduced without sufficient balancing of post-processing resources and workforce allocation.

Overall, the analysis highlights that simple system configurations—specifically, those involving a balanced one-to-one-to-one ratio of DLP machines, manual washing machines, and operators—are not only the most productive but also offer the most consistent performance. The results suggest that scaling up production by simply increasing the number of printers does not linearly translate into higher throughput. Instead, it often introduces bottlenecks and resource conflicts that degrade system performance. Therefore, future scaling strategies must consider proportional adjustments across all stages of the production process to ensure that efficiency and stability are maintained.

7-2 Production line for geometry II

Table 13 presents the output analysis for the second geometry, based on simulations conducted in FlexSim. The primary performance metric evaluated is system throughput, defined as the total number of parts successfully produced and transferred to the output warehouse over the simulation period. For this geometry, the throughput reached 3,216 parts, reflecting the system's productivity under the specified configuration, assumptions, and operational parameters.

Table 13 Output Analysis – Geometry II

Object	Throughput
Output Warehouse	3,216

Table 14 summarizes the simulation outcomes across multiple scenarios to identify the most efficient production configuration. These results offer a comprehensive evaluation of the system's monthly production performance under varying operational conditions.

Table 14 Production Rate Comparison- geometry II

Scenario #	Production (Mean, std)	Scenario #	Production (Mean, std)
1	(3050.26, 336.45)	15	(3797.70, 393.65)
2	(3486.64, 317.63)	16	(4428.02, 332.75)
3	(3394.16, 296.15)	17	(5218.10, 730.25)
4	(3903.96, 594.26)	18	(5567.72, 782.89)
5	(3939.88, 323.80)	19	(6754.90, 766.99)
6	(3982.22, 239.62)	20	(5661.50, 646.09)
7	(3741.94, 130.63)	21	(5508.76, 679.88)
8	(4349.24, 591.98)	22	(4899.06, 161.32)
9	(4081.36, 560.83)	23	(5044.90, 690.58)
10	(5002.74, 725.42)	24	(6381.00, 1117.56)
11	(4706.16, 481.99)	25	(5984.72, 917.45)
12	(4992.10, 803.85)	26	(4994.12, 1110.22)
13	(4031.08, 126.16)	27	(4646.23, 421.62)
14	(4060.08, 714.52)		

The production rates vary significantly across scenarios, reflecting the sensitivity of output to changes in machine and operator configurations defined in Table 9. Among all scenarios, Scenario 19 achieves the highest average production rate with 6,754.90 units, followed by Scenario 24 with 6,381.00 units and Scenario 18 with 5,567.72 units. These results underscore the importance of optimized resource allocation in mixed-part production lines, especially for more complex or longer-duration parts such as Geometry II.

Scenario 19 again stands out, not only delivering the highest output but doing so with a lean configuration of 3 DLP machines, 1 manual washing machine, and 1 operator, confirming its overall system efficiency observed previously in the mixed production line analysis. This configuration balances high core production capacity with minimal but sufficient support resources, resulting in a system that is both productive and resource-efficient. Scenario 24, with a more resource-intensive setup (3 DLP, 2 washing machines, 3 operators), offers a high output but comes with the highest

standard deviation (1,117.56 units), indicating increased variability in system performance, likely due to complexities in coordinating a larger number of resources.

Scenario 18 (3 DLP, 1 washing machine, 3 operators) also achieves a high mean output, but like Scenario 24, it suffers from elevated variability (std = 782.89). This suggests that increasing the operator count without adjusting process control or task scheduling may contribute to inconsistent production performance. In contrast, lower-performing configurations, such as Scenario 1 (mean = 3,050.26 units) and Scenario 2 (mean = 3,486.64 units), are characterized by fewer DLP machines (only one), confirming that the number of core printing units remains the most critical factor influencing throughput for Geometry II.

The observed standard deviations across scenarios indicate that the production of Geometry II is particularly sensitive to the synchronization between printing and post-processing stages. Since this geometry likely involves longer DLP printing times or more intensive post-processing, asynchronous resource availability and queue buildup can exacerbate performance fluctuations. Scenarios with high throughput also tend to exhibit high variability, which reflects the complex dynamics of mixed-part scheduling and resource contention in shared environments.

To reduce variability and improve the stability of Geometry II production, strategic interventions such as geometry-based job prioritization, dynamic resource allocation, or buffer tuning can be implemented. These approaches could help streamline flow and reduce delays caused by mismatches in resource timing or competition between part types.

Overall, Scenario 19 emerges as the most balanced and optimal configuration for producing Geometry II, achieving the highest output with minimal support resources and acceptable variability. This further validates its suitability for efficient, high-throughput production in mixed-line additive manufacturing systems. Other high-output scenarios, such as 24 and 18, demonstrate potential but would require better control over operational variability to be considered equally effective.

To further support these findings and reduce redundancy, a replication plot—illustrated in Figure 51—is proposed specifically for Geometry II, providing a clear visual comparison of monthly production outputs across all scenarios.

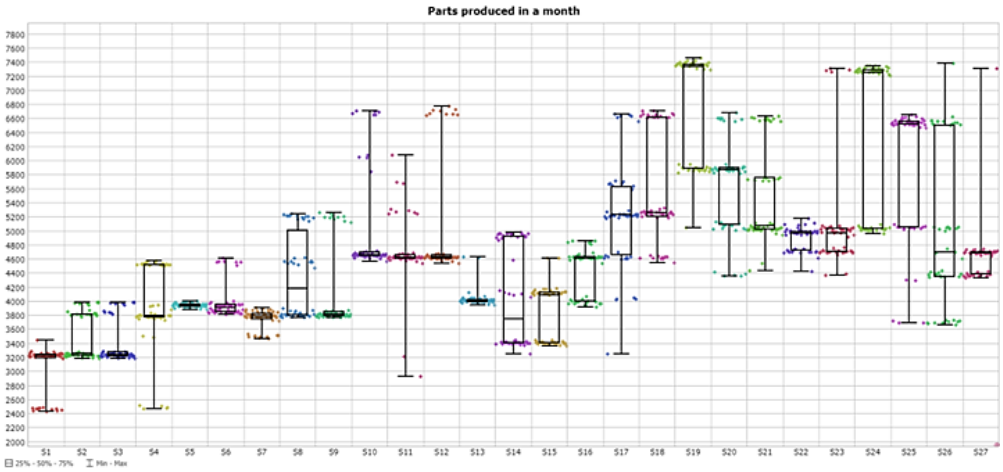

Figure 51 Replication Plot of Monthly Production Outputs for Scenarios - geometry II

This visualization enables a clearer comparison of production performance across scenarios, supporting the identification of the optimal configuration by balancing production output and operational efficiency.

7-3 Mix production line for geometry I and II

After defining the necessary parameters and assumptions in the FlexSim model, the simulation was executed to analyse the production performance of the integrated system. The results, as presented in Table 15, provide insights into the total production output and the distribution of part types within the system. The table shows that the Output Warehouse processed a total of 5,367 parts during the simulation period. This total is further broken down by geometry type: 2,775 parts correspond to Type 1 (Geometry I), while 2,592 parts correspond to Type 2 (Geometry II). These findings highlight the system's overall production efficiency and demonstrate a slightly higher throughput for Type 1 parts compared to Type 2.

Table 15 Production Throughput Summary - Mix Production Line

Category	Type	Throughput
Total Output	–------	5,367
By Geometry Type	Type 1	2,775
By Geometry Type	Type 2	2,592

Transitioning from single-part to mixed-part production introduced several operational challenges that significantly impacted overall throughput. As shown in Table 15, the total output in the mixed production configuration reached 5,367 parts, with 2,775 units of Geometry I and 2,592 units of Geometry II. This performance is notably lower compared to the dedicated lines, where throughput

reached 11,193 parts for Geometry I (see Table 11) and 3,216 parts for Geometry II (see Table 13). Despite using a similar machine configuration across setups, the mixed production line produced less than half the output of the Geometry I line and approximately 1,500 fewer parts than the Geometry II line. This substantial decline in productivity is attributed to the increased system complexity when simultaneously processing parts with different geometrical and temporal characteristics, particularly in the DLP printing stage, where processing times vary between the two geometries.

Moreover, the mixed line introduced greater competition for shared resources such as washing machines and operators. The need to dynamically coordinate task assignments across part types added further strain to scheduling efficiency, often resulting in longer queue times and idle machine states. These inefficiencies were reflected in higher standard deviations for several scenarios in Table 16, underscoring variability and instability in mixed production conditions. Collectively, these findings highlight the trade-off between production flexibility and operational efficiency—while mixed-line setups support diverse part outputs within a single workflow, they require more sophisticated scheduling strategies and resource synchronization to avoid substantial performance degradation compared to dedicated production lines.

To determine the most effective production setup, various scenarios were analysed. The results, summarized in Table 16, reveal the production rates achieved under different configurations of DLP machines, manual washing machines, and operators, as defined in Table 9. Among the 27 evaluated scenarios, Scenarios 19, 20, and 21 demonstrated the highest production rates. Scenario 20 achieved the peak output of 7,395 units using six machines (3 DLP, 2 washing machines, and 1 operator), followed closely by Scenario 21 with 7,176 units (3 DLP, 2 washing machines, 2 operators). Although Scenario 19 produced a slightly lower output of 7,046 units, it did so with only five machines (3 DLP, 1 washing machine, and 1 operator), positioning it as a highly efficient configuration in terms of both performance and resource utilization.

These top-performing scenarios all share the use of three DLP machines—the maximum tested—highlighting that the number of DLP units is the dominant factor in maximizing throughput. However, differences in the number of supporting resources reveal that increasing manual washing machines and operators beyond a certain point does not yield proportional productivity gains and may introduce inefficiencies. For example, although Scenario 26 employed the same number of DLP machines and even more support resources (3 washing machines and 2 operators), its output (7,223 units) was still marginally lower than Scenario 20's, suggesting diminishing returns when resource allocation exceeds process demand.

Table 16 Production Rate Comparison - Mix Production Line

Scenario #	Production (Mean, std)	Scenario #	Production (Mean, std)
1	(4054, 1406)	15	(5957, 1412)
2	(3952, 1383)	16	(6661, 1288)
3	(4254, 1346)	17	(6206, 1482)
4	(3628, 1076)	18	(6197, 1409)
5	(3918, 1317)	19	(7046, 1768)
6	(3865, 1321)	20	(7395, 1225)
7	(4073, 1294)	21	(7176, 1682)
8	(3866, 1300)	22	(6266, 1655)
9	(4140, 1268)	23	(6768, 1463)
10	(6730, 1454)	24	(6653, 1245)
11	(6513, 1255)	25	(6983, 1512)
12	(6956, 1321)	26	(7223, 1277)
13	(6866, 1234)	27	(6956, 1342)
14	(6422, 1067)		

The relatively high standard deviations observed in Table 16 reflect the increased variability and operational uncertainty inherent in mixed-part production lines. This variability arises primarily from the differences in processing times between Geometry I and Geometry II, particularly during the DLP printing stage, which leads to asynchronous machine availability and fluctuating queue lengths. Additionally, the shared utilization of machines and post-processing resources introduces dynamic competition between part types, further amplifying performance fluctuations across simulation replications. To mitigate this variability and lower the standard deviation, operational strategies such as implementing geometry-specific buffering or batching mechanisms and refining scheduling rules to prioritize part flow based on processing time or downstream availability could be considered. These adjustments aim to enhance the consistency of production performance without compromising the flexibility of mixed-line manufacturing.

8 Conclusions and Future Works

Conclusions

This thesis has investigated the application of Discrete Event Simulation (DES) to optimize production workflows in Additive Manufacturing (AM), specifically targeting the efficiency, scalability, and reliability of industrial-scale 3D printing. The research developed and validated a simulation-driven framework using FlexSim to analyze and improve production strategies across three AM technologies: Selective Laser Sintering (SLS), Stereolithography (SLA), and Digital Light Processing (DLP).

Through the use of FlexSim-based case studies, this work demonstrates that DES enables a systematic evaluation of machine utilization, post-processing dynamics, and job scheduling strategies. The findings underscore that simulation not only supports performance optimization during system design but also provides continuous improvement opportunities during operational phases. Notably, DES proves effective in identifying bottlenecks, minimizing idle time, and improving resource allocation in complex AM workflows. The thesis makes several contributions to the field of AM:

- Proposing an adaptable DES framework tailored to the unique challenges of AM systems.
- Validating this framework across multiple AM technologies and production scenarios.
- Demonstrating how DES can support data-driven decision-making to improve throughput, reduce costs, and increase production consistency.

Although notable progress has been made, the research recognizes several limitations, including its dependence on precise input data and the necessary simplifications involved in building any simulation model. Moreover, while the study centers on three additive manufacturing technologies, its broader applicability could be enhanced by incorporating further case studies involving different printing techniques and post-processing settings.

In summary, this study underscores the value of Discrete Event Simulation as a key enabler in advancing the industrialization of Additive Manufacturing. Connecting theoretical models with real-world applications, it aids AM stakeholders in developing more efficient, scalable, and data-driven production systems.

Future Work

Building upon the results and limitations of this thesis, several directions are proposed for future research:

- Real-Time Data Integration: Integrating live production data with simulation models could enable adaptive planning and real-time monitoring for dynamic decision-making.
- Hybrid Simulation Models: Combining DES with Agent-Based Modeling (ABM) or System Dynamics (SD) may provide a more comprehensive analysis of complex and long-term interactions in AM systems.
- AI-Enhanced Optimization: Future work may explore embedding artificial intelligence and machine learning into simulation environments to automate process optimization, scheduling, and defect prediction.
- Expansion to Additional AM Technologies: Future studies could extend the framework to include other printing methods, such as Fused Deposition Modeling (FDM) and Binder Jetting, to improve generalizability and broaden industrial relevance.
- Environmental and Economic Metrics: Incorporating life-cycle assessment (LCA), energy consumption, and waste reduction into DES models would support the development of sustainable and cost-effective AM production strategies.

Pursuing these research avenues will further solidify simulation's pivotal role in evolving additive manufacturing into a robust, scalable, and fully industrialized production framework.

Bibliography

[1] A.M. Law, W.D. Kelton, W.D. Kelton, Simulation modeling and analysis, Mcgraw-hill New York, 2007.
[2] J. Fleischer, S. Niggeschmidt, M. Wawerla, Optimizing the life-cycle-performance of machine tools by reliability and availability prognosis, in: Advances in Life Cycle Engineering for Sustainable Manufacturing Businesses: Proceedings of the 14th CIRP Conference on Life Cycle Engineering, Waseda University, Tokyo, Japan, June 11th–13th, 2007, Springer, 2007, pp. 329-334.
[3] G. Gao, J. Sun, The application of program analysis method in streamline balance, Machinery Design and Manufacture, 7 (2007) 204-206.
[4] A. Anglani, A. Grieco, M. Pacella, T. Tolio, Object-oriented modeling and simulation of flexible manufacturing systems: a rule-based procedure, Simulation Modelling Practice and Theory, 10 (2002) 209-234.
[5] D. Hounshell, From the American system to mass production, 1800-1932: The development of manufacturing technology in the United States, Jhu Press, 1984.
[6] K.H. Oh, Expert line balancing system (ELBS), Computers & industrial engineering, 33 (1997) 303-306.
[7] H. Pierreval, C. Caux, J. Paris, F. Viguier, Evolutionary approaches to the design and organization of manufacturing systems, Computers & Industrial Engineering, 44 (2003) 339-364.
[8] Z. Xuelong, Work research applied to enterprise production line optimization redesign-case study, Modern Manufacturing Engineering, 3 (2015) 27-32.
[9] M.H. Rais, Y. Li, I. Ahmed, Dynamic-thermal and localized filament-kinetic attacks on fused filament fabrication based 3D printing process, Additive Manufacturing, 46 (2021) 102200.
[10] D.K. Sahini, J. Ghose, S.K. Jha, A. Behera, A. Mandal, Optimization and simulation of additive manufacturing processes: challenges and opportunities–a review, Additive manufacturing applications for metals and composites, (2020) 187-209.
[11] A. Imširović, G. Kumnova, Utilizing 3D Printing to Provide Customized Joysticks, Gothenburg, Sweden: Chalmers University of Technology, (2017).
[12] A.J. Pontes, Designing for additive manufacturing, Design and Manufacturing of Plastics Products; Elsevier: Amsterdam, The Netherlands, (2021) 249-292.
[13] K.V. Wong, A. Hernandez, A review of additive manufacturing, International scholarly research notices, 2012 (2012) 208760.
[14] T. Kermavnar, A. Shannon, L.W. O'Sullivan, The application of additive manufacturing/3D printing in ergonomic aspects of product design: A systematic review, Applied Ergonomics, 97 (2021) 103528.
[15] D. Popescu, D. Laptoiu, Rapid prototyping for patient-specific surgical orthopaedics guides: A systematic literature review, Proceedings of the Institution of Mechanical Engineers, Part H: Journal of Engineering in Medicine, 230 (2016) 495-515.
[16] K.E. Madden, A.D. Deshpande, On integration of additive manufacturing during the design and development of a rehabilitation robot: a case study, Journal of Mechanical Design, 137 (2015) 111417.
[17] L.J. Tan, W. Zhu, K. Zhou, Recent progress on polymer materials for additive manufacturing, Advanced Functional Materials, 30 (2020) 2003062.
[18] B. Redwood, F. Schffer, B. Garret, The 3D printing handbook: technologies, design and applications, 3D Hubs, 2017.
[19] A. Bandyopadhyay, S. Bose, Additive manufacturing, CRC press, 2019.
[20] C. Petropolis, D. Kozan, L. Sigurdson, Accuracy of medical models made by consumer-grade fused deposition modelling printers, Plastic Surgery, 23 (2015) 91-94.

[21] M. George, K.R. Aroom, H.G. Hawes, B.S. Gill, J. Love, 3D printed surgical instruments: the design and fabrication process, World journal of surgery, 41 (2017) 314-319.
[22] R. Singh, A. Suri, S. Anand, B. Baby, Validation of reverse-engineered and additive-manufactured microsurgical instrument prototype, Surgical innovation, 23 (2016) 606-612.
[23] S.-H. Kim, J. Kwon, Y.-J. Kim, H.-J. Lee, H.-C. Seo, S.B. Lim, S. Joo, D.-W. Seo, W.-Y. Kim, S.-B. Hong, Impact of a custom-made 3D printed ergonomic grip for direct laryngoscopy on novice intubation performance in a simulated easy and difficult airway scenario—a manikin study, PLoS One, 13 (2018) e0207445.
[24] R. Jafri, S.A. Ali, Utilizing 3D printing to assist the blind, in: 2015 International Conference on Health Informatics and Medical Systems (HIMS'15)(Las Vegas, Nevada, 2015), 2015, pp. 55-61.
[25] Z.X. Khoo, J.E.M. Teoh, Y. Liu, C.K. Chua, S. Yang, J. An, K.F. Leong, W.Y. Yeong, 3D printing of smart materials: A review on recent progresses in 4D printing, Virtual and Physical Prototyping, 10 (2015) 103-122.
[26] Y. Huang, M.C. Leu, J. Mazumder, A. Donmez, Additive manufacturing: current state, future potential, gaps and needs, and recommendations, Journal of Manufacturing Science and Engineering, 137 (2015) 014001.
[27] T. Wohlers, Wohlers report 2019: 3D printing and additive manufacturing state of the industry, (No Title), (2019).
[28] R. Krishna, M. Manjaiah, C. Mohan, Developments in additive manufacturing, in: Additive manufacturing, Elsevier, 2021, pp. 37-62.
[29] S.D. Kumar, D. Karthik, A. Mandal, J.P. Kumar, Optimization of Thixoforging process parameters of A356 alloy using Taguchi's experimental design and DEFORM Simulation, Materials Today: Proceedings, 4 (2017) 9987-9991.
[30] D.B. Kim, P. Witherell, R. Lipman, S.C. Feng, Streamlining the additive manufacturing digital spectrum: A systems approach, Additive manufacturing, 5 (2015) 20-30.
[31] Y. Lu, S. Choi, P. Witherell, Towards an integrated data schema design for additive manufacturing: Conceptual modeling, in: International design engineering technical conferences and computers and information in engineering conference, American Society of Mechanical Engineers, 2015, pp. V01AT02A032.
[32] D.B. Kim, P. Witherell, Y. Lu, S. Feng, Toward a digital thread and data package for metals-additive manufacturing, Smart and sustainable manufacturing systems, 1 (2017) 75-99.
[33] Z. Isania, M.P. Fanti, G. Casalino, Some Challenges and Opportunities in Additive Manufacturing Industrialization Process, in: International Conference on Flexible Automation and Intelligent Manufacturing, Springer, 2023, pp. 311-318.
[34] Y. Zhai, D.A. Lados, J.L. LaGoy, Additive manufacturing: making imagination the major limitation, Jom, 66 (2014) 808-816.
[35] C.K. Chua, C.H. Wong, W.Y. Yeong, Standards, quality control, and measurement sciences in 3D printing and additive manufacturing, Academic Press, 2017.
[36] J. Wang, D. Gu, Z. Yu, C. Tan, L. Zhou, A framework for 3D model reconstruction in reverse engineering, Computers & Industrial Engineering, 63 (2012) 1189-1200.
[37] S.U. AMM, A. DM D, K.H. Harib, T. Lin, Fractals and additive manufacturing, International Journal of Automation Technology, 10 (2016) 222-230.
[38] P. Mohan Pandey, N. Venkata Reddy, S.G. Dhande, Slicing procedures in layered manufacturing: a review, Rapid prototyping journal, 9 (2003) 274-288.
[39] R. Ponche, O. Kerbrat, P. Mognol, J.-Y. Hascoet, A novel methodology of design for Additive Manufacturing applied to Additive Laser Manufacturing process, Robotics and Computer-Integrated Manufacturing, 30 (2014) 389-398.
[40] G.A. Adam, D. Zimmer, Design for Additive Manufacturing—Element transitions and aggregated structures, CIRP Journal of Manufacturing Science and Technology, 7 (2014) 20-28.
[41] R. Wauthle, B. Vrancken, B. Beynaerts, K. Jorissen, J. Schrooten, J.-P. Kruth, J. Van

Humbeeck, Effects of build orientation and heat treatment on the microstructure and mechanical properties of selective laser melted Ti6Al4V lattice structures, Additive manufacturing, 5 (2015) 77-84.
[42] N. Gardan, A. Schneider, Topological optimization of internal patterns and support in additive manufacturing, Journal of Manufacturing Systems, 37 (2015) 417-425.
[43] I. ASTM, ASTM52915-13, Standard specification for additive manufacturing file format (AMF) Version 1.1, ASTM International, West Conshohocken, PA, 52915 (2013) 2013.
[44] A. Cooke, J. Slotwinski, Properties of metal powders for additive manufacturing: a review of the state of the art of metal powder property testing, (2012).
[45] S. Moylan, J. Slotwinski, A. Cooke, K. Jurrens, M.A. Donmez, An additive manufacturing test artifact, Journal of research of the National Institute of Standards and Technology, 119 (2014) 429.
[46] W.E. Frazier, Metal additive manufacturing: a review, Journal of Materials Engineering and performance, 23 (2014) 1917-1928.
[47] A.C. Kak, M. Slaney, Principles of computerized tomographic imaging, SIAM, 2001.
[48] S.A. Khairallah, A.T. Anderson, A. Rubenchik, W.E. King, Laser powder-bed fusion additive manufacturing: Physics of complex melt flow and formation mechanisms of pores, spatter, and denudation zones, Acta Materialia, 108 (2016) 36-45.
[49] B. Salzbrenner, B. Boyce, B.H. Jared, J. Rodelas, J.R. Laing, Defect Characterization for Material Assurance in Metal Additive Manufacturing (FY15-0664), in, Sandia National Lab.(SNL-NM), Albuquerque, NM (United States), 2016.
[50] J.M. Waller, B.H. Parker, K.L. Hodges, E.R. Burke, J.L. Walker, Nondestructive evaluation of additive manufacturing state-of-the-discipline report, in, 2014.
[51] J.A. Slotwinski, E.J. Garboczi, K.M. Hebenstreit, Porosity measurements and analysis for metal additive manufacturing process control, Journal of research of the National Institute of Standards and Technology, 119 (2014) 494.
[52] J.J. Lewandowski, M. Seifi, Metal additive manufacturing: a review of mechanical properties, Annual review of materials research, 46 (2016) 151-186.
[53] J. Slotwinski, A. Cooke, S. Moylan, Mechanical properties testing for metal parts made via additive manufacturing: a review of the state of the art of mechanical property testing, National Institute of Standards and Technology, (2012).
[54] J.-Y. Lee, J. An, C.K. Chua, Fundamentals and applications of 3D printing for novel materials, Applied materials today, 7 (2017) 120-133.
[55] E. Atzeni, A. Salmi, Economics of additive manufacturing for end-usable metal parts, The International Journal of Advanced Manufacturing Technology, 62 (2012) 1147-1155.
[56] N. Guo, M.C. Leu, Additive manufacturing: technology, applications and research needs, Frontiers of mechanical engineering, 8 (2013) 215-243.
[57] A. Gogate, S. Pande, Intelligent layout planning for rapid prototyping, International Journal of Production Research, 46 (2008) 5607-5631.
[58] R. Liu, X. Xie, K. Yu, Q. Hu, A survey on simulation optimization for the manufacturing system operation, International Journal of Modelling and Simulation, 38 (2018) 116-127.
[59] Siemens, The factory of the future for 3D printing (Access date: 19 Sep 2024), https://blog.siemens.com/2023/05/the-factory-of-the-future-for-3d-printing/.
[60] W. ElMaraghy, H. ElMaraghy, T. Tomiyama, L. Monostori, Complexity in engineering design and manufacturing, CIRP annals, 61 (2012) 793-814.
[61] F. Tao, Q. Qi, L. Wang, A. Nee, Digital twins and cyber–physical systems toward smart manufacturing and industry 4.0: Correlation and comparison, Engineering, 5 (2019) 653-661.
[62] L. Morabito, M. Ippolito, E. Pastore, A. Alfieri, F. Montagna, A discrete event simulation based approach for digital twin implementation, IFAC-PapersOnLine, 54 (2021) 414-419.
[63] U. Dahmen, J. Rossmann, Experimentable digital twins for a modeling and simulation-based engineering approach, in: 2018 IEEE International Systems Engineering Symposium (ISSE), IEEE,

2018, pp. 1-8.
[64] W. Kritzinger, M. Karner, G. Traar, J. Henjes, W. Sihn, Digital Twin in manufacturing: A categorical literature review and classification, Ifac-PapersOnline, 51 (2018) 1016-1022.
[65] S. Lidberg, L. Pehrsson, M. Frantzén, Applying aggregated line modeling techniques to optimize real world manufacturing systems, Procedia Manufacturing, 25 (2018) 89-96.
[66] I.R. Iriondo, A.U. Zearra, A.K. Igartua, DISCRETE EVENT SIMULATION PROCEDURE TO BUILD THE PRODUCTION DIGITAL TWIN OF HIGHLY AUTOMATED AND COMPLEX PRODUCTION SYSTEMS.
[67] H. Qin, H. Wang, Y. Zhang, L. Lin, Constructing digital twin for smart manufacturing, in: 2021 IEEE 24th International Conference on Computer Supported Cooperative Work in Design (CSCWD), IEEE, 2021, pp. 638-642.
[68] A. Negahban, J.S. Smith, Simulation for manufacturing system design and operation: Literature review and analysis, Journal of manufacturing systems, 33 (2014) 241-261.
[69] B.H. Huynh, H. Akhtar, W. Li, Discrete event simulation for manufacturing performance management and optimization: a case study for model factory, in: 2020 9th International Conference on Industrial Technology and Management (ICITM), IEEE, 2020, pp. 16-20.
[70] O. Omogbai, K. Salonitis, Manufacturing system lean improvement design using discrete event simulation, Procedia CIRP, 57 (2016) 195-200.
[71] S. Velumani, H. Tang, Operations status and bottleneck analysis and improvement of a batch process manufacturing line using discrete event simulation, Procedia Manufacturing, 10 (2017) 100-111.
[72] N. Prajapat, T. Waller, J. Young, A. Tiwari, Layout optimization of a repair facility using discrete event simulation, Procedia CIRP, 56 (2016) 574-579.
[73] S.A. White, Introduction to BPMN, Ibm Cooperation, 2 (2004) 0.
[74] M. Weske, Concepts, languages, architectures, Business Process Management, (2007).
[75] W.M. Van der Aalst, Business process management: a comprehensive survey, International Scholarly Research Notices, 2013 (2013) 507984.
[76] B.P. Model, Notation (BPMN) version 2.0, OMG Specification, Object Management Group, 19 (2011) 52-60.
[77] M. Owen, J. Raj, BPMN and business process management, Introduction to the new business process modeling standard, (2003) 1-27.
[78] S. Sholiq, R. Sarno, E.S. Astuti, Generating BPMN diagram from textual requirements, Journal of King Saud University-Computer and Information Sciences, 34 (2022) 10079-10093.
[79] C. Larman, Applying UML and patterns: an introduction to object-oriented analysis and design and iterative development, Pearson Education India, 2005.
[80] M. Dumas, M. La Rosa, J. Mendling, H.A. Reijers, Fundamentals of business process management, Springer, 2013.
[81] N. Prajapat, A. Tiwari, A review of assembly optimisation applications using discrete event simulation, International Journal of Computer Integrated Manufacturing, 30 (2017) 215-228.
[82] D. Goldsman, P. Goldsman, Discrete-event simulation, in: Modeling and Simulation in the Systems Engineering Life Cycle: Core Concepts and Accompanying Lectures, Springer, 2015, pp. 103-109.
[83] M. Jamil, N.M. Razali, Simulation of assembly line balancing in automotive component manufacturing, in: IOP Conference Series: Materials Science and Engineering, IOP Publishing, 2016, pp. 012049.
[84] R. Mansharamani, An overview of discrete event simulation methodologies and implementation, Sadhana, 22 (1997) 611-627.
[85] N. Karanjkar, A. Joglekar, S. Mohanty, V. Prabhu, D. Raghunath, R. Sundaresan, Digital twin for energy optimization in an SMT-PCB assembly line, in: 2018 IEEE international conference on Internet of Things and intelligence system (IOTAIS), IEEE, 2018, pp. 85-89.

[86] C.J. Turner, W. Hutabarat, J. Oyekan, A. Tiwari, Discrete event simulation and virtual reality use in industry: new opportunities and future trends, IEEE Transactions on Human-Machine Systems, 46 (2016) 882-894.
[87] A. Ingemansson, T. Ylipää, G.S. Bolmsjö, Reducing bottle-necks in a manufacturing system with automatic data collection and discrete-event simulation, Journal of Manufacturing Technology Management, 16 (2005) 615-628.
[88] A. Kampa, G. Gołda, I. Paprocka, Discrete event simulation method as a tool for improvement of manufacturing systems, Computers, 6 (2017) 10.
[89] S. Pfeiffer, Robots, Industry 4.0 and humans, or why assembly work is more than routine work, Societies, 6 (2016) 16.
[90] M. Albrecht, P. Az, Introduction to discrete event simulation, PE (AZ), (2010).
[91] R. Söderberg, K. Wärmefjord, J.S. Carlson, L. Lindkvist, Toward a Digital Twin for real-time geometry assurance in individualized production, CIRP annals, 66 (2017) 137-140.
[92] M. Schluse, M. Priggemeyer, L. Atorf, J. Rossmann, Experimentable digital twins—Streamlining simulation-based systems engineering for industry 4.0, IEEE Transactions on industrial informatics, 14 (2018) 1722-1731.
[93] T. Ziarnetzky, L. Mönch, A. Biele, Simulation of low-volume mixed model assembly lines: modeling aspects and case study, in: Proceedings of the Winter Simulation Conference 2014, IEEE, 2014, pp. 2101-2112.
[94] G. Weigert, T. Henlich, Simulation-based scheduling of assembly operations, International Journal of Computer Integrated Manufacturing, 22 (2009) 325-333.
[95] R.B. Detty, J.C. Yingling, Quantifying benefits of conversion to lean manufacturing with discrete event simulation: a case study, International journal of production research, 38 (2000) 429-445.
[96] S. Kumar, P. Phrommathed, Improving a manufacturing process by mapping and simulation of critical operations, Journal of Manufacturing Technology Management, 17 (2006) 104-132.
[97] M. Dewa, L. Chidzuu, Managing bottlenecks in manual automobile assembly systems using discrete event simulation: case study, South African Journal of Industrial Engineering, 24 (2013) 155-166.
[98] Z. Wang, H. Wang, Simulation and optimization of the mixed assembly line based on Flexsim software, Modular Maching Tool & Automatic Manufacturing Technique, (2015) 142-145.
[99] Nordgren, FlexSim simulation environment, in: Proceedings of the 2003 Winter Simulation Conference, 2003., 2003, pp. 197-200 Vol.191.
[100] A.A.M. Ruwaida Aliyu, Research Advances in the Application of FlexSim: A Perspective on Machine Reliability, Availability, and Maintainability Optimization, Journal of Hunan University Natural Sciences, 48 (2021).
[101] G. Li-xiong, T. Guo, H. Min, Simulation and optimization of motorcycle coating product line based on Flexsim, Industrial Engineering and Management, 19 (2014) 122-126.
[102] H. Yuan, Y. Luo, Simulation and optimization of the technological processes based on Flexsim, Journal of Hubei University of technology, 22 (2007) 81-82.
[103] E. Gelenbe, H. Guennouni, FLEXSIM: A flexible manufacturing system simulator, European journal of operational research, 53 (1991) 149-165.
[104] J.W. Kim, J.S. Park, S.K. Kim, Application of FlexSim software for developing cyber learning factory for smart factory education and training, Multimedia Tools and Applications, 79 (2020) 16281-16297.
[105] Z. Wei-Feng, F. Qi, Simulation of complex logistics and it's research status, Acta Simulata Systematica Sinica. vol15, (2003) 353-356.
[106] S. Bao, H. Chen, G. Jiang, X. Zhou, Optimizing the logistics of streamline based on software Flexsim, industrial engineering and management, 13 (2008) 106-109.
[107] E.M. Sefene, State-of-the-art of selective laser melting process: A comprehensive review,

Journal of Manufacturing Systems, 63 (2022) 250-274.
[108] N. Pradhan, A compilation of design principles and guidelines for selective laser sintering, in, 2016.
[109] Y.A. Gueche, N.M. Sanchez-Ballester, S. Cailleaux, B. Bataille, I. Soulairol, Selective laser sintering (SLS), a new chapter in the production of solid oral forms (SOFs) by 3D printing, Pharmaceutics, 13 (2021) 1212.
[110] J. Wang, F. Qiao, F. Zhao, J.W. Sutherland, A data-driven model for energy consumption in the sintering process, Journal of Manufacturing Science and Engineering, 138 (2016) 101001.
[111] A. Alfaify, M. Saleh, F.M. Abdullah, A.M. Al-Ahmari, Design for additive manufacturing: A systematic review, Sustainability, 12 (2020) 7936.
[112] A. Kowalski, R. Waszkowski, Layout guidelines for 3D printing devices, Applied Sciences, 10 (2020) 6333.
[113] M. Chinosi, A. Trombetta, BPMN: An introduction to the standard, Computer Standards & Interfaces, 34 (2012) 124-134.
[114] C.R. Deckard, Method and apparatus for producing parts by selective sintering, (1991).
[115] J.W. Stansbury, M.J. Idacavage, 3D printing with polymers: Challenges among expanding options and opportunities, Dental materials, 32 (2016) 54-64.
[116] Installation Conditions FORMIGA P 110. Laser-Sintering System for Plastics, Krailling, Germany, (2013).
[117] Q. Cheng, H. Shen, H. Chu, Z. Liu, C. Zhang, J. Ren, Research on logistics simulation and optimization of die forging production line based on flexsim, in: Journal of Physics: Conference Series, IOP Publishing, 2020, pp. 022063.
[118] T. Wallin, J. Pikul, R.F. Shepherd, 3D printing of soft robotic systems, Nature Reviews Materials, 3 (2018) 84-100.
[119] T.D. Ngo, A. Kashani, G. Imbalzano, K.T. Nguyen, D. Hui, Additive manufacturing (3D printing): A review of materials, methods, applications and challenges, Composites Part B: Engineering, 143 (2018) 172-196.
[120] J. Huang, Q. Qin, J. Wang, A review of stereolithography: Processes and systems, Processes, 8 (2020) 1138.
[121] P. Bartolo, J. Gaspar, Metal filled resin for stereolithography metal part, CIRP annals, 57 (2008) 235-238.
[122] W.K. Swainson, Method, medium and apparatus for producing three-dimensional figure product, in, Google Patents, 1977.
[123] A.J. Herbert, Solid object generation, Jour Appl Photo Eng, (1982) 185-188.
[124] C.W. Hull, Apparatus for production of three-dimensional objects by stereolithography, United States Patent, Appl., No. 638905, Filed, (1984).
[125] Stereolithography (SLA) 3D printing Technology overview, in, 8 September 2023.
[126] J.R. Tumbleston, D. Shirvanyants, N. Ermoshkin, R. Janusziewicz, A.R. Johnson, D. Kelly, K. Chen, R. Pinschmidt, J.P. Rolland, A. Ermoshkin, Continuous liquid interface production of 3D objects, Science, 347 (2015) 1349-1352.
[127] B.E. Kelly, I. Bhattacharya, H. Heidari, M. Shusteff, C.M. Spadaccini, H.K. Taylor, Volumetric additive manufacturing via tomographic reconstruction, Science, 363 (2019) 1075-1079.
[128] M. Shusteff, A.E. Browar, B.E. Kelly, J. Henriksson, T.H. Weisgraber, R.M. Panas, N.X. Fang, C.M. Spadaccini, One-step volumetric additive manufacturing of complex polymer structures, Science advances, 3 (2017) eaao5496.
[129] M. Shusteff, R.M. Panas, J. Henriksson, B.E. Kelly, A.E. Browar, Additive fabrication of 3d structures by holographic lithography, (2016).
[130] A. Kataria, D.W. Rosen, Building around inserts: methods for fabricating complex devices in stereolithography, in: International Design Engineering Technical Conferences and Computers and Information in Engineering Conference, American Society of Mechanical Engineers, 2000, pp. 1387-

1397.
[131] N.J. Mankovich, A.M. Cheeseman, N.G. Stoker, The display of three-dimensional anatomy with stereolithographic models, Journal of digital imaging, 3 (1990) 200-203.
[132] D. Miedzińska, E. Małek, A. Popławski, Numerical modelling of resins used in stereolitography rapid prototyping, Applied Computer Science, 15 (2019).
[133] S. Korga, M. Barszcz, K. Dziedzic, Development of software for identification of filaments used in 3d printing technology, Applied Computer Science, 15 (2019) 74--83.
[134] X. Wang, M. Jiang, Z. Zhou, J. Gou, D. Hui, 3D printing of polymer matrix composites: A review and prospective, Composites Part B: Engineering, 110 (2017) 442-458.
[135] J. Miltenburg, U-shaped production lines: A review of theory and practice, International journal of production economics, 70 (2001) 201-214.
[136] R. Aliyu, A. Mokhtar, H. Hussin, Research advances on the application of FLEXSIM in maintenance processes: A mini review, in: AIP Conference Proceedings, AIP Publishing, 2024.
[137] K. Kovbasiuk, K. Židek, M. Balog, L. Dobrovolska, Analysis of the selected simulation software packages: a study, Acta Tecnología, 7 (2021) 111-120.
[138] J. Butt, A strategic roadmap for the manufacturing industry to implement industry 4.0, Designs, 4 (2020) 11.
[139] Gray 3D printing resin. Website: https://www.directindustry.com/prod/druckwege/product-4560415-2535000.html.